This is to certify that the

dissertation entitled

FINITE ELEMENT ANALYSIS OF HYDROLOGIC RESPONSE AREAS USING GEOGRAPHIC INFORMATION SYSTEMS

presented by

BAXTER E. VIEUX

has been accepted towards fulfillment
of the requirements for

Ph.D. degree in Agricultural Engineering

Major Professor

Date July 21, 1988

ABSTRACT

FINITE ELEMENT ANALYSIS OF HYDROLOGIC RESPONSE AREAS USING GEOGRAPHIC INFORMATION SYSTEMS

By

Baxter Ernest Vieux

The methodology developed in this research utilizes a Geographic Information System and the finite element Galerkin formulation to solve the kinematic wave equation for overland flow in a watershed. The watershed studied was number 4H, located in Webster County, Nebraska, and was operated by the USDA-Agricultural Research Service.

The one- and two-dimensional forms of the equation were studied and the resulting outflow hydrograph was compared to an actual storm event, May 4, 1959. Rainfall excess was calculated using the Green and Ampt infiltration equation for an unsteady rainfall.

Hydrologic response areas were formed based on slope with the aid of the ARC-INFO Geographic Information System developed by ESRI, Redlands, Ca. A finite element grid representing streamlines and equipotential lines was formed such that the direction of slope forms the streamlines of flow and the elevational contours form the equipotential lines. This results in nodal slope values perpendicular and parallel to the sides of the elements. Kinematic shock was avoided due to the use of nodal slope values. This formulation allowed solution of the overland flow equations

FINITE ELEMENT ANALYSIS OF HYDROLOGIC RESPONSE AREAS USING GEOGRAPHIC INFORMATION SYSTEMS

By

Baxter Ernest Vieux

A DISSERTATION

Submitted to
Michigan State University
in partial fulfillment of the requirements
for the degree of

DOCTOR OF PHILOSOPHY

Department of Agricultural Engineering

1988

ABSTRACT

FINITE ELEMENT ANALYSIS OF HYDROLOGIC RESPONSE AREAS USING GEOGRAPHIC INFORMATION SYSTEMS

By

Baxter Ernest Vieux

The methodology developed in this research utilizes a Geographic Information System and the finite element Galerkin formulation to solve the kinematic wave equation for overland flow in a watershed. The watershed studied was number 4H, located in Webster County, Nebraska, and was operated by the USDA-Agricultural Research Service.

The one- and two-dimensional forms of the equation were studied and the resulting outflow hydrograph was compared to an actual storm event, May 4, 1959. Rainfall excess was calculated using the Green and Ampt infiltration equation for an unsteady rainfall.

Hydrologic response areas were formed based on slope with the aid of the ARC-INFO Geographic Information System developed by ESRI, Redlands, Ca. A finite element grid representing streamlines and equipotential lines was formed such that the direction of slope forms the streamlines of flow and the elevational contours form the equipotential lines. This results in nodal slope values perpendicular and parallel to the sides of the elements. Kinematic shock was avoided due to the use of nodal slope values. This formulation allowed solution of the overland flow equations

for a watershed as a continuum rather than as a series of independent cascades.

The method developed through this research provides a more accurate description of the hydrologic processes in a watershed. Through more accurate description of hydrologic processes insight is provided into transport phenomena of agricultural pollution such as pesticides and nutrients in surface and subsurface water as affected by overland flow and infiltration for an agricultural watershed.

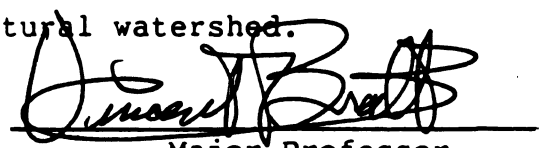

Major Professor

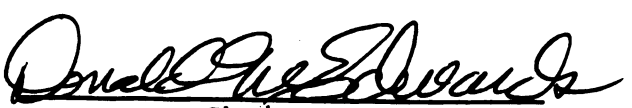

Chairperson

DEDICATION

I wish to dedicate this work to my wife Jean and our children William, Ellen, Laura, Anne, and Kimberly who all helped in their own way, and to my mother and father who inspired my love of science at an early age.

ACKNOWLEDGMENT

To my advisor, Dr. Vincent Bralts, I owe a debt of gratitude for the inspiration to complete this work. To the members of my guidance committee I must thank them as a team that as a whole provided more than guidance.

To the other members of the guidance committee, I individually wish to thank Dr. Larry Segerlind for his insight into the finite element method and for his more than finite patience and encouragement; Dr. Donald Edwards for his oversight and greatly appreciated support; Dr. Jon Bartholic for his efforts to provide direction to and synthesis of this work, and Dr. Roger Wallace for his unrelenting insight into the physical problem formulation.

I also wish to thank Dr. Walter Rawls, of the USDA-ARS Hydrology Laboratory for his valued assistance in the infiltration component of the Water Erosion Prediction Project (WEPP) used in this research.

TABLE OF CONTENTS

LIST OF TABLES

LIST OF FIGURES

LIST OF SYMBOLS

A = Cross-sectional area of flow.

$\{A\}$ = Nodal flow area vector for a channel of irregular cross section.

$[a]$ = $\int_{\Omega} \{N\}^T (\{N\}\{w\})\{N\}d\Omega$.

$[Bx]^T$ = Transpose matrix of the derivatives of the shape functions with respect to x.

$[By]^T$ = Transpose matrix of the derivatives of the shape functions with respect to y.

c = Speed of a gravity wave or (5/3)V.

$[C]$ = Capacitance matrix

dA = Differential element of the control surface, cs.

$d\Lambda$ = Differential element of control volume, cv.

$\{F\}$ = Force vector.

F_p = Pressure in elemental control volume = $\rho gh^2/2$.

F_g = Gravitational force.

F_o = Froude number.

F_s = Frictional resistance = $\rho hgS_f\Delta x$.

g = Gravitational acceleration.

h = Water depth.

h_e = $\sum_{1}^{n} N_i(x,y)h_i$ piecewise continuous shape function approximation of the flow depth h.

h_i = Nodal values of the flow depth h.

$\{\dot{h}\}$ = Vector of time derivatives of the flow depth h.

h^* = Rainfall impact overpressure or induced head.

i = Infiltration rate.

k = Kinematic wave number.

$[K]$ = Stiffness matrix.

N_i = Shape function at the ith node.

N_j = Shape function at the jth node.

$[N]^T$ = Transpose matrix of the shape functions.

ρ = Fluid density.

$\{Q\}$ = Nodal flow rate vector.

r = Rainfall intensity.

R = Rainfall excess = (r-i) .

$\{R\}^{(e)}$ = Elemental residual.

R_x = Angle between the horizontal axis and the x-axis.

s = Local coordinate system in the x-direction.

S_f = Friction slope defined by either of the Chezy or Manning equations.
S_{fx} = Friction slope in x-direction.
S_{fy} = Friction slope in y-direction.
S_o = Slope of the channel bottom.
S_x = Slope in the x-direction.
S_y = Slope in the y-direction.
u = $u(x,y,z,t)$, velocity in the x-direction.

$\bar{u}$ = Depth-averaged velocities in the x-direction.
u_e = $\sum_{1}^{n} N_i(x,y)u_i$ piecewise continuous shape function approximation of the velocity u.
u_i = Nodal values of the velocity u.
v = $v(x,y,z,t)$, velocity in the y-direction.

$\bar{v}$ = Depth-averaged velocities in the y-direction.
v_e = $\sum_{1}^{n} N_i(x,y)v_i$ piecewise continuous shape function approximation of the velocity v.
v_i = Nodal values of the velocity v.
V = Velocity vector.
$V \cdot \hat{n}$ = Dot product of the velocity vector to the normal unit vector of the control surface.
w = $w(x,y,z,t)$, velocity in the z-direction or flow width of the element.
Δt = Time step.
Δx = Distance increment or element length.
x = Coordinate in the primary flow direction.
y = Coordinate perpendicular to the x-direction.
z = Vertical coordinate or direction perpendicular to the channel bottom.
β, β_L = Momentum correction factors for main and lateral flows.
β_r = Momentum correction factor for raindrop terminal velocity.
η = Eta natural coordinate corresponding to the global y-direction.
ξ = Ksi natural coordinate corresponding to the global x-direction.
λ = Eigenvalue.
Λ = Elemental control volume or mean terminal velocity of fall of raindrops.
Ω = Two-dimensional element domain.
$\theta_{x,y,z}$ = Angle with the respective direction.
Φ_x = Angle of inclination between the terminal velocity vector and the vertical axis.

I. INTRODUCTION

Agricultural pollution by pesticides and nutrients threatens both surface and subsurface waters due to hydrologic transport of these contaminants. The locations within a watershed that produce similar contributions to surface and subsurface waters may be termed hydrologic response units or areas. To successfully reduce subsurface water contamination, reduce sedimentation, and control erosion, land treatment measures must be focused on those geographic areas that will yield the greatest mitigation. Hydrologic modeling has recently been the subject of more and more attention in addressing watershed management. Modeling may be mathematical, if described by a mathematical equation, or physical if a scale model is built to represent dimensional similitude to the actual watershed. In either case the model is a conceptualization of the actual watershed. Mathematical modeling generally seeks to define the mathematical relation between a set of independent variables and a response or dependent variable.

The twentieth century has witnessed a rapid acceleration in the quantitative modeling of physical processes. The mathematical description of natural phenomena in the hydrologic cycle is not, however, a child of this century. The history of quantitative hydrology has

been marked by important milestones. Achievements of each scientist have served as the foundation for advances by the next scientist. Of the classical period the most notable treatise (in 66 AD) that makes mention of the hydrologic cycle was Vitruvius' "Ten Books of Architecture" (Morgan, 1960). Vitruvius' description in Book VIII on how to find water, we read

> The valleys among the mountains receive the rains most abundantly, and on account of the thick woods the snow is kept in them longer by the shade of the trees and mountains. Afterwards, on melting, it filters through the fissures in the ground, and thus reaches the very foot of the mountains, from which gushing springs come belching out.

Though not without some misconceptions, Vitruvius essentially understood the origin of springs and groundwaters. Not until the seventeenth century did ideas of quantitative hydrology emerge. Biswas (1968) presented the following matter on the beginnings of quantitative hydrology.

Pierre Perrault anonymously published the book De l'Origine des Fountaines in 1674 (Biswas, 1968). In this work he calculates the quantity of water that would accumulate from the rainfall in the catchment of the Seine River, France. He found that a sixth part of the rain and snow water is necessary to make the river run continually throughout the year. For the first time experimental evidence proved the pluvial origin of rivers. The greatest contribution of Perrault and other contemporaries--including Edmond Halley, who calculated the volume of water

required to supply the rivers in the evaporation-precipitation cycle, and Edme Mariotte who expanded on the pluvial origins of rivers--was that they proved their hypotheses through quantitative methods.

Watershed hydrology can be treated as either a lumped or distributed parameter model as well as by a stochastic or a deterministic method. A lumped model tends to utilize the average of a set of independent variables that represent a sub-basin or an entire watershed. A distributed model utilizes the spatial location of the independent variables and computes the dependent variable directly at the spatial location of each independent variable. Distributed models represent spatial distribution as a set of grids or a series of finite elements, each with its own physical properties. The degree to which physical properties--e.g., soil infiltration parameters, surface roughness, or slope--are averaged, represents the degree to which the model is lumped. The direct computation utilizing these parameters is a deterministic method as opposed to a stochastic method.

Scope and Objectives

Early modeling efforts neglected the spatial variability of the independent variables. Lumping of these parameters does not allow visualization of the spatially distributed runoff and infiltration processes.

Distributed parameter models, which can readily handle complex geometry and spatial distributions of the independent variables, have typically used approximations of the actual watershed by using arbitrary grids, planes or elements. The observation of the spatial and temporal distribution of infiltration and runoff is one of the benefits claimed by proponents of distributed models. In actual practice, however, the volume of input data prevented accurate representation of the spatial character of the input data. Proper location of land treatment measures required knowing the spatial and temporal distribution of the infiltration and runoff processes. In order to achieve an accurate characterization of the spatially distributed input parameters, an improved method of defining hydrologic response areas is needed.

The value of processing a watershed by a Geographic Information System (GIS) is evident within the context of the finite element method as shown in Figure 1. The GIS serves as a spatial data management system. Soils maps, landuse and other geographic data are represented in a digital media using a common coordinate system. The first step in the finite element method is to define elements over which the differential equations of overland flow may be

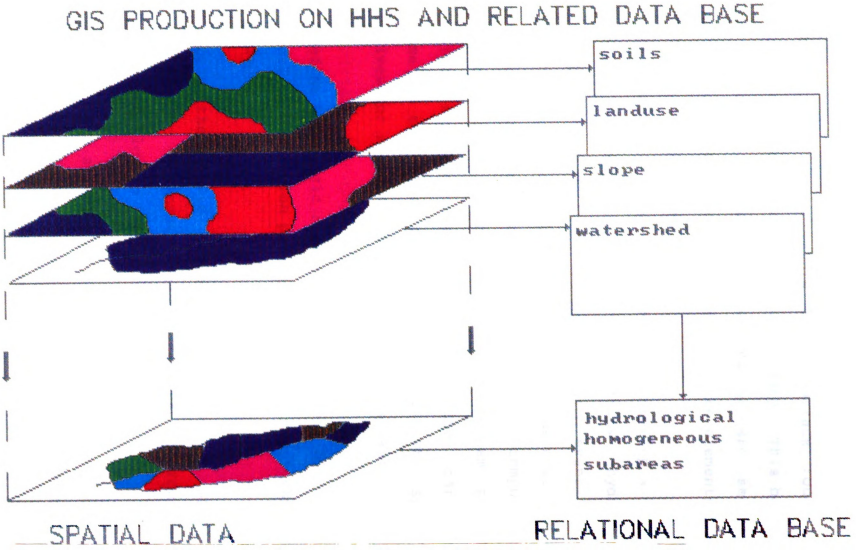

Figure 1. Geographic Information System Definition of Areas With Similar Attributes.

integrated. The efficiency of the Geographic Information System is realized when areas of like attribute values, such as infiltration parameters, slope, surface roughness, and so on, are aggregated within a boundary. This boundary forms a polygon consisting of vectors or arc segments. These polygons then become the set of finite elements used to model the runoff process.

The purpose of this research was to develop a method that more accurately predicts the outflow hydrograph resulting from runoff during a rainstorm event for a watershed with spatially non-uniform parameters. This method utilized the finite element method to compute the runoff rates and a Geographic Information System to more accurately represent the spatially distributed parameters for use in the computation of the runoff. The specific objectives for reaching this goal are as follows:

1) Define hydrologic response areas that exhibit similar soil infiltration parameters, surface roughness, and slope.

2) Apply the finite element method to the specific hydrologic response areas to compute and route the overland flow to the outlet.

3) Compare the accuracy of the outflow hydrographs to the actual outflow hydrograph for a given rainstorm event for the following two cases:

i) A finite element grid that is of an arbitrary spatial form.

ii) A finite element grid formed from hydrologic response areas defined by the Geographic Information System.

It was hypothesized that the combination of the Geographic Information System and the finite element method would result in a mathematical model that predicted the outflow hydrograph from a finite element grid formed of hydrologic response areas more accurately than from a finite element grid that was of an arbitrary spatial form. Validation of this hypothesis was accomplished if the method developed through this research more accurately predicted the actual outflow hydrograph from a watershed of non-uniform, spatially distributed parameters such as infiltration parameters, surface roughness, and slope.

i) A finite element grid that is of an arbitrary spatial form.

ii) A finite element grid formed from hydrologic response areas defined by the Geographic Information System.

It was hypothesized that the combination of the Geographic Information System and the finite element method would result in a mathematical model that predicted the outflow hydrograph from a finite element grid formed of hydrologic response areas more accurately than from a finite element grid that was of an arbitrary spatial form. Validation of this hypothesis was accomplished if the method developed through this research more accurately predicted the actual outflow hydrograph from a watershed of non-uniform, spatially distributed parameters such as infiltration parameters, surface roughness, and slope.

II. REVIEW OF THEORY AND LITERATURE

Since the seventeenth century, the science of hydrology evolved together with mechanical and industrial developments. The twentieth century and recent decades in particular, have seen great strides in the science of hydrology. The industrial age, which effected environmental degradation also necessitated more and greater strides in hydrologic methods. One such method, the mathematical model, through recent technical elaborations has allowed the direct modeling of spatially distributed hydrologic processes.

Hydrologic processes, when described by physically based equations, are termed deterministic. This review expounds the theory in the literature on deterministic hydrologic models, particularly those utilizing finite difference and finite element methods to describe the spatially distributed hydrologic process of a rainfall storm event over a watershed.

A. Hydrologic Modeling

The physically correct representation of the surface runoff and infiltration processes in a watershed, field, or plot depends on many factors. To categorize these factors, several distinctions should be made in general as to the

modeling process that seeks to represent the physical process. Abstraction is the mind's attempt to disengage the essence of something from that which is non-essential or only incidental to its make-up (V.E. Smith, 1950). The order of abstraction required in mathematical modeling is to consider the mathematical relation between cause and effect for the abstracted, conceptual model. The conceptual model strips the processes that are considered incidental or nonessential. The mathematical model then describes those essential processes contained in the conceptual model. Considering the complexity of the real world, it is necessary to use a conceptual model in order to successfully apply the mathematical model. This however is not without drawbacks, considering the interdependence of the many hydrologic processes. Modeling a particular process in the absence of another that is affecting the modeled process may result in a physically invalid model and would represent a poor choice of a conceptual model.

These drawbacks notwithstanding, we will examine first some mathematical models that seek to model deterministically the physical process of the rainfall event. This process may include infiltration, overland flow of the rainfall excess, and channel routing of the lateral inflow from the overland flow portion of the watershed. Smith and Woolhiser (1971) developed a mathematical model that modeled a coupled system of two complex, natural processes of an elemental watershed. The

conceptual model included only infiltration and overland flow. Channel flow was not considered because the conceptual model was limited to the upland portion of the watershed where channel flow is not well established. The infiltration model provides insight into the process by which rainfall becomes either runoff or subsurface water. The kinematic equations provide insight into the depth and velocity of the runoff as it accelerated down the watershed. The infiltration and the kinematic equation were coupled mathematically such that the rainfall excess as defined by the infiltration model was the boundary value for solution of the kinematic equation.

A distributed, deterministic system results when the inherent spatial nature of the processes are preserved in the solution method. A model such as Smith and Woolhiser's provides the opportunity to model the outflow of the watershed and, more importantly, the spatial and temporal distribution of the runoff-infiltration process within that watershed.

1. Distributed Parameter Models

Huggins and Burney (1982) observed that hydrologic modeling is most differentiated by the manner in which parameters or input values are handled. Lumping or averaging certain parameters yields a lumped parameter model. Distributed parameter watershed models treat the individual input parameters directly without lumping. Such models avoid the errors caused by averaging of nonlinear

variables or threshold values (Huggins and Burney, 1982).

Distributed parameter models are relatively new and are the subject of intense research. The principal advantage of distributed models is that the geographical variation of data within the watershed is preserved. Furthermore, with measured parameters, ungaged watersheds may be investigated for the effect of landuse changes. Finally, water quality simulations on a distributed basis identify the source areas within a watershed of hydrodynamic transport of pollutants.

Distributed parameter watershed models are more complex, require more computing time and increased input data. The value of the knowledge derived from distributed models must be considered vis-a-vis the increased time and costs of developing and using this class of model. High speed digital computers, however, obviate the restrictions on increased computing time and complexity allowing more and more complex, distributed models to be used.

Huggins and Monke (1966) developed the ANSWERS model, a distributed parameter model that uses a grid as a method of preserving the geographic heterogeneity of the input parameters. Each cell of the grid represents the hydrologic unit over which the model equations are solved using the finite difference method.

The ANSWERS model uses a fundamental method of computing distributed processes. The continuum of the watershed is resolved into discrete elements and

preserves the spatial heterogeneity of the input parameters.

2. Hydrodynamic Model Approach

The hydrodynamic approach proposed by C.L. Chen and Ven Te Chow (1971) considered watershed hydrology as a distributed continuum, where the hydrodynamic principles of fluid flow apply. The solution of the hydrodynamic equations yields a deterministic model capable of defining distributed flow velocities and depths over the watershed.

The hydrodynamic equations have been derived and solved by various methods. There are two distinct categories of flow in a watershed--overland flow, characterized by shallow flow, and channel flow, characterized by well-defined channel geometry. The boundary between these two flows changes with time and distance and therefore are modeled with difficulty.

Chen and Chow formulated a comprehensive watershed-flow model. They classified watershed hydrology by a molecular approach, a microscopic hydrodynamic approach, and a macroscopic hydrodynamic approach. The microscopic and macroscopic hydrodynamic approaches both derive the Navier-Stokes equation of motion for fluid flow with suitable boundary conditions. The difference between the micro- and the macro- approaches is that the latter utilizes averaging of variables in certain flow directions in order to simplify the Navier-Stokes equation.

The approach of Chen and Chow formulated the equations of continuity and momentum for flow of a Newtonian fluid in a three dimensional space. A Cartesian coordinate system is used whereby the average velocity is taken parallel to the ground surface with the x- and y-directions along the bottom of the flow. Temperature variations are not considered, so the fluid is assumed to be of a homogeneous viscosity. Their derivation is summarized as follows.

a. Conservation of Mass

The conservation of mass is derived by integrating in the vertical direction such that the differential variation in flow is considered only in the x- and y-directions with vertical variation as defined by the depth of flow h.

$$\frac{\partial h}{\partial t} + \frac{\partial (uh)}{\partial x} + \frac{\partial (vh)}{\partial y} = r - i \qquad [1]$$

where

h = the depth of flow measured in the vertical axis z'

u = depth-averaged velocity in the x-direction,

v = depth-averaged velocity in the y-direction,

r = rainfall, and

i = infiltration, positive when moving out of channel, negative when moving into channel.

The coordinate system used assumes that the primary flow directions are parallel to the ground surface. This requires that the z-direction makes an angle θ inclination

with the force of gravity. Equation [1] is in terms of vertically oriented variables h, r, and i. The x- and y-directions are not orthogonal with the vertical z-axis.

b. Conservation of Momentum

The conservation of momentum is derived by balancing momentum and forces for an elemental control volume. The resulting equation is the Navier-Stokes equation and is a fundamental equation of fluid mechanics. Chen and Chow (1971) begin with the Navier-Stokes equation and simplify it according to appropriate boundary conditions and assumptions. This rather convoluted approach yields the general momentum equation for watershed flow in the x-direction.

$$\frac{\partial(AV)}{\partial t} + \frac{\partial(\beta AV^2)}{\partial t} - \beta_r r \Lambda T \cos\Phi_X - \beta_L V q_L$$

$$= gA\sin\theta_X - g\frac{\partial}{\partial x}[A(h\cos^2\theta_Z + h^*)] - gAS_{fx} \qquad [2]$$

where

$\theta_{x,y,z}$ = angle with the respective direction,

h = depth of the centroid of the cross-sectional area,

h^* = rainfall impact overpressure or induced head,

A = cross-sectional area of flow,

S_{fx} = friction slope in x-direction,

β, β_L = momentum correction factors for main and lateral flows,

β_r = momentum correction factor for raindrop

terminal velocity,

Λ = mean terminal velocity of fall of raindrops, and

Φ_x = angle of inclination between the terminal velocity vector and the vertical axis.

Because they are applicable to both overland and channel flow, equations [1] and [2] for the conservation of continuity and momentum, form the description of the watershed problem. They are the complete dynamic form of the shallow water equations. The continuity or conservation of mass and the one-dimensional, conservative form of the conservation of momentum are commonly known as the St. Venant equation derived by St. Venant in 1871. The general form, ignoring the momentum of the rainfall impact and overpressure, is expressed by [3] as a set of equations

$$A\frac{\partial V}{\partial x} + V\frac{\partial A}{\partial x} + \frac{\partial A}{\partial t} = q$$

and

$$V\frac{\partial V}{\partial x} + \frac{\partial V}{\partial t} + \frac{g}{A}\frac{\partial(\bar{y}A)}{\partial x} = g(S_o - S_f) - \frac{Vq}{A} \qquad [3]$$

where

A = cross-sectional flow area,

$\bar{y}$ = depth of flow,

V = mean water velocity,

q = lateral inflow per unit length of channel,

y = distance from the water surface of the centroid,

S_o = channel slope, and

S_f = friction slope.

These are the conservation of mass and momentum in the x-direction.

Abdel-Razaq (1967) applied the finite difference solution to the above St. Venant equations. Brutsaert (1971) experimentally verified the solution, and Yen (1973) recapitulated the open channel flow equations emphasizing the origin of the St. Venant equations as the special form of the conservation of mass and momentum. Previous researchers had simplified these equations before formulating a mathematical model. The significant contribution is that these researchers applied these equations to a watershed flow domain.

The solution of the partial differential equations requires initial and boundary conditions. If the flow domain is considered to be the watershed as a whole, then only one boundary condition on the watershed divide and one at the outlet are needed if the flow is subcritical. If supercritical, then only one boundary condition is required at the watershed divide to give a unique solution.

If the flow domain is divided artificially into overland flow and channel flow, then there are two subdomains separated by an internal boundary. This boundary is not known prior to the solution yet is required in the solution. This difficulty may be removed by estimating a likely location of such an internal divide and treating the system of channel and overland flow as

uncoupled. This approach allows the computed values of the overland flow to act as lateral inflow for the channel flow equation.

3. Kinematic Wave Equation

A comprehensive treatment of the kinematic wave equation was examined by Woolhiser (1975) as a means of computing hydrographs with the assumption of both the Chezy and Manning equations as friction relations. Grace and Eagleson (1966) developed the full dynamic equations using the control volume technique for conservation of momentum and mass. Normalized equations were then established and an order of magnitude analysis produced. This approach allows simplification of the governing equations by discarding small order terms maintaining similarity between model and prototype. Brutsaert (1968) obtained an analytical solution to the shallow water or St. Venant equations. This was done within a small solution domain bounded by the forward and backward characteristics and the x-axis from 0 to L of the plane. The series solution provides good initial values for numeric analysis of overland flow in the initial stages of the hydrograph development. Of importance is that for large slopes, for a large roughness coefficient of the plane, or for very small constant lateral inflow, the series solution reduces to the kinematic wave equation, which is an approximation to the full dynamic equation.

Following is an illustration of the simplifications that

can be made to the full dynamic equation, ignoring lateral inflow:

$$V\frac{\partial V}{\partial x} + \frac{\partial V}{\partial t} + \frac{g}{A}\frac{\partial (yA)}{\partial x} = g\,(S_o - S_f) \qquad [4]$$

or

$$\underbrace{S_f = S_o}_{\text{KINEMATIC}} - \underbrace{\frac{g}{A}\frac{\partial (yA)}{\partial x}}_{\text{DIFFUSION}} - \underbrace{V\frac{\partial V}{\partial x} - \frac{\partial V}{\partial t}}_{\text{FULL DYNAMIC}} \qquad [5]$$

The terms in equation [5] represent the possible analogies for the modeling of the momentum equation. Through simplification or elimination of low order-of-magnitude terms, the significant terms are used in computing the fluid's dynamic behavior. The elimination of these terms in the above analogies introduces an error in the solution. The magnitude of the error dictates the acceptability of the analogy used under the physical conditions of the problem.

Woolhiser and Liggett (1967) examined in depth the errors introduced by the kinematic wave analogy applied to the full dynamic equation for the rising hydrograph. They discovered that the kinematic analogy can be applied within a certain range of input parameters. To quantify this range, the equations of continuity and the momentum equation are first normalized, constituting a nondimensional form of the full dynamic or shallow water equations. Then,

the kinematic equation or continuity plus the Chezy relation is normalized, yielding the equation of motion without the momentum terms.

Kibler and Woolhiser (1970) described the kinematic cascade as a hydrologic model. The concept here is to reduce not only the full dynamic equation momentum to a simplified form but also the geometry of the watershed to simple geometric cascades, through which the overland flow is routed to the outlet of the watershed. This approach results in a distributed parameter watershed model. The kinematic equation used is the Chezy equation together with the equation of continuity.

$$u = \alpha h^{N-1} \qquad [6]$$

and

$$\frac{\partial h}{\partial t} + \frac{\partial uh}{\partial x} = q \qquad [7]$$

N = 3/2 for wide channels,

α = $C\sqrt{S}$, where C is the Chezy roughness coefficient and S is the slope, and

h = the depth of overland flow.

In order to quantify the range of input parameters for which the kinematic analogy is applicable, equations [6] and [7] are normalized or made dimensionless.

Dimensionless Form

Equations [6] and [7] are normalized to yield

dimensionless equations dividing each term by a characteristic length or time. The Chezy equation is substituted into the equation for continuity and then solved using the method of characteristics. The dimensionless parametric equation is

$$\frac{\partial h^*}{\partial t^*} + \beta h^{*N-1} \frac{\partial h^*}{\partial x^*} = q^* \qquad [8]$$

where

q^* = normalized lateral inflow q,

h^* = normalized depth,

$\beta = N L_k / \sum_{i=1}^{n} l_i$,

l_i = length of plane i in feet,

L_k = normalizing depth for plane k,

N = Chezy parameter defined as above.

The dimensionless characteristic equations derived from the above normalized, nondimensional equation is

$$\frac{dx^*}{dt^*} = \beta h^{*N-1} \qquad [9]$$

and

$$\frac{dh^*}{dt^*} = q^* \qquad [10]$$

The earliest solution method was the method of characteristics, which had its origins in the nineteenth century. This method is also related to a separation of variables technique. In both instances, the partial

differential equation is reduced to ordinary derivatives. These are then solved graphically, numerically, or by a combination of both in the x-t domain (Henderson, 1966). The value of this method is that it presents information on the partial differential equation solution. Looking at the ordinary differential equations for the characteristics, we obtain a velocity dx/dt at which information can be transmitted through the system. This velocity leads to the Courant condition, which states the limit at which a disturbance can move. This velocity is the celerity of a gravity wave.

Kibler and Woolhiser (1970) made a thorough analysis of the kinematic cascade as a distributed parameter mathematical watershed model. One difficulty they encountered was the numerical phenomenon of the kinematic shock. When a disturbance occurs in an open channel system, its propagation may be described by the method of characteristics. Simple wave theory explains that when there is a change in slope between planes in the cascade, a shock or wave front is propagated within the system. The shock represents a numeric difficulty in the computation of the hydrograph. The shock parameter used to predict occurrence is defined as

$$P_s = \frac{w_{k-1}}{w_k} \frac{\alpha_{k-1}}{\alpha_k} > 1 \qquad [11]$$

where

w = width of the k and k-1

planes,

α = Chezy coefficient or $C\sqrt{S}$.

Observing the shock parameter inequality will ensure that shocks will not be propagated along characteristic lines emanating from the upstream boundary and the line $x = 0$.

Morris and Woolhiser (1980) re-examined the validity of the kinematic assumption under partial equilibrium. They found that the full dynamic or diffusion equations should be used for flat grassy slopes. The criterion

$$F_o^2 k \geq 5$$

should be observed when using the kinematic analogy. The physical significance of $F_o^2 k$ or $S_o L_o/H_o$ represents the ratio between the difference in elevation between the top and bottom of the plane ($S_o L_o$) and the normal flow depth at the downstream boundary(H_o). This criterion provides a convenient method of deciding the validity of the kinematic analogy. Earlier work (Woolhiser and Liggett, 1967) suggested that at full equilibrium the criterion

$$k = S_o L_o/H_o \geq 10$$

should be observed when using the kinematic analogy. If the kinematic number k is less than 10, then the full dynamic equations should be used. This condition does not normally occur in agricultural watersheds but may occur in urban areas where short, smooth watersheds with low lateral inflows prevalent.

4. Infiltration

When modeling overland flow in a pervious watershed, it is necessary to calculate the rainfall excess that results when the rainfall intensity exceeds the infiltration capacity of the soil and the surface storage. The rainfall excess is treated as lateral inflow in the overland flow equations. The right-hand side of equation [7] is the lateral inflow and can be viewed as the forcing function. In order to characterize an infiltrating natural watershed, it is necessary that

1. The conceptual model accounts for all processes of interest, e.g., unsteady rain, snow melt, etc.
2. The mathematical model adequately describes the conceptual model.
3. Soil properties within the watershed are taken into account.
4. Input parameters can be obtained for the domain of interest and successfully applied towards the solution.

The USDA-Soil Conservation Service developed a procedure to estimate direct runoff from ungaged watersheds. Rallison (1980) gives a detailed synopsis of the development of this procedure from its inception to its final form and application to ungaged watersheds. Work on this procedure began in the mid 1950s in response to the passage of the Watershed Protection and Flood Prevention Act (P.L. 83-566). Due to the work authorized by this act, SCS anticipated the need for a simplified method of hydrologic computation. Based on extensive analyses of

gaged, experimental watersheds and infiltrometer studies, a relation between rainfall and runoff was developed (Andrews, 1954, and Mockus, 1949). The basic relation was derived by plotting the accumulated natural runoff versus the accumulated rainfall. It was observed that the relation is asymptotic to a line at a 45 degree slope. This shows that the runoff rate approaches rainfall rate as the accumulation of both continues. Also, the difference between rainfall and runoff, the maximum retention, approaches a constant value. Rainfall intensity and the surface sealing effects of rainfall were not considered in the analysis. The basic hypothesis is

$$\frac{F}{S} = \frac{Q}{P_a} \qquad [12]$$

where

F = actual retention of precipitation during a storm,

S = potential maximum retention,

Q = direct runoff,

P_a = rainfall after initial abstraction.

Curve numbers are related to S by

$$CN = \frac{1000}{S+10} . \qquad [13]$$

The range of curve numbers for a watershed are due primarily to variations in storm duration and intensity. In the original analysis the CN chosen was an average of a

range of values for the particular soil-cover complex. For a particular storm, the CN may possibly fall outside the range originally established. Infiltration patterns are not accounted for within a storm period since no time variation was incorporated into the procedure. Consequently, the curve number method is not applicable to modeling infiltration under a variable intensity rainfall.

Infiltration equations that respond to variations of rainfall intensity have since been developed. Mein and Larson (1971) presented an extensive analysis of infiltration modeling as it relates to watershed modeling. They classified models as being empirical, theoretically derived algebraic, or soil moisture flow models. The Green and Ampt equation falls into the category of theoretically derived algebraic equations. The approach of Mein and Larson was to predict the time between the inception of rainfall and the inception of runoff. Their methodology was to modify the decay function of the infiltration capacity as defined by the Green and Ampt equation. This modification is necessary in order to account for the infiltration that occurs prior to surface ponding. The result of this effort was a simple model that relates infiltration to a constant rainfall intensity, homogeneous soil properties, and uniform initial soil moisture.

Brakensiek and Onstad (1977) presented a parameter estimation for the Green and Ampt infiltration equation. They observed that if watershed runoff is to be accurately

predicted, an accurate estimation of the infiltration capacity is needed. The sensitivity of runoff rate and volume was very sensitive to the fillable porosity and the hydraulic conductivity. A runoff model using the kinematic wave equation for direct runoff from a plane predicted the effect of varying the Green and Ampt parameters. The volume of runoff, for the conditions modeled, was most sensitive to fillable porosity. This is termed by some researchers to be the initial soil moisture deficit. The sensitivity expressed as a ratio of the dependent to the independent variable is as follows:

$$\frac{Q_v}{C} = 5.79$$

$$\frac{Q_p}{C} = 3.47$$

where

Q_p = peak runoff rate,

Q_v = volume of runoff,

C = fillable porosity.

For each 1% error in fillable porosity there is a corresponding 5.79% error in the volume of runoff. The sensitivity of hydraulic conductivity is

$$\frac{Q_v}{K} = 4.41$$

$$\frac{Q_p}{K} = 2.68$$

where

Q_p = peak runoff rate,

Q_v = volume of runoff,

K = hydraulic conductivity.

The sensitivity of these parameters indicates which parameters must be estimated with the greatest accuracy. The sensitivity indicates which parameters most easily bring the model into agreement with the observed event. The least sensitive parameter is the wetting front suction head. This would indicate that in a parameter optimization scheme, convergence may not be as rapid for the wetting front suction head parameter as for the others.

Chu (1978) studied infiltration under an unsteady rain. His study extended the application of the Green and Ampt equation to predicting the infiltration under an unsteady rainfall intensity. During an unsteady rainfall event, the intensity may recurrently shift from falling below to exceeding the infiltration capacity. The purpose of Chu's study was to extend the Green and Ampt equation to account for variable periods of rainfall intensity. The accomplished purpose is a transformed time scale that allows the computation of the infiltration with time under an unsteady rainfall.

Agricultural management affects the infiltration process. Rawls, Brakensiek, and Soni (1983) present guidelines for predicting the effects of tillage on the Green and Ampt parameters. Using the soil texture data, a

regression analysis was made to predict the increase in porosity due to tillage of a given soil. With time, the increased porosity decreases due to consolidation. The estimated change in porosity is a basis for estimating the change in the Green and Ampt parameters of capillary pressure of the wetting front and the hydraulic conductivity parameter, which is a fraction of the saturated hydraulic conductivity. The effect of tillage is accounted for by this procedure.

Brakensiek and Rawls (1983) presented the effects of surface sealing or crusting on the Green and Ampt parameters. A two layered, hydraulic conductivity is assumed to represent crusting. The wetting front capillary head is assumed to be that of the pre-crusted soil. The crusting thickness is assumed to be 0.5 cm. The effective hydraulic conductivity is calculated for pre-ponded and post-ponded periods during a rainfall event. The model predicts the infiltration to within an order of the effects of a crust formation under a rainfall simulator.

B. Numerical Solution of the Hydrodynamic Equations

The solution of the full dynamic equations poses significant problems due primarily to the nonlinearity of such terms as $u\partial u/\partial x$. Such problems give motivation to identify the domain in which reasonably accurate solutions to the simplified equations may be obtained. Further motivation to simplify the full dynamic equations is the

difficulty to provide the appropriate boundary conditions and incorporate them into the solution method.

The finite difference method has achieved extensive use in the computer solution of the full dynamic and simplified equations of fluid flow. Abdel-Razaq (1967) provided a finite difference solution to the surface runoff problem defined by the conservation of mass and the one-dimensional conservative form of the conservation of momentum equations.

The method of characteristics is a semi-graphical solution of the full dynamic and the simplified equations of fluid flow. Henderson (1966) gives an in-depth procedure for the solution of the full dynamic equation and the kinematic wave equations for channel flow. The method of characteristics also yields information on grid spacing in the finite differencing domain. This is related to the partial differential equation theory. The goal of these methods is to reduce the partial differential equations to ordinary and the ordinary to a linear system of equations amenable to solution.

1. Finite Difference Method

The finite difference method seeks to replace a continuum with discrete points between which the differentials are approximated. By replacing the partial differential terms with a finite difference approximation, the continuous domain is replaced by a network of isolated, discrete points. This procedure reduces a continuous

problem to an approximating eigenvalue matrix amenable to solution (Crandall, 1956).

The solution of the finite element formulation in time is most commonly done by the finite difference method. For example, the equation

$$[C]\{\dot{A}\} + [K]\{Q\} = \{F\} \qquad [14]$$

requires that a temporal solution of the time derivatives $\{\dot{A}\}$, $\partial A/\partial t$ be computed. This may be accomplished by writing the finite difference form of the time derivative as

$$\frac{\partial A(\xi)}{\partial t} = \frac{A(a) - A(b)}{\Delta t} \qquad [15]$$

The mean value theorem indicates that ξ must lie within the interval of $a \geq \xi \geq b$.

Not knowing where ξ lies within this interval we must define the parameter

$$\theta = \frac{(\xi - a)}{\Delta t} \qquad [16]$$

and use it as

$$A(\xi) = (1-\theta)A(a) + \theta A(b) \qquad [17]$$

Substituting [16] into [17] yields the relation for $\xi = t$ as

$$A = (1-\theta)A_a + \theta A_b \qquad [18]$$

Similarly for the right-hand force vector {F}

$$F = (1-\theta)F_a + \theta F_b \qquad [19]$$

where the b values are new values at the next time step. The four common values adopted for θ are

θ=0, ξ=a, the forward difference method.

θ=1/2, ξ=Δt/2, the central difference method.

θ=2/3, ξ=2Δt/3, the Galerkin's method.

θ=1, ξ=b, the backward difference method.

Equations [14] through [19] form the basis for the finite difference solution in time commonly used in conjunction with the finite element method

2. Finite Element Method

The solution of the hydrodynamic equations for fluid flow has encompassed a wide variety of disciplines, including

1. surface water equations for tidal estuaries,
2. boundary layer equations,
3. Navier-Stokes and St. Venant equations for closed and free surface fluid systems,
4. meteorological dynamics, and
5. groundwater flow.

The application of the finite element method is used extensively in fluid mechanics, as evidenced by the large volume of literature dealing with the solution of the Navier-Stokes equation especially in mechanical engineering

applications. The application of the finite element method to watershed or catchment hydrology is the subject at hand and is discussed herewith.

C. Finite Element Hydrologic Models

The finite element method was first used by Guymon (1972) in the solution of the hydrodynamic equations for free surface water flow. He solved the equations assuming a constant depth over a region using the variational principle. He concluded that the finite element method was a suitably efficient solution technique for surface water problems.

Researchers have typically approached the watershed or catchment problem as a model composed of two distinct parts--overland and channel flow. Judah (1973) applied the finite element method to this two-part model. He used the kinematic simplification of the momentum equation and the continuity equation and the Manning equation as the friction relation.

Judah's application of the Galerkin principle utilized linear shape and weighting functions to approximate depth and velocity. The element was one dimensional, having an average slope in the direction of flow. Rainfall excesses were not modeled because the model was tested for storms for which the rainfall excess was already known. Several watersheds, both experimental and natural, were modeled. Close agreement was generally found in the simulations of

the outflow hydrographs. It should be emphasized that rectangular strips (one-dimensional elements with an average top width) were used to represent the watersheds. The Rocky Run Branch Watershed in Brunswick County, Virginia, was subdivided into nine finite elements representing a total drainage of 555 acres.

Taylor (1974), using a Navier-Stokes formulation for the momentum equation, derived the two-dimensional form for watershed flow with the kinematic wave assumption. This application of the Galerkin method resulted in a coupled set of equations of the form

$$[M]\{q\}_t = \{F\}_t \qquad [20]$$

where the vector

$$\{q\} = \begin{Bmatrix} u \\ v \\ h \end{Bmatrix} \qquad [21]$$

is the vector containing the nodal values of the velocity u in the x-direction, v in the y-direction, and the flow depth h. Solution was confined to a one-dimensional impervious plane. The friction relations used were the Chezy and Manning equations. When compared to results for a kinematic cascade presented by Kibler and Woolhiser (1972), excellent agreement was found for the plane. Kinematic shocks were observed when two planes of different slope were treated as one domain. The solution, however, showed no smoothing, as is often the case when using finite

difference techniques.

Jayawardena (1976) represented the natural watershed by a large number or series of variable width strips. These strips were one-dimensional elements with a width that varied linearly over the length. Using linear shape functions the width was approximated by

$$w(x) = N_1W_1 + N_2W_2 \qquad [22]$$

Throughflow and infiltration were also modeled as saturated processes. Overland and channel flow were treated separately. An application was made with reasonable success to the Plynlimon and Wye catchments in Central Wales. Significant errors were introduced due to kinematic shock, which occurred where there was sufficient change in slope and flow parameters. These errors might be avoided by using a single set of slope and parameters within a strip composed of several elements.

Taylor (1976) proposed a two-dimensional, isoparametric element in the solution of the continuity and the kinematic equation for overland flow. The friction equations were the Chezy and the Manning equations. The finite element formulation used the vector defined by [21] for the nodal values. Time integration was performed by the central difference method with successive relaxation. Only a cascade of two elements was simulated with the two-dimensional elements. The kinematic equations and full dynamic equations were compared for a slope change of four

times. Kinematic shocks were observed, but it was Taylor's opinion that they caused no problem. This opinion conflicted with previous observations showing that continuity and peak discharge values were in error (cf. Jayawardena, 1976). The chief manifestation of the shock is that the profile of the water surface at the change in slope and the flow rate is discontinuous at this junction.

Judah, Shanholtz, and Contractor (1975) presented a simulation of a flood hydrograph for the Rocky Run Watershed in Brunswick County, Virginia. They used the same Galerkin formulation Judah used in 1973, and the watershed was represented by one-dimensional elements with variable width. The watershed was therefore composed of strips perpendicular to the contours. The researchers stated that their ultimate goal was to select sub-areas or elements that were hydrologically homogeneous. As other researchers have noted, significant changes in slope produce errors in shape and peak discharge of the outflow hydrograph. In the modeling of a surface coal mine, exaggerated changes in slope occur between benches. It was these changes that produced errors in the discharge hydrograph due to kinematic shock. Another problem encountered was the definition of rainfall excess. The Stanford Watershed Model was used to calculate rainfall excess. It was noted that some errors in the outflow volume were due to inaccurate prediction of rainfall excess. It should be noted, however, that the author's

assumption that there was a uniform rainfall distribution over the entire watershed may hold considerable error.

Jayawardena and White (1979) modeled the Severn and Wye catchments using the finite element method (cf. Jayawardena, 1976). The catchment was divided into strips flowing from the top of each slope to major drainage paths. These strips were further divided into finite elements. Each strip was computed separately with the outflow becoming the inflow boundary condition when the receiving strip was computed. A global matrix of strips for the watershed was not formed. This approach was used to avoid difficulty with kinematic shock. Errors due to inaccurate rainfall excess computations caused poor correlation of runoff volumes. Significant errors arose from using discrete elements to represent a continuum and from inaccurate parameter values. The former was estimated to be on the order of 1.5% due to the coarseness of the finite element representation. The latter, parameter errors, caused from 7 to 73% rms error in predicting the recorded hydrograph discharges. All parameters were assumed to be constant over the watershed.

Taylor and Huyakorn (1978) compared finite element based solution schemes for overland flow. The mathematical model they used was the kinematic wave equation for direct runoff from an impervious plane surface. Previous researchers encountered instability and excessively small time steps in the solution with time when solving the

equations with all terms except the partial derivative in time on the right hand side. The advent of unsymmetric matrix solvers has eliminated the need to cast the equations to be solved in such a manner. Several schemes were calculated. The implicit Newton-Raphson scheme resulted in quick and unconditional convergence, though it required significantly more work in preparing matrices for the solution. The implicit Newton-Raphson method is more efficient than both the consistent and lumped mass matrix explicit iteration schemes. Of the two explicit schemes, the lumped mass matrix method was most efficient in terms of computer time since it resulted in an uncoupled system of equations. The solution schemes were also tested on a two-plane cascade of slopes 0.04 and 0.01. The Newton-Raphson was again superior in time of computation.

Morris, Blyth, and Clarke (1980) described the finite element application to the headwaters of the Wye and Severn rivers on the slopes of Plynlimon in Central Wales. The Plynlimon study was motivated by the desire to quantify the effect of landuse changes to hydrologic processes. For the objectives of the study, the infiltration process was modeled along with overland and channel flow.

The watershed was divided into elements of equal slope representing both overland and channel flow. These elements were solved separately. Within each element, soil properties were averaged due to variations but due to the variations were not subdivided . The assumption was that

if slope, soil type, and vegetation were used as the criteria of watershed subdivision, the number of elements would become too large--presumably too large to handle efficiently.

The finite element method was applied to the St. Venant equations for shallow water on a plane surface (one dimensional) using the kinematic wave assumption. The rainfall excess was modeled for the soil types using Richard's equation for infiltration and throughflow. The paper was merely a suggested methodology and not an actual application. Their suggested improvement for modeling the Plynlimon catchment was that the more sophisticated Richard infiltration equation would lead to better results than had been achieved by others using the Darcian flow analogy (cf. Jayawardena, 1976).

As evidenced by the foregoing review of the finite element solution of watershed models, the application has been limited by several difficulties. Though the finite element method is a promising technique it has been plagued by problems such as kinematic shock and voluminous input data. To accurately represent the variation of slope, soils, and rainfall depth in a watershed, a more efficient means of subdividing the watershed into discrete elements is needed. Another implicit limitation of past research has been the use of one-dimensional elements to represent a two-dimensional continuum. This limitation has increased the difficulty in accurately modeling a continuous two-

dimensional domain such as a watershed.

D. Geographic Information Systems

Geographic Information Systems (GISs) have become highly sophisticated database management systems for spatially distributed attributes. In the area of natural resources, these spatially distributed attribute values may include such things as soils and soil properties, landuse and cover, rainfall, runoff, infiltration, agricultural pollutants, and crop yields.

Many computer software products are available that provide varied analysis techniques. Spatially distributed databases used in analyses ensure that the integrated resource base is accurately portrayed in the final result. Techniques such as environmental and hydrologic models and GISs are indispensable to proper landuse and natural resource planning.

GISs encompass a broad area of research. The scope of this dissertation and this review of literature and theory is directed towards the application of such systems to modeling environmental and hydrologic processes.

Analytic uses of spatially integrated databases for data analysis and input to environmental and hydrologic models are being developed. As models and GISs are linked, their usefulness increases.

Bartholic and Kittleson (1985) observed the spatially distributed effects of vegetation on temperature and

reflectance, as well as heat and vapor fluxes. Using spatially distributed databases the change in the environment due to landuse changes was detected. Landuse changes have been found to increase surface temperatures by as much as 10 to 15 degrees Celsius.

These temperature changes have an impact on the net radiation balance and consequently the quantity of evapotranspiration. Such profound changes greatly affect watershed hydrology. Changes are easily observed using a GIS coupled with remote sensing techniques. To quantify these changes, a suitable, spatially distributed watershed model is needed.

Mathematic modeling of a physical process is enhanced when spatially distributed data are processed by a GIS. The uses of a data value can be generalized into six categories (Zobrist, 1976):

1. Physical Analog: The pixel value represents a physical variable such as elevation, rainfall, smog, density, etc.

2. District Identification: The pixel value is a numerical identifier for the district and includes that pixel area.

3. Class Identification: The pixel value is a numerical identifier for the landuse, landcover, or other area-classification schemes.

4. Tabular Pointer: The pixel value is a record pointer to a tabular record which applies to the pixel geographic area.

5. Point Identification: The pixel value identifies a point, or the nearest of a set of lines, or the distance to the nearest set of points.

6. Line Identification: The pixel value identifies a point, or the nearest of a set of lines, or the

III. METHODOLOGY

A. Research Objective and Approach

The goal of this research has been achieved by accomplishing the following three objectives and appropriate approaches.

Objective 1. Define hydrologic response areas that exhibit similar soil infiltration parameters, surface roughness, and slope for a given watershed.

Approach: A geographical information system was used to search, smooth and aggregate areas of similar soil infiltration parameters, surface roughness, and slope, thus producing the specific hydrologic response areas.

Objective 2. Apply the finite element method to the specific hydrologic response areas to compute and route the overland flow to the outlet.

Approach: The rate and volume of infiltration was modeled by the Green and Ampt infiltration equation. The equation parameters were calibrated for the watershed using an arbitrary finite element grid. The rainfall excess thus defined becomes the lateral inflow for use in solution of the overland flow equations.

Objective 3. Compare the accuracy of the outflow hydrographs to the actual outflow hydrograph for a given

distance to the nearest of a set of lines.

These categories pertain primarily to grid-based systems that analyze geographic information by cells or pixels. Such rectilinear image elements combine to provide the full image called a raster. Another class of GISs are polygon based. This class of GIS analyzes directly the polygons that delineate the geographic element. No conversion between the input data to a grid-based system is needed.

Band (1986) described a method of partioning a watershed into areas bounded by drainage divides and stream channels using a GIS. He used a digital elevation model formed from a raster of grid cells. The grid cell attributes are the elevations. By sequentially examining each grid cell in a three-by-three cell window, the grid cell is classified as a linking a stream channel or drainage divide. Band's technique provides an automated method of identifying not only the drainage divides and stream channels but also the drainage areas associated with them. The map of these drainage areas is useful in distributed hydrologic models.

The Phase I, Oconee River Basin Flood Plain Information Scope Study, Savannah District Corps of Engineers (1973) presents a comprehensive study in which a GIS serves as a database manager for the hydrologic model input parameters. The hydrologic model used was the Army Corps of Engineers HEC-1 to calculate and route the hydrograph downstream. The rainfall excess and unit

hydrographs are calculated using the USDA-SCS rainfall-runoff method. By forming landuse, hydrologic soil group, subbasin boundary, surface slope, and the SCS runoff curve number grid representations, the effect on the downstream hydrograph of landuse changes at specified locations were investigated.

Grayman (1975) presented the results of an environmental management computer system applied to water quality planning for the James River Basin, Virginia. The system called ADAPT (Areal Design and Planning Tool) modeled not only wastewater treatment discharges but also the water-borne wastes from land development and nonpoint source pollution. Such a tool is capable of modeling the large-scale development effects within a developing river basin. The spatial data was represented by triangular subareas. The mathematical model was solved for each subarea and the result routed downstream to receiving subareas.

The spatial data management and the mathematical modeling linked together formed a system capable of providing the least-cost alternatives for wastewater treatment plants that met water quality goals. These goals were established by the U.S. Environmental Protection Agency. The conclusions from the study were as follows:

1. The cost of technically feasible systems was insensitive to system layout or location.
2. The economies of regionalized, large treatment plants were limited by escalating costs for

transport of the wastes through undeveloped areas.

These conclusions seem to contradict each other but illustrate the decisions that can be reached with the aid of a model, such as ADAPT, linked to a GIS.

Gupta and Solomon (1977) described an information system for use with a distributed parameter hydrologic model. Their main argument is that distributed parameter models provide insight into the hydrologic process in a river basin. However, one limitation is the large amount of input data required by such models. The information system used to store and manipulate the spatial data is the means for avoiding this difficulty. The spatial data set becomes the input data for modeling hydrologic processes.

E. Synoptic Evaluation of Current Theories

The difficulties encountered in applying a deterministic, distributed parameter model to watershed hydrology fall into three categories.

1. Numeric errors--those that arise from the method itself such as inaccuracies and instability in the time solution of the finite element method.

2. Model equation errors--which arise from the simplification of the full dynamic equation by the kinematic or diffusion analogy and kinematic shocks.

3. Parameter estimation errors--arising from uncertainty and from spatial variation of infiltration, rainfall, roughness and other parameters over the watershed domain. These errors may result from

a. the assumption that infiltration, rainfall, roughness and other parameters are uniform over the entire watershed.

b. the use of elements that do not maintain faithful representation of the hydrologically homogeneous character of subareas within the watershed.

c. an incomplete knowledge of the parameters and the variation over the watershed or with time during the modeling process. Rainfall excess was found to be the most significant error-producing parameter.

These difficulties must be overcome in order to accurately model the hydrologic response areas within a particular watershed during an unsteady rainstorm. The first two difficulties relate to the mathematical model, the third relates to the spatial data management. The finite element method holds promise as a mathematical model capable of accurately and efficiently solving the distributed, deterministic surface water equations in a watershed. The Geographic Information System holds promise as an efficient means of handling the large volume of input data required by distributed, deterministic models.

III. METHODOLOGY

A. Research Objective and Approach

The goal of this research has been achieved by accomplishing the following three objectives and appropriate approaches.

Objective 1. Define hydrologic response areas that exhibit similar soil infiltration parameters, surface roughness, and slope for a given watershed.

Approach: A Geographic information system was used to search, smooth and aggregate areas of similar soil infiltration parameters, surface roughness, and slope, thus producing the specific hydrologic response areas.

Objective 2. Apply the finite element method to the specific hydrologic response areas to compute and route the overland flow to the outlet.

Approach: The rate and volume of infiltration was modeled by the Green and Ampt infiltration equation. The equation parameters were calibrated for the watershed using an arbitrary finite element grid. The rainfall excess thus defined becomes the lateral inflow for use in solution of the overland flow equations.

Objective 3. Compare the accuracy of the outflow hydrographs to the actual outflow hydrograph for a given

rainstorm event for the following two cases.

a. A finite element grid that is of an arbitrary spatial form.

b. A finite element grid formed from hydrologic response areas defined by the Geographic Information System.

Approach: The rate and volume of runoff was modeled by the finite difference/finite element method of solving the kinematic wave equation for overland flow. The excess rainfall was defined by the infiltration equation. The outflow hydrograph was calculated for the outlet of the watershed for the two cases described above. A finite element model, which is capable of computing the overland flow equations for geometric elements and routing the flow to the outlet, was used to perform this modeling. The validity of the method was checked by comparing the computed and actual outflow hydrographs.

The modeled watershed is the USDA-ARS research watershed number 4H, located near Hastings, Nebraska. This watershed was selected because it has been modeled using a finite element model together with the Green-Ampt equation for an unsteady rainfall, July 4, 1959 (Peters, Blandford, and Meadows, 1983). The Geographic Information System was used as described above to better characterize the spatially distributed input parameters. The finite element

modeling was done first for a set of one-dimensional, linear elements of arbitrary spatial form. The present research will demonstrate that the proposed methodology more accurately predicts the outflow hydrograph when hydrologic response areas of uniform spatial parameters are modeled with the finite element method. If it does, then it will be concluded that the method developed through this research predicts more accurately than previous methods the actual outflow hydrograph from a watershed of nonuniform, spatially distributed parameters such as infiltration parameters, surface roughness and slope.

B. Theoretical Development

The basic equations to be solved fall into the general class called the shallow water equations. These are the continuity of mass and the conservation of momentum. They are derived using the assumption of shallow water theory, that the pressure varies hydrostatically in the vertical direction, or

$$P = \rho g(h-z), \quad z > 0 \qquad [23]$$

where

z = the vertical coordinate,

h = the water depth,

ρ = fluid density,

g = gravitational acceleration.

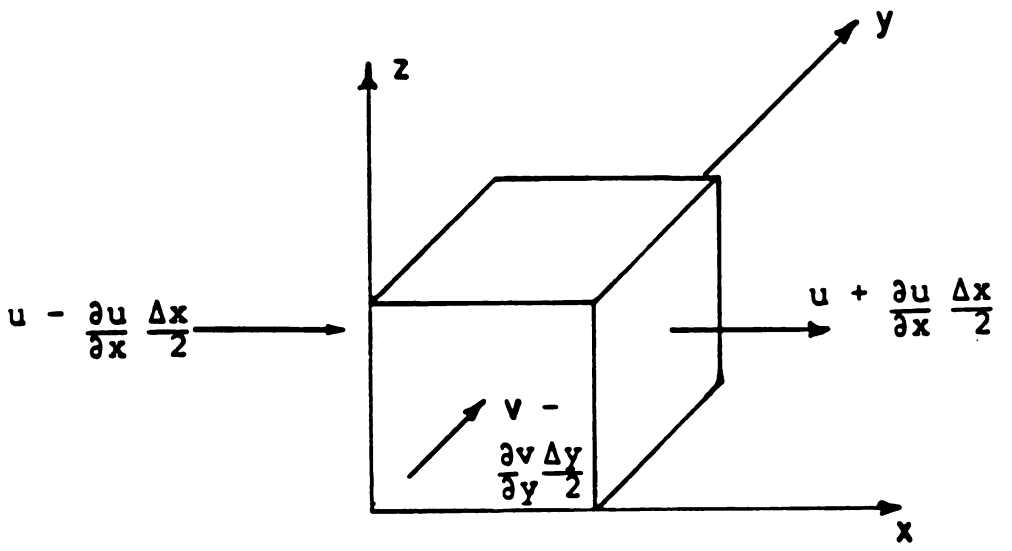

Figure 2 Coordinate System Definition

The coordinate system is defined as follows:

x = horizontal direction of primary flow, parallel to the bottom of the flow surface.

y = horizontal direction perpendicular to primary flow, parallel to bottom of the flow surface.

z = vertical direction.

The time averaged local flow velocities in the elemental volume are:

$u \pm \frac{\partial u}{\partial x} \frac{\Delta x}{2}$ = velocity in x-direction on up- and downstream face.

$v \pm \frac{\partial v}{\partial y} \frac{\Delta y}{2}$ = velocity in y-direction on up- and downstream face.

The hydrostatic equation is the basic assumption of the first-order shallow water theory and is prevalent in engineering applications (Liggett, 1975). The hydrostatic equation implies that the flow lines possess no curvature. Other assumptions implied or not listed include:

1. There is no Coriollis acceleration.
2. Streamlines are not curved such that the pressure variation with depth is linear.
3. Turbulent velocities are time-averaged.

Turbulent fluctuation velocities are not considered since on time average the net effect is present as represented in the conservation of mass and momentum equations by the Reynolds stress $\overline{u'v'}$ (Potter and Foss, 1982).

In the one-dimensional case, velocities are depth-averaged, thus suppressing the vertical dimension in the conservation equations. U is the primary flow velocity and

is a function of x and t. The x- direction is such that $\cos\theta \approx 1$. The control volume and vector convention in Figure 3, is used in the Reynolds Transport equations.

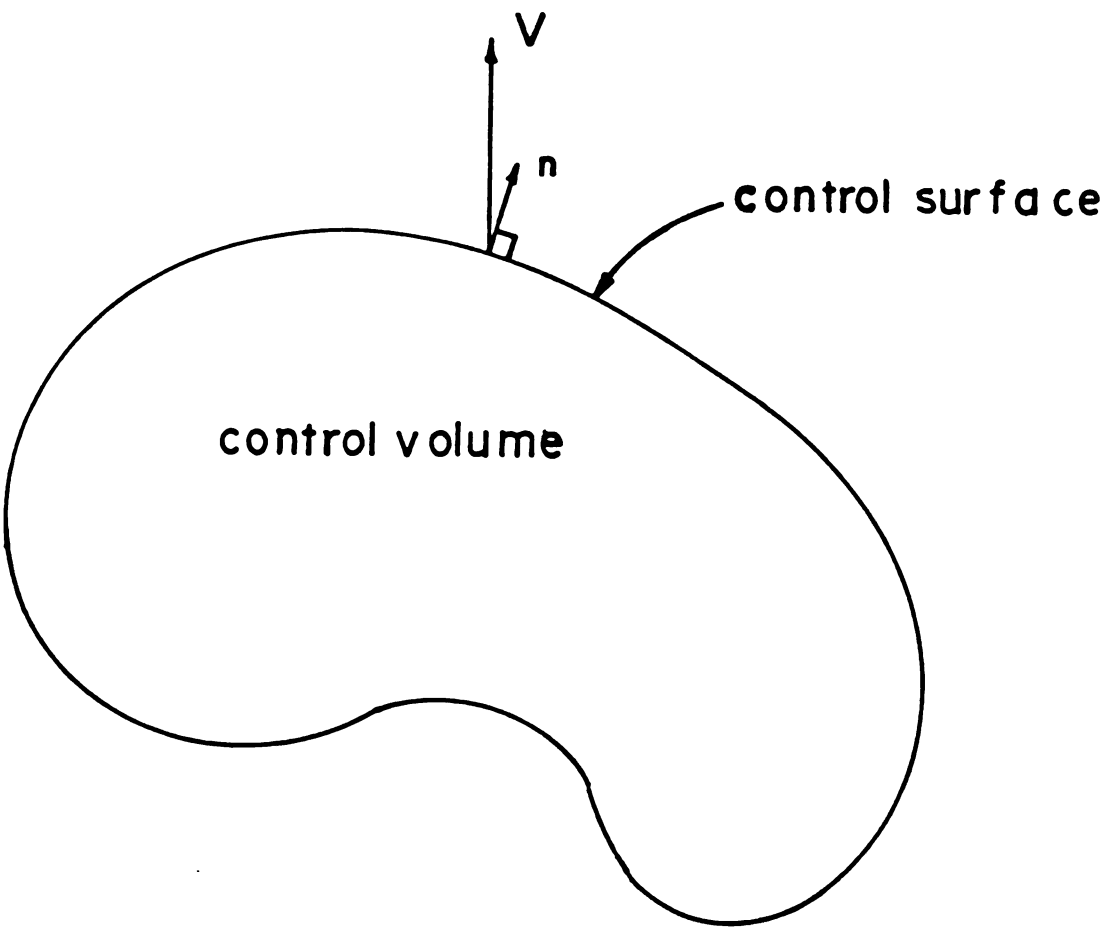

Figure 3 Control Volume Definition

The Reynolds Transport theorem provides a method of describing, among other thermodynamic quantities, the transport of mass and momentum into and out of a control volume (Potter and Foss, 1982).

1. Conservation of Mass

The Reynolds Transport equation for conservation of mass requires that

$$\frac{\partial}{\partial t}\int_{cv} d\Lambda + \int_{cs} (V\cdot\hat{n})dA = 0 \qquad [24]$$

where

V = velocity vector,

$d\Lambda$ = differential element of control volume, cv,

$V\cdot\hat{n}$ = dot product of the velocity vector to the normal unit vector of the control surface,

dA = differential element of the control surface, cs.

The mass balance for a differential volume of height h(x,t) is

$$\left(u - \frac{\partial u}{\partial x}\frac{\Delta x}{2}\right)\left(h - \frac{\partial h}{\partial x}\frac{\Delta x}{2}\right)$$

$$- \left(u + \frac{\partial u}{\partial x}\frac{\Delta x}{2}\right)\left(h + \frac{\partial h}{\partial x}\frac{\Delta x}{2}\right) = \frac{\partial h}{\partial t}\Delta x \qquad [25]$$

Expanding, summing like terms, and disregarding higher order terms such as

$$\frac{\partial u}{\partial x}\frac{\partial h}{\partial x}$$

yields the discrete form

$$-\frac{\partial h}{\partial x}\Delta x - h\frac{\partial u}{\partial x}\Delta x = \frac{\partial h}{\partial t}\Delta x \quad , \qquad [26]$$

which is useful in finite difference computational methods.

The differential form of the conservation of mass equation is

$$\frac{\partial h}{\partial t} + \frac{\partial (uh)}{\partial x} = 0 \qquad [27]$$

for one dimensional, depth-averaged, time-averaged, flow.

2. Conservation of Momentum

The conservation of momentum equation is derived in a similar manner to the conservation of mass. The Reynolds Transport equation for momentum requires that

$$\frac{\partial}{\partial t} \int_{cv} (\rho V) \, d\Lambda + \int_{cs} (\rho V)(V \cdot \hat{n}) dA = \Sigma F \qquad [28]$$

where

V = velocity vector,

$d\Lambda$ = control volume,

ρ = mass density of water,

$V \cdot \hat{n}$ = dot product of the velocity vector to the normal unit vector of the control surface,

ΣF = summation of forces acting on control volume.

Substitution of the velocity components for the depth-averaged elemental control volume results in

$$\frac{\partial (\rho U h) \Delta x}{\partial t} - \left[U(uh) - \frac{\partial (U(uh))}{\partial x} \frac{\Delta x}{2} \right] + \left[U(uh) + \frac{\partial (U(uh))}{\partial x} \frac{\Delta x}{2} \right] = \Sigma F_x \qquad [29]$$

Upper case variables are vectors and lower case variables

are scalar values. The term ΣF_x is the vector summation of forces in the x-direction. These forces are

1. Gravitational, $F_g = \rho g h \Delta x \sin\theta_x = \rho g h S_x \Delta x$ where θ_x = angle between the horizontal axis and the x-axis. $\sin\theta_x = \tan\theta_x$ for small slope; $S_x = \tan\theta_x = \sin\theta$.

2. Pressure, $F_p = \int_0^h \rho dz = \rho g \int_0^h (h-z)dz = \rho g h^2/2$

3. Frictional resistance, $F_s = \rho h g S_f \Delta x$ where S_f is the frictional slope defined by either of Manning equations,

$$u = \frac{1.486}{n} R^{2/3} S_f 1/2 \quad \text{(english units)}, \qquad [30]$$

$$u = \frac{1}{n} R^{2/3} S_f 1/2 \quad \text{(SI units)}, \qquad [31]$$

or the Chezy equation,

$$u = C(RS_f)^{1/2} \quad \text{(SI or english units)}. \qquad [32]$$

Combining these equations using the Manning equation results in

$$\rho\left(U(uh) - \frac{\partial U(uh)\Delta x}{\partial x}\frac{}{2}\right) - \rho\left(U(uh) + \frac{\partial U(uh)\Delta x}{\partial x}\frac{}{2}\right)$$

$$+ \rho g h S_x \Delta x + 1/2 \rho g\left(h^2 - \frac{\partial (h^2)\Delta x}{\partial x}\frac{}{2} - \left(h^2 + \frac{\partial (h^2)\Delta x}{\partial x}\frac{}{2}\right)\right)$$

$$+ \rho g h S_f \Delta x = \frac{\partial (\rho U h)\Delta x}{\partial t} \qquad [33]$$

Rearranging and disregarding higher order terms and taking the limit $\Delta x \to 0$ yields

$$h\frac{\partial U}{\partial t} + U\frac{\partial h}{\partial t} + U\frac{\partial (uh)}{\partial x} + uh\frac{\partial U}{\partial x} + gh\frac{\partial h}{\partial x} = gh(S_x - S_f) \qquad [34]$$

By substitution of the differential form of the conservation of mass,

$$\frac{\partial h}{\partial t} + \frac{\partial (uh)}{\partial x} = 0 \qquad [27]$$

into the above equation [34] the conservative form of the one-dimensional, depth-averaged, time-averaged, conservation of momentum equation is obtained

$$\frac{\partial U}{\partial t} + U\frac{\partial u}{\partial x} + g\frac{\partial h}{\partial x} = g(S_x - S_f) \qquad [35]$$

The two-dimensional case is derived similarly except that momentum in the x-direction may now be transported into and out of the differential control volume on both the x- and y-faces. The general form of the Reynolds Transport equation in the case of conservation of mass is

$$\frac{\partial}{\partial t}\int_{cv} d\Lambda + \int_{cs} (V \cdot \hat{n}) dA = 0 \qquad [24]$$

where

V = velocity vector,

$d\Lambda$ = differential element of control volume, cv,

$V \cdot \hat{n}$ = dot product of the velocity vector to the normal unit vector of the control surface,

dA = differential element of the control surface, cs.

Substitution of the values for the two dimensional control

volume results in

$$\frac{\partial(\rho h)}{\partial t} - \left(Uh - \frac{\partial(uh)}{\partial x}\frac{\Delta x}{2}\right) + \left(Uh + \frac{\partial(uh)}{\partial x}\frac{\Delta x}{2}\right)$$

$$- \left(Vh - \frac{\partial(vh)}{\partial y}\frac{\Delta y}{2}\right) + \left(Vh + \frac{\partial(vh)}{\partial y}\frac{\Delta y}{2}\right) = 0 \qquad [36]$$

Combining terms yields

$$\frac{\partial h}{\partial t} + \frac{\partial(uh)}{\partial x} + \frac{\partial(vh)}{\partial y} = 0 \qquad [37]$$

The Reynolds transport equation applied to the conservation of momentum yields

$$\frac{\partial}{\partial t}\int_{cv}(\rho V)\, d\Lambda + \int_{cs}(\rho V)(V\cdot\hat{n})dA = \Sigma F \qquad [28]$$

where

V = velocity vector,

$d\Lambda$ = control volume,

ρ = mass density of water,

$V\cdot\hat{n}$ = dot product of the velocity vector to the normal unit vector of the control surface,

ΣF = summation of forces acting on control volume.

Substitution of the velocity components for the depth-averaged elemental control volume produces

$$\frac{\partial(Vh)}{\partial t} - \left(V - \frac{\partial v}{\partial y}\frac{\Delta y}{2}\right)(uh) + \left(V + \frac{\partial v}{\partial y}\frac{\Delta y}{2}\right)(uh)$$

$$- \left(U(uh) - \frac{\partial(U(uh))}{\partial x}\frac{\Delta x}{2}\right) + \left(U(uh) + \frac{\partial(U(uh))}{\partial x}\frac{\Delta x}{2}\right) \qquad [38]$$

Simplifying, the x-momentum equation results in

$$\frac{\partial(uh)}{\partial t} + \frac{\partial(u^2h)}{\partial x} + \frac{\partial(uvh)}{\partial y} + \frac{g\partial(h^2)}{2\partial x} = gh(S_x - S_f) \quad [39]$$

and the y-momentum equation becomes

$$\frac{\partial(vh)}{\partial t} + \frac{\partial(uvh)}{\partial x} + \frac{\partial(v^2h)}{\partial y} + \frac{g\partial(h^2)}{2\partial y} = gh(S_y - S_f) \quad [40]$$

Incorporating the continuity equation,

$$\frac{\partial u}{\partial x} + \frac{\partial v}{\partial y} = 0 \quad , \quad [41]$$

yields the x-momentum conservative form:

$$\frac{\partial u}{\partial t} + u\frac{\partial u}{\partial x} + v\frac{\partial u}{\partial y} + g\frac{\partial h}{\partial x} = g(S_x - S_{fx}) \quad . \quad [42]$$

The y-momentum conservative form is derived similarly as

$$\frac{\partial v}{\partial t} + u\frac{\partial v}{\partial x} + v\frac{\partial v}{\partial y} + g\frac{\partial h}{\partial y} = g(S_y - S_{fy}) \quad . \quad [43]$$

Assumptions implied in the above derivation include.

1. The above derivations do not include lateral inflow or other inflow/outflows such as rainfall or infiltration.

2. The channel is prismatic and of a rectangular cross-section.

3. Irregular Cross-section

In deriving the above conservation of mass and momentum equations, the cross-section of the channel was assumed to be rectangular. However, in the application to

natural channels, a more general form is needed in which the depth h is assumed to vary across the y-direction. The irregular cross-section is shown in Figure 4.

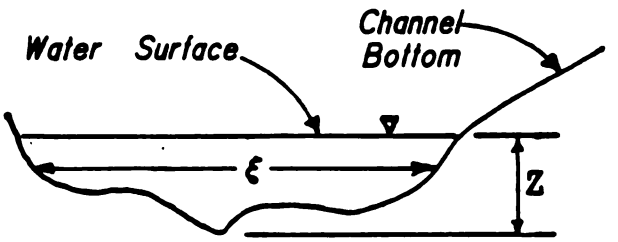

Figure 4 Irregular Cross-section of a Channel.

In the derivation of the conservation of mass and momentum the depth h times the unit or differential width of the control volume was used as the dA in the Reynolds Transport equation. The Reynolds Transport equation for conservation of mass requires that

$$\frac{\partial}{\partial t}\int_{cv}\partial\Lambda + \int_{cs}(V\cdot\hat{n})dA = 0 \qquad [24]$$

where

V = velocity vector,

dx = differential element of control volume cv,

$V\cdot\hat{n}$ = dot product of the velocity vector to the normal unit vector of the control surface,

dA = differential element of the control surface cs.

If instead of the depth h times the unit or differential width in the y-direction, the area A, which is a function of f(y,z), is replaced, we obtain

$$\frac{\partial A}{\partial t} + \frac{\partial (UA)}{\partial x} = 0 \qquad [44]$$

and

$$\frac{\partial (UA)}{\partial t} + \frac{\partial (U^2)}{\partial x} + F_p = gA(S_x - S_f) \qquad [45]$$

The pressure term F_p is the force on the face of the control volume

$$F_p = \int_0^h g(h-z)\xi(z)dz \qquad [46]$$

in which $\xi(z)$ is the channel width at the height z above the bottom of the channel. The net force in the downstream direction is

$$F_p - (F_p + \frac{\partial F_p}{\partial x}\Delta x) = -\frac{\partial}{\partial x} \int_0^h \rho g(h - z)\ \xi(z)dz \quad \Delta x \qquad [47]$$

By simplifying the right of [47] using the Leibnitz rule we have,

$$-\frac{\partial}{\partial x} \int_0^h \rho g(h - z)\ \xi(z)dz =$$

$$-\rho g \int_0^h \frac{\partial}{\partial x} [\ (h - z)\xi(z)]dz$$

$$= -\rho g[\frac{\partial h}{\partial x} \int_0^h \xi(z)dz + \int_0^h (h - z)\ \frac{\partial \xi(z)}{\partial x}\ dz]$$

The first integral on the right defines the cross-sectional area. The second term $\partial\xi(z)/\partial x$ is assumed to be zero, which is the prismatic channel assumption. If the channel narrows or widens, then an additional force is exerted on the channel walls. Therefore, the pressure term in the conservation of momentum equation is interpreted as

$$F_p = gA \frac{\partial h}{\partial x} \qquad [48]$$

and the conservation of momentum equation

$$\frac{\partial(UA)}{\partial t} + \frac{\partial(U^2)}{\partial x} + F_p = gA(S_x - S_f) \qquad [49]$$

becomes

$$\frac{\partial(UA)}{\partial t} + \frac{\partial(U^2)}{\partial x} + gA \frac{\partial h}{\partial x} = gA(S_x - S_f) \qquad [50]$$

Using this conservation of mass equation for an irregular cross-section [50] the conservation of momentum equation becomes

$$\frac{\partial U}{\partial t} + U\frac{\partial u}{\partial x} + g\frac{\partial h}{\partial x} = g(S_x - S_f) \ , \qquad [51]$$

which is the same as the conservation of momentum for one dimension. It was assumed that the channel width variation is negligible so that $\partial\xi(z)/\partial x$ is zero.

4. Lateral Inflow

Lateral inflow must be incorporated into the conservation equations, if for example, distributed inflow

from groundwater, infiltration, tributary inflow, rainfall, or overland flow occurs. In this derivation inflow is regarded as positive and outflow as negative. Let the symbol q represent lateral inflow/outflow with dimensions of $[L^3]/[TL^2]$ when used in the one-dimensional equations or $[L^3]/[TL]$ when used in the two-dimensional equations. The conservation of mass equation incorporating lateral inflow would be

$$\frac{\partial h}{\partial t} + \frac{\partial (Uh)}{\partial x} = q \qquad [52]$$

for the one-dimensional case and similarly for the two-dimensional case for rectangular or irregular channel cross-sections.

The conservation of momentum equation must account for the momentum entering and leaving the control volume transported by the lateral inflow or outflow. The additional momentum entering is $\rho g u_q \Delta x$ where u_q is the downstream component of velocity of the lateral inflow. Upon leaving the control volume the velocity of the lateral inflow is assumed to have the same velocity as the downstream velocity of the fluid, so that the momentum of the lateral inflow leaving is $\rho q U \Delta x$:

$$h\frac{\partial U}{\partial t} + U\frac{\partial h}{\partial t} + U\frac{\partial (uh)}{\partial x} + uh\frac{\partial u}{\partial x} + gh\frac{\partial h}{\partial x} =$$

$$gh(S_x - S_f) + q(u_q - U) \qquad [53]$$

for the two dimensional conservation of momentum

equation and

$$\frac{\partial(UA)}{\partial t} + \frac{\partial(U^2)}{\partial x} + gA\frac{\partial h}{\partial x} = gA(S_x - S_f) + q(u_q - U) \qquad [54]$$

for the two dimensional conservation of momentum equation for irregular cross-section.

C. Finite Element Model Formulation

The form of the partial differential equations governing direct runoff have been derived by use of the Reynolds Transport theorem. These partial differential equations are used in the finite element method, Galerkin formulation of the surface water equations.

The equation of continuity for an incompressible fluid is written as

$$\frac{\partial u}{\partial x} + \frac{\partial v}{\partial y} + \frac{\partial w}{\partial z} = 0 \qquad [55]$$

where

u = u(x,y,z,t), velocity in the x-direction,

v = v(x,y,z,t), velocity in the y-direction,

w = w(x,y,z,t), velocity in the z-direction.

On integration in the z-direction and using appropriate boundary conditions, we obtain:

$$\frac{\partial h}{\partial t} + \frac{\partial(\bar{u}h)}{\partial x} + \frac{\partial(\bar{v}h)}{\partial y} = r - i \qquad [56]$$

where

$\bar{u},\bar{v}$ = depth-averaged velocities,

h = vertical depth of flow,

r,i = rainfall intensity and infiltration rate respectively.

The equation of momentum, the Navier-Stokes equation for two-dimensional flow with appropriate boundary conditions, is

$$\frac{\partial \bar{u}}{\partial t} + u\frac{\partial \bar{u}}{\partial x} + v\frac{\partial \bar{u}}{\partial y} + g\frac{\partial h}{\partial x} = g(S_{ox} - S_{fx}) - \frac{\bar{u}}{h}(r-i) \quad [57]$$

and

$$\frac{\partial \bar{v}}{\partial t} + u\frac{\partial \bar{v}}{\partial x} + v\frac{\partial \bar{v}}{\partial y} + g\frac{\partial h}{\partial y} = g(S_{oy} - S_{fy}) - \frac{\bar{v}}{h}(r-i) \quad [58]$$

where S_{ox} and S_{oy} are the slopes of the element in the x- and y-direction respectively. S_{fx} and S_{fy} are the frictional slopes in the x- and y-direction respectively (Taylor, 1974).

The continuity and momentum equations form the governing equations for watershed surface hydrology. Woolhiser and Liggett (1967) and other researchers have documented the adequacy of using the kinematic wave simplifying assumption, where all terms on the left-hand side of the momentum equation are assumed negligible. The general form then becomes

$$V = m\, h^{\alpha} \quad [59]$$

where m and α are constants such as in the Chezy or the Manning equation, and v is velocity in the direction of flow.

If the above assumption is made, then only the continuity and kinematic wave formulas need to be solved over each element. This in effect reduces a nonlinear set of simultaneous, partial differential equations to a linear set. The validity of this simplifying assumption is considered only if

$$\frac{LS_o}{F_o^2 h_o} > 10 \qquad [60]$$

where L is the length of domain and F_o and h_o are the Froude number and depth of flow at the downstream location end under steady-state conditions. This restriction is dependent on the finite element grid and hydraulic parameters used to describe the watershed.

The finite element formulation is applied by writing approximating functions of the form

$$\phi_e = \sum_{i=1}^{n} N_i(x,y)\Phi_i \qquad [61]$$

where Φ_i are known values of the function ϕ at each of the n nodal points. $N_i(x,y)$ is a shape function, which approximates the function ϕ_e based on the n nodal values (Segerlind, 1984).

The watershed surface flow variables are approximated as follows:

$$u_e = \sum_{i=1}^{n} N_i(x,y)\bar{u}_i \qquad [62]$$

$$v_e = \sum_{i=1}^{n} N_i(x,y)\bar{v}_i \qquad [63]$$

$$h_e = \sum_{i=1}^{n} N_i(x,y)h_i \qquad [64]$$

where u_e, v_e and h_e are the approximate values of the velocities in the x- and y-directions, and the depth, respectively, within the finite element domain.

The assembly of the elemental equations into a global matrix form for the entire domain or watershed constitutes the system of equations that models overland flow runoff. Iterative solution procedures are required (such as the Newton-Raphson technique) to obtain the solution of these equations in the time domain.

1. Element Equations

The application of the Galerkin method to the kinematic equation for overland flow is performed as follows: The convention of {} representing a vector quantity and [] representing a matrix quantity will be used.

For two dimensions:

$$\int\int [N]^T \left(\frac{\partial h}{\partial t} + \frac{\partial (\bar{u}h)}{\partial x} + \frac{\partial (\bar{v}h)}{\partial y} - (r - i) \right) dxdy = 0 \quad [65]$$

For one dimension:

$$\int [N]^T \left(\frac{\partial h}{\partial t} + \frac{\partial (\bar{u}h)}{\partial x} - (r - i) \right) dx = 0 \quad [66]$$

Applying the kinematic wave assumption, the momentum equation is reduced to

$$S_o = S_f \quad [67]$$

Utilizing the Manning equation that relates the depth of flow to discharge for turbulent flow, we have

$$Q_x = \frac{1.49}{n} R^{2/3} S^{1/2} A \quad [68]$$

For a wide channel or overland flow, the hydraulic radius is $R = A/P \simeq A$, so that the discharge relation becomes

$$Q = \frac{1.49}{n} A^{5/3} S^{1/2} \quad [69]$$

Recognizing that the cross-sectional area A is, in the case of overland flow, equivalent to the flow depth defined above as h, the wide channel assumption of R = h, and the vector Q in [69] is resolved into its respective directional components in the x and y direction, with θ as the angle with the x-axis results in

$$\bar{u}h = Q_x = Q \cos\theta \quad [70]$$

$$- \int [N]^T \, dx\{r-i\} \qquad [72]$$

and for two-dimensions,

$$\{R\}^{(e)} = \int [N]^T[N]\{\dot{A}\}dx + \int[N]^T[\partial N_i/\partial x \quad \partial N_j/\partial x]\{Qx\} + \int[N]^T[\partial N_i/\partial y \quad \partial N_j/\partial y]\{Qy\} - \int [N]^T \, dx\{r-i\} \, . \qquad [73]$$

It should be observed that the discharge values

$$Q_{\beta x} = \frac{1.486}{n_\beta} R^{2/3} S_\beta^{1/2} A_\beta \qquad [74]$$

and

$$Q_{\beta y} = \frac{1.486}{n_\beta} R^{2/3} S_\beta^{1/2} A_\beta \qquad [75]$$

are the β nodal values. The concept of the nodal discharge values based on nodal values of slope in the x- and y-directions and the nodal values of roughness n_β is of paramount importance if the effects of kinematic shocks are to be avoided between elements where abrupt changes in slope or roughness would otherwise occur. By causing the nodal values of discharge to be computed with nodal values of slope and roughness, a linear variation over the element of these values effects a linear variation in Q without abrupt discontinuities at the inter-element nodes. The numeric difficulty encountered by other researchers is thus avoided (personal correspondence with D.A. Woolhiser and G.A. Blandford). This is due to the elimination of the diffusion term $\partial h/\partial x$ along with the other terms in the

over the element of these values effects a linear variation in Q without abrupt discontinuities at the inter-element nodes. The numeric difficulty encountered by other researchers is thus avoided (personal correspondence with D.A. Woolhiser and G.A. Blandford). This is due to the elimination of the diffusion term $\partial h/\partial x$ along with the other terms in the full dynamic equation because of the kinematic assumption. Because of this, there is no possibility other than a discontinuity in flow depth at the inter-element nodes. To avoid this difficulty, the values that relate h to Q--i.e., the slope and roughness--must be considered as nodal values. The value of Q is a vector quantity in the direction of nodal slope subsequently resolved into x- and y-direction components according to the orientation of the slope with the global coordinate system.

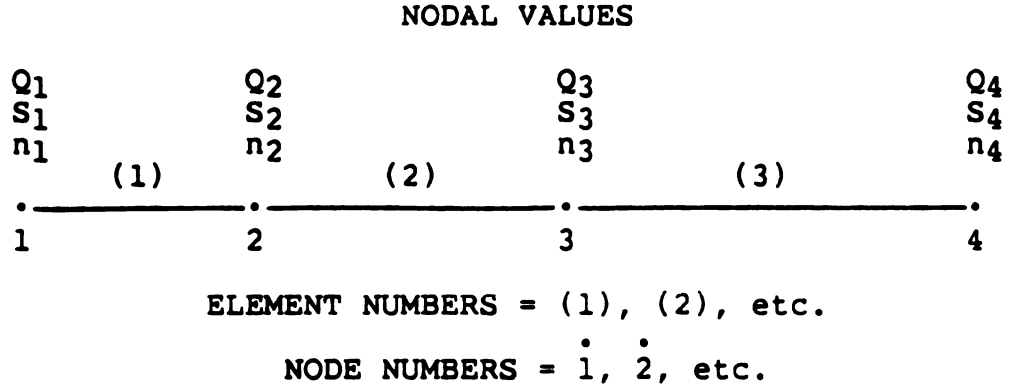

Figure 5 Element and Node Numbering Convention

The convention illustrated in Figure 5 is the nodal

representation by nodal values of the independent variables. With this methodology, the discontinuities in function values are avoided at the inter-element nodes.

2. Shape Functions

The shape functions provide the basis of writing the linear variation across the element of the approximated functions. The local coordinate system allows easier integration over an element. For this reason the following system is defined

s = x-direction with limits of $0 \leq s \leq L$

for a one-dimensional linear element of length L. The shape functions are

$$N_i = 1 - s/L \qquad [76]$$

$$N_j = s/L \qquad [77]$$

or, in matrix form

$$[N]^T = \begin{bmatrix} 1-s/L \\ s/L \end{bmatrix} \qquad [78]$$

The partial derivative is computed by taking the partial derivative of the shape functions, since the approximating function is

$$\phi(x) = N_i\Phi_i + N_j\Phi_j \qquad [79]$$

where the nodal values Φ are constants with respect to the x- or s-space dimension. The derivative is

x- or s-space dimension. The derivative is

$$\frac{\partial \phi(x)}{\partial x} = \frac{\partial N_i}{\partial x}\Phi_i + \frac{\partial N_j}{\partial x}\Phi_j \qquad [80]$$

The derivatives of the shape functions with respect to x or s--which are equivalent locally within the element--are

$$\frac{\partial N_i}{\partial x} = \frac{-1}{L} \qquad [81]$$

$$\frac{\partial N_j}{\partial x} = \frac{1}{L} \qquad [82]$$

In matrix form this is

$$[bx]^T = \begin{bmatrix} \frac{\partial N_i}{\partial x} \\ \frac{\partial N_j}{\partial x} \end{bmatrix} = \frac{1}{L}\begin{bmatrix} -1 \\ 1 \end{bmatrix} \qquad [83]$$

Writing the individual integrals from the residual

$$\{R\}^{(e)} = \int [N]^T[N]\{A\}dx + \int [N]^T[\partial N_i/\partial x \ \partial N_j/\partial x]\{Q\} - \int [N]^T dx\{r\text{-}i\} \qquad [84]$$

and integrating over the element length L we have

$$\int [N]^T[N]\{A\}dx = \int \begin{bmatrix} 1 \\ s/L \end{bmatrix}\begin{bmatrix} 1-s/L & s/L \end{bmatrix}\{\dot{A}\}\, dx$$

$$= \frac{L}{6}\begin{bmatrix} 2 & 1 \\ 1 & 2 \end{bmatrix}\{\dot{A}\}$$

$$= [C]\{\dot{A}\} \qquad [86]$$

The discharge term in the residual is

$$\int [N]^T [b]\{Q\} = \int_0^L \begin{bmatrix} 1 \\ s/L \end{bmatrix} \begin{bmatrix} -1 & 1 \\ \overline{L} & \overline{L} \end{bmatrix} \{Q\}$$

$$= \frac{1}{2} \begin{bmatrix} -1 & 1 \\ -1 & 1 \end{bmatrix} \{Q\}$$

$$= [bx]\{Q\} \qquad [87]$$

The lateral inflow term is

$$\int_0^L [N]^T \, dx(r-i) = \int_0^L \begin{bmatrix} 1 \\ s/L \end{bmatrix} dx(r-i)$$

$$= \frac{(r-i)L}{2} \begin{Bmatrix} 1 \\ 1 \end{Bmatrix} \qquad [88]$$

Assembling the results of [86], [87], and [88] into the residual expression, we have

$$\{R\}^{(e)} = \frac{L}{6} \begin{bmatrix} 2 & 1 \\ 1 & 2 \end{bmatrix} \{\dot{A}\} + \frac{1}{2} \begin{bmatrix} -1 & 1 \\ -1 & 1 \end{bmatrix} \{Q\} - \frac{(r-i)L}{2} \begin{Bmatrix} 1 \\ 1 \end{Bmatrix} \qquad [89]$$

The residual $\{R\}^{(e)}$ in [89] is minimized over the system of elements only when assembled in the global form.

3. Global Matrix

The global matrix form of the assembled elemental residuals may be formed by the direct stiffness procedure when local node numbering schemes are used. An expanded

form will also be examined, which uses a global nodal numbering system. The direct stiffness procedure results in a banded matrix as follows.

Given a three-element, four node system as shown in Figure 5, it can be seen that node 2 receives contributions from the elements (1) and (2); node 3 from elements (2) and (3); and nodes 1 and 4 from elements (1) and (4) respectively.

Assemblage by the direct stiffness procedure is as follows for elements of equal length:

$$\frac{L}{6}\begin{bmatrix} 2 & 1 & & \\ 1 & (2+2) & 1 & \\ & 1 & (2+2) & 1 \\ & & 1 & 2 \end{bmatrix}\begin{Bmatrix} \dot{A}_1 \\ \dot{A}_2 \\ \dot{A}_3 \\ \dot{A}_4 \end{Bmatrix} + \frac{1}{2}\begin{bmatrix} -1 & 1 & & \\ -1 & (1-1) & 1 & \\ & -1 & (1-1) & 1 \\ & & -1 & 1 \end{bmatrix}\begin{Bmatrix} Q_1 \\ Q_2 \\ Q_3 \\ Q_4 \end{Bmatrix} =$$

$$\frac{rL}{2}\begin{Bmatrix} 1 \\ 2 \\ 2 \\ 1 \end{Bmatrix} \qquad [90]$$

The nodal values of Q are related to A by the Chezy or Manning equations, resulting in a nonlinear set of differential equations with respect to time. Alternately, with [C], [K], and {F} as defined above in [86-88] without the (e) elemental designation we have

$$[C]\{\dot{A}\} + [bx]\{Q\} = \{F\} \qquad [91]$$

This matrix equation represents the system of equations to be solved. Note that the left-hand side contains the time derivatives of the cross-sectional area {A}. A solution in time is needed such as a finite difference scheme. Note also that the discharge values of Q contain the cross-sectional area A in the Manning equation. Therefore, at each time step, when A is solved, a new set of Q's must be computed. Depending on the time weighting coefficient, an implicit or explicit solution for A and Q results. The rL values are considered constant over each element. This results in the form of a forcing function vector on the right hand side.

The finite difference solution utilizing the form of equations [14-19] for the time dependent matrix equation [91] is

$$[C]\{A\}_{new} = [C]\{A\}_{old} - \Delta t[bx]((1-\theta)\{Q\}_{old} + \theta\{Q\}_{new}) + \Delta t((1-\theta)\{F\}_{old} + \theta\{F\}_{new}) \quad [92]$$

The time dependent finite difference form of equation [91] can be recast into the nonlinear form

$$[C]\{A\}_{new} = \{F^*\} \quad [93]$$

where $\{F^*\}$ is the combination of the right-hand-side terms in [93]. The right-hand-side contains terms such as $\{Q\}_{new}$ that are functions of the left-hand-side term $\{A\}_{new}$. This forms a set of nonlinear equations requiring special solution techniques such as a simple iteration scheme or

The iterative schemes are preferred for large systems because, unlike the Newton-Raphson Method, no matrix inverses are required. At each time step the value of the rainfall excess intensities are placed in $\{F^*\}$, the old and new values of $\{A\}$ are assumed equal. At the first time step the old values are the initial values. Then the system of equations are solved by standard methods. The new values thus solved for become the new values for the next recursion until the solution converges to within a set tolerance. This recursion is repeated at the next time step with the new values from before becoming the old values for the present time step.

4. Expanded Form

The expanded form of the global system of equations is as follows for the system of elements depicted in Figure 5. The approximating shape functions are written for each element and assembled into the expanded elemental equations:

$$\phi^{(1)} = N_1(1)\Phi_1 + N_2(1)\Phi_2 + 0\Phi_3 + 0\Phi_4$$
$$\phi^{(2)} = 0\Phi_1 + N_2(2)\Phi_2 + N_3(2)\Phi_3 + 0\Phi_4$$
$$\phi^{(3)} = 0\Phi_1 + 0\Phi_2 + N_3(3)\Phi_3 + N_3(3)\Phi_4$$

or, in matrix notation,

$$\begin{Bmatrix} \{\phi\}^{(1)} \\ \{\phi\}^{(2)} \\ \{\phi\}^{(3)} \end{Bmatrix} = \begin{bmatrix} N_1 & N_2 & 0 & 0 \\ 0 & N_2 & N_3 & 0 \\ 0 & 0 & N_3 & N_4 \end{bmatrix} \begin{Bmatrix} \Phi_1 \\ \Phi_2 \\ \Phi_3 \\ \Phi_4 \end{Bmatrix} \qquad [94]$$

It is now possible to combine the elemental equations into a single region equation (Segerlind, 1976):

$$\phi = \sum_{e=1}^{E} \phi^{(e)} \qquad [95]$$

This results in the equation

$$\phi = [N_1(1)]\Phi_1 + [N_2(1) + N_2(2)]\Phi_2 + [N_3(2) + N_3(3)]\Phi_3 + [N_3(3)]\Phi_4 \qquad [96]$$

The importance of this region equation is seen when an element region in two dimensions is formed from simpler finite elements. For example, a region as follows may form an element region,

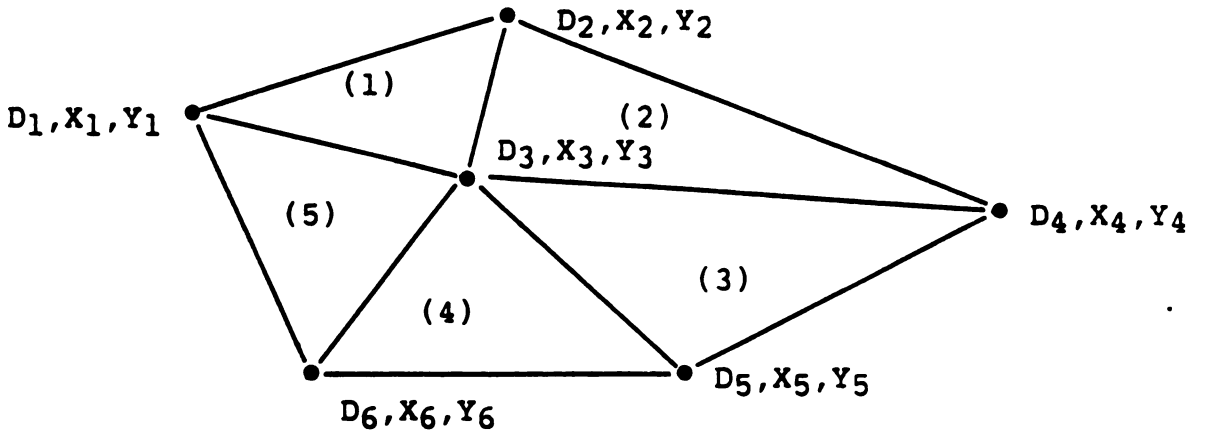

Figure 6 Five-Element Region

Writing the set of element equations, we have

$$\begin{matrix}\{\phi\}^{(1)}\\ \{\phi\}^{(2)}\\ \{\phi\}^{(3)}\\ \{\phi\}^{(4)}\\ \{\phi\}^{(5)}\end{matrix} = \begin{bmatrix} N_1 & N_2 & N_3 & 0 & 0 & 0 \\ 0 & N_2 & N_3 & N_4 & 0 & 0 \\ 0 & 0 & N_3 & N_4 & N_5 & 0 \\ 0 & 0 & N_3 & 0 & N_5 & N_6 \\ N_1 & 0 & N_3 & 0 & 0 & N_6 \end{bmatrix} \begin{Bmatrix} \Phi_1 \\ \Phi_2 \\ \Phi_3 \\ \Phi_4 \\ \Phi_5 \\ \Phi_6 \end{Bmatrix} \qquad [98]$$

This regional equation could be considered as an expanded element defined by triangular elements and area coordinate shape functions. The utility of such an approach is in the modeling of irregular patches as defined by the hydrologically homogeneous areas. By building an expanded region the irregular patch can be handled.

Substructuring removes the internal node if no nodal value is desired at that point. This is done after the global matrix is constructed. By solving the matrix for removal of a nodal value and associated constants, the resulting set reflects its contribution but is not present in the set of equations.

6. Isoparametric Elements

Another technique for representing finite element regions is one using isoparametric elements. This class of elements utilizes a coordinate transformation technique that maps the element in the global coordinate system into a natural coordinate system. The natural coordinate system for a linear, one-dimensional element is the ξ system corresponding to the global x-coordinate system. The ξ system varies from -1 to +1 with the origin at the center of the element. The element matrices such as [C], [B], and {F} are integrated numerically in the ξ coordinate system.

The coordinate transformation is written in terms of the same element shape functions as used to represent the state variables, hence, the name isoparametric. Super- and sub-parametric elements are those that use higher or lower order shape functions to perform the transformation.

The transformation is done by writing the global coordinate system in terms of the nodal coordinates and the shape functions:

$$x = N_1(\xi)X_1 + N_2(\xi)X_2 \qquad [99]$$

where

$$N_1 = 1/2(1-\xi) \quad \text{and}$$

$$N_2 = 1/2(1+\xi) \quad .$$

The change of variable in any integral is accomplished by writing

$$\int_{x_i}^{x_j} f(x)dx = \int_{-1}^{+1} g(\xi) \left(\frac{d(x(\xi))}{d\xi} \right) d\xi \quad . \qquad [100]$$

The Jacobian of the transformation is

$$\frac{d(x(\xi))}{d\xi} = -\frac{X_i}{2} + \frac{X_j}{2} = \frac{L}{2} \qquad [101]$$

Jacobian transformations are done similarly for two-dimensional elements. The four-node quadrilateral has four shape functions in ξ and η. The coordinate transformation is accomplished by writing the global coordinates in terms

of ξ and η such that,

$$x = N_1(\xi,\eta)X_1 + N_2(\xi,\eta)X_2 + N_3(\xi,\eta)X_3 + N_4(\xi,\eta)X_4 \qquad [102]$$

and

$$y = N_1(\xi,\eta)Y_1 + N_2(\xi,\eta)Y_2 + N_3(\xi,\eta)Y_3 + N_4(\xi,\eta)Y_4 \qquad [103]$$

where

$$N_1 = 1/4(1-\xi)(1-\eta) \ ,$$

$$N_2 = 1/4(1+\xi)(1-\eta) \ ,$$

$$N_3 = 1/4(1+\xi)(1+\eta) \ ,$$

$$N_4 = 1/4(1-\xi)(1+\eta) \ .$$

The Jacobian of the transformation is

$$[J] = \begin{bmatrix} \frac{\partial N}{\partial \xi^1} & \frac{\partial N}{\partial \xi^2} & \frac{\partial N}{\partial \xi^3} & \frac{\partial N}{\partial \xi^4} \\ \frac{\partial N}{\partial \eta^1} & \frac{\partial N}{\partial \eta^2} & \frac{\partial N}{\partial \eta^3} & \frac{\partial N}{\partial \eta^4} \end{bmatrix} \begin{bmatrix} X_1 & Y_1 \\ X_2 & Y_2 \\ X_3 & Y_3 \\ X_4 & Y_4 \end{bmatrix} \qquad [104]$$

The Jacobian for the linear triangle finite element is

$$[J] = \begin{bmatrix} \frac{\partial x}{\partial L_1} & \frac{\partial y}{\partial L_1} \\ \frac{\partial x}{\partial L_2} & \frac{\partial y}{\partial L_2} \end{bmatrix} = \begin{bmatrix} (X_1 - X_3) & (Y_1 - Y_3) \\ (X_2 - X_3) & (Y_2 - Y_3) \end{bmatrix} \qquad [105]$$

where

$L_1 = \frac{A}{A^1}$, the area coordinate and shape function 1,

$L_2 = \frac{A}{A^2}$, the area coordinate and shape function 2,

$L_3 = 1 - L_1 - L_2$, the area coordinate and shape function 3,

A, A_1, A_2 = total area, and partial areas of local coordinate.

The isoparametric, linear and quadratic quadrilateral are useful for representing odd shaped and curved boundaries. The integration of the element matrices are performed on the transformed element in the natural coordinate system. The integration method most commonly used for integrating functions is the Gauss-Legendre quadrature. This method replaces the integral with a summation of the function at mxn integration points multiplied by mxn weighting coefficients. This represented by the following equation [106] and is the method used to integrate the shape functions as used in [86-88].

$$\int_{-1}^{1}\int_{-1}^{1} g(\xi,\eta)d\xi d\eta = \sum_{i=1}^{m}\sum_{j=1}^{n} W_i W_j\, g(\xi_i,\eta_j) \qquad [106]$$

The number of integration points depends on the highest power of the function to be integrated. This means that a polynomial of power (2n-1) may be integrated exactly with n sampling points at which the element is evaluated

(Segerlind, 1983). Figure 7 depicts the isoparametric linear, one-dimensional and two-dimensional triangle and quadrilateral elements together with the integration points and weighting coefficients for the highest polynomial power of ξ^2 and η^2 .

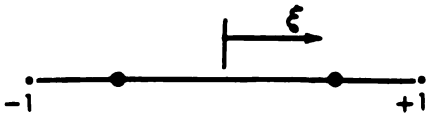

$n=2 \quad \xi_i = \pm 0.577350 \quad W_i = 1.0$

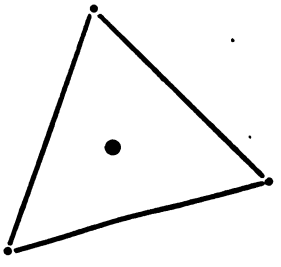

$L_1 = L_2 = 1/3 \qquad W = 1/2$

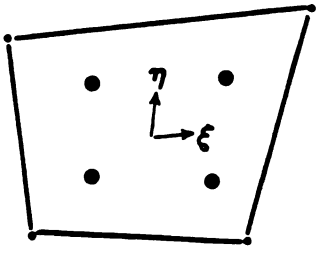

$\xi = \eta = \pm\ 0.577350 \qquad W = 1.0$

Figure 7 Isoparametric Elements and Integration Points.

7. Consistent Stress Approach

Nodal values of discharge Q, slope S, roughness n, and rainfall r can be considered either as constants over an element or as nodal values. It is necessary to maintain continuity at the inter-elemental nodes. The difficulty arises whenever the state variable is either

a) known at the nodes and it is required to be used as an elemental constant, or
b) known as an elemental constant and it is required to be used as a nodal value.

The consistent stress approach provides the correct method of computing these values. The form is

$$[C]\{\Phi\} = r\{F\} \qquad [107]$$

The vector $\{\Phi\}$ contains the nodal values, whereas r represents the constant values over the element (Segerlind, 1976).

In summary, the governing equations have been developed for use in modeling the overland flow from an infiltrating watershed using a Galerkin formulation. The governing equations may be solved for the steady-state and the time-dependent cases. Computation may be done by hand for a small number of elements or by a computer program for larger systems. Before initiation of the computation, a check should be made on the applicability of the kinematic

wave approximation to the specific set of variables or problem. This may be done by using equation [52] to compute the kinematic number k, which must be larger than 10 for the maximum intensity. In addition, the Froude number should be computed to determine where the boundary condition should be applied--upstream or downstream--for sub- and supercritical flow, respectively.

The time solution requires the selection of a time step Δt. This time step must not be larger than the time during which a gravity wave can travel over the length of the element. This is the Courant condition and should not be violated.

Provided these conditions are met, computation of the time-dependent solution of the overland flow equations may be performed using the Galerkin finite element formulation. The method is applicable to both one-dimensional and two-dimensional finite elements using the assembled form of equation [91] and solved by any of the standard finite difference, time-domain solution techniques represented by equations [14] through [19] as shown in [92] and [93].

IV. RESULTS AND ANALYSIS

The results obtained and analysis performed are presented in the following order: The finite element formulation, Geographic Information System analysis, input parameters, hydrologic response areas. The watershed modeled was Watershed 4H near Hastings, Nebraska. The rainstorm event selected was 0.33 cm on May 4, 1959.

A. Finite Element Formulation

The Galerkin finite element formulation was used to solve the kinematic wave equation. The Green-Ampt infiltration equation was used to compute the rainfall excess. The excess rainfall intensity was calculated using the Green and Ampt runoff model from the USDA-ARS Water Erosion Prediction Program (WEPP) project (under development).

The Galerkin formulation of the kinematic wave equation has been presented in the theoretical development and will not be repeated here. The elements used for the arbitrary finite element grid were linear, one-dimensional elements. The formulation used variable width to represent trapezoidal areas. The elements used in the hydrologic response area finite element grid were the linear, two-dimensional, isoparametric four-node quadrilateral elements

and three-node triangles. The system of equations solved by time integration for the one-dimensional, arbitrary grid was

$$[a]\{\dot{h}\} + [b]\{Q\} = [a]\{i_e\} \qquad [108]$$

where

$$[a] = \int_{\Omega} \{N\}^T (\{N\}\{w\})\{N\} d\Omega \ ,$$

$$[b] = \int_{\Omega} \{N\}^T d\{N\}/dx \ d\Omega \ ,$$

$\{\dot{h}\}$ = $\{dh/dt\}$,

i = rainfall excess,

Q = flow rates,

h = flow depth,

w = flow width of the element.

The system of equations solved for the two-dimensional hydrologic response area grid was

$$[a]\{\dot{h}\} + [bx]\{Q\} + [by]\{Q\} = i\{F\} \qquad [109]$$

where

$$[a] = \int_{\Omega} \{N\}^T \{N\} d\Omega \ ,$$

and

$$[bx] = \int_{\Omega} \{N\}^T d\{N\}/dx \; d\Omega \;,$$

$$[by] = \int_{\Omega} \{N\}^T d\{N\}/dy \; d\Omega \;,$$

$$\{F\} = \int_{\Omega} \{N\}^T \; d\Omega \;,$$

$\{\dot{h}\} = \{dh/dt\}$,

i = rainfall excess,

Q = flow rates,

h = flow depth.

Since [109] is a two-dimensional formulation and the equations are integrated over the two-dimensional element domain Ω, no variable width w is needed in the system. The nodal flow rates are for a unit width.

The system of equations in [108] and [109] may be solved with any of the common time integration schemes--

Forward Difference

Central Difference

Galerkins

Backward Difference

depending on the time weighting coefficient chosen. Stability and accuracy of the solution will dictate the proper time weighting coefficient. The Central Difference scheme was used in this analysis. This corresponds to a value of $\theta = 1/2$. No numeric oscillations were observed, which may result from choices of time integration schemes

that are inconsistent with the finite element grid.

A criterion that must be met is the kinematic number after Woolhiser and Liggett (1967). This comes from the kinematic approximation to the full momentum equation. The approximation is accurate to within 10 % if $k = LS_o g/V^2 > 10$. The steps used to check this criterion are to calculate the equilibrium outflow, which is the maximum rainfall excess, solve for the corresponding flow depth using the Manning equation, solve for velocity, and check the Froude number and the kinematic number.

The actual time step used in the time integration scheme must not be longer than that time during which a gravity wave front may propagate through the system. This is known as the Courant condition:

$$\Delta t < \Delta x/c \quad ,$$

where

Δt = time step,

Δx = distance increment or element length,

c = speed of a gravity wave or (5/3)V.

If this condition is violated the partial differential equation theory is violated. This condition arises from the theory of the Method of Characteristics. A time step of one minute was selected as shown in the Appendix.

B. Geographic Information System Analysis

The spatial analysis of the ARS Watershed 4H near Hastings, Nebraska was performed using the ARC-INFO GIS, version 3.2, developed by Environmental Systems Research Institute, Inc., Redlands, California. Several layers were digitized in order to perform an overlay analysis of the landuse, soils, and slope data. This overlay effects a delineation of areas containing homogeneous parameters. In this case, the hydrologic response areas of homogeneous parameters consisted of only the slope interior to the watershed boundary.

The landuse was digitized for the watershed according to the landuse at the time of the May 4, 1959 rainstorm event. This watershed, like many of the ARS research watersheds, was under a single crop and tillage practice. The landuse for this watershed was fallow under good residue cover at the time of the rainstorm event. Figure 8 depicts the landuse at the time of the event on May 4, 1959.

The soils in this watershed are the Hastings silty loam, Hastings silty clay loam, and a Colby silt loam. These soil names are the 1939 soil survey names originally mapped for this watershed by the USDA-Soil Conservation Service. Figure 9 shows the three soil delineations for the watershed. The Hastings silty clay loam is an eroded profile of the Hastings soil series. The B-horizon properties were used in the Green and Ampt modeling for

this mapping unit. The Green and Ampt equation was solved for this storm and these soils using the soil properties from soil samples sampled April 21, 1965 by the USDA-Soil Conservation Service. The location of the Hastings soil sample was in Webster County, 0.15 miles west and 180 feet south of northeast corner of Sec. 1, T3N, R10W. The soil properties were taken from the Hastings Soil No. S65NE-91-1 data, Sample Nos: 20449-20456. The Colby soil properties were taken from the Soils-5 data sheet for the series. This information was contained in the soils data base at the USDA-Soil Conservation Service, National Soil Survey Laboratory, Lincoln, Nebraska. The soil properties are contained in Table 1.

TABLE 1 Soil Properties

1939 SOIL SURVEY NAME	% > 3 in	% > #10	% SAND	% CLAY	BULK DENSITY GM/CC	PERCENT ORGANIC MATTER	CEC/ CLAY
COLBY Si L	0	0	10	21	1.40	1.50	0.65
HASTINGS Si L	0	0	10	24	1.27	2.50	0.79
HASTINGS Si C L	0	0	8	34	1.26	1.77	0.67

Figure 8 Watershed 4H Landuse.

Figure 9 Watershed 4H Soils Map.

The slope and topography was obtained from two-foot contour maps provided by the USDA-Soil Conservation Service in a 1942 plane table survey. Figure 10 shows the digitized elevation map derived from the plane table survey. The ARC-INFO GIS, utilizing the Triangular Irregular Network (TIN) subroutine, calculates the slope of each triangular area from the elevations of the vertices. The TIN slope map is shown in Figure 11. The slopes required for the finite element modeling are at the nodes of the elements. To achieve this, the finite element grid was overlaid on to the slope map an the slope at the node tabulated in the INFO Database for each node. As the finite elements decrease in size, the elemental slopes tend toward nodal slopes in the limit. The slope map in Figure 11 shows increased complexity primarily due to the delineation of not only slope but aspect. The aspect of the slope is the direction measured in degrees between the principal slope and the north direction. The aspect and principal slope are resolved into x- and y-direction slopes for use in the finite element model. In the kinematic wave equation the friction relation, Manning or Chezy, contains the square root of the slope. When modeling the two-dimensional flow equations, the flow is caluclated in the direction of and using the principal slope. This flow rate is then resolved into x- and y-direction flow rates for use in calculating the $\partial(uh)/\partial x$ and $\partial(vh)/\partial y$ terms. To relate the orientation of all vector quantities to the watershed

map, such as velocity or flow rate, the aspect anlge of the principal slope was used.

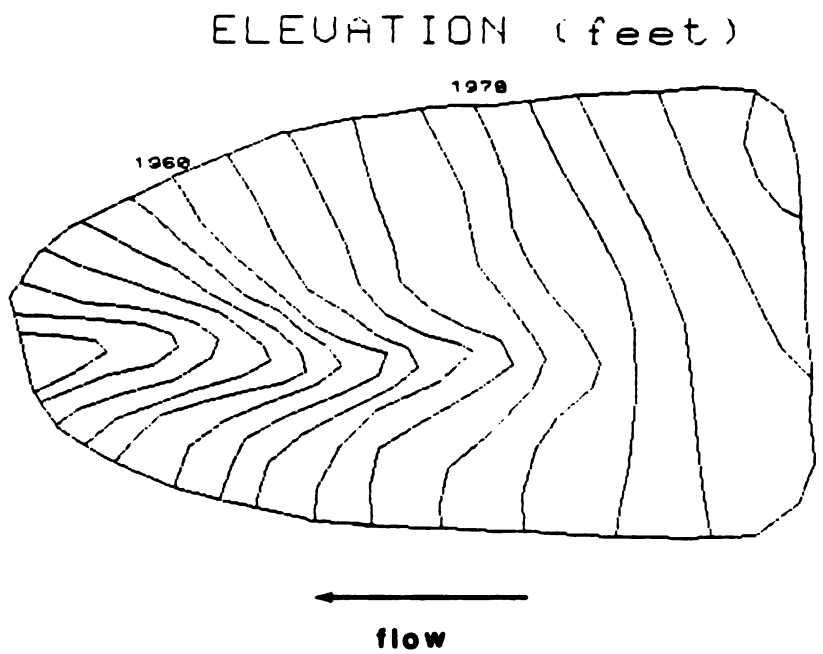

Figure 10 Watershed 4H Elevation Map.

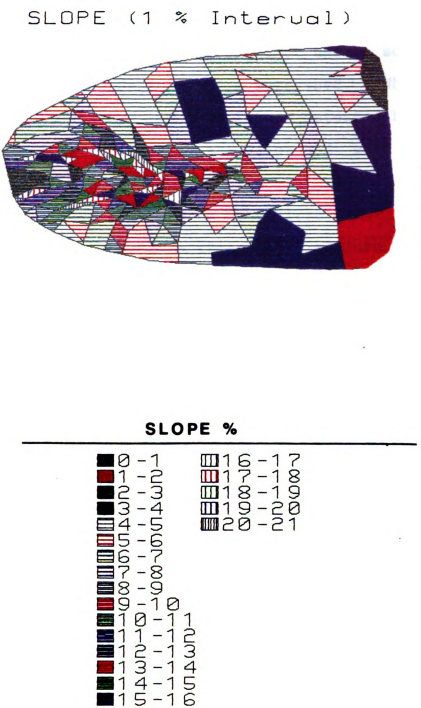

Figure 11 ARC-INFO TIN Slope Map.

Figure 12 depicts the rainfall excesses for the three soils as defined by the Green and Ampt equation--no significant difference was observed. For the purposes of computing runoff and infiltration, these soils may be treated as one for the entire watershed. While spatial nonhomogeneity may exist it is not detected by the soil mapping units interior to the watershed when considering infiltration.

Figure 13 illustrates the first case analyzed, a finite element grid of arbitrary spatial form. That is, a set of linear elements of variable width. This is the same finite element grid, slopes and Manning n's as used by Peters, Blandford and Meadows (1983). Table 2 contains the arbitrary finite element grid input data.

Table 2 Arbitrary Grid Finite Element Input Data.

ELEMENT NUMBER	NODE NUMBER	X-COORD	NODAL SLOPE	MANNING n	WIDTH (FEET)
(1)	1	0	0.0406	0.035	353
	2	171	0.0406	0.035	
(2)	2	171	0.0406	0.035	333
	3	342	0.0669	0.035	
(3)	4	342	0.0669	0.035	206
	4	507	0.0562	0.035	

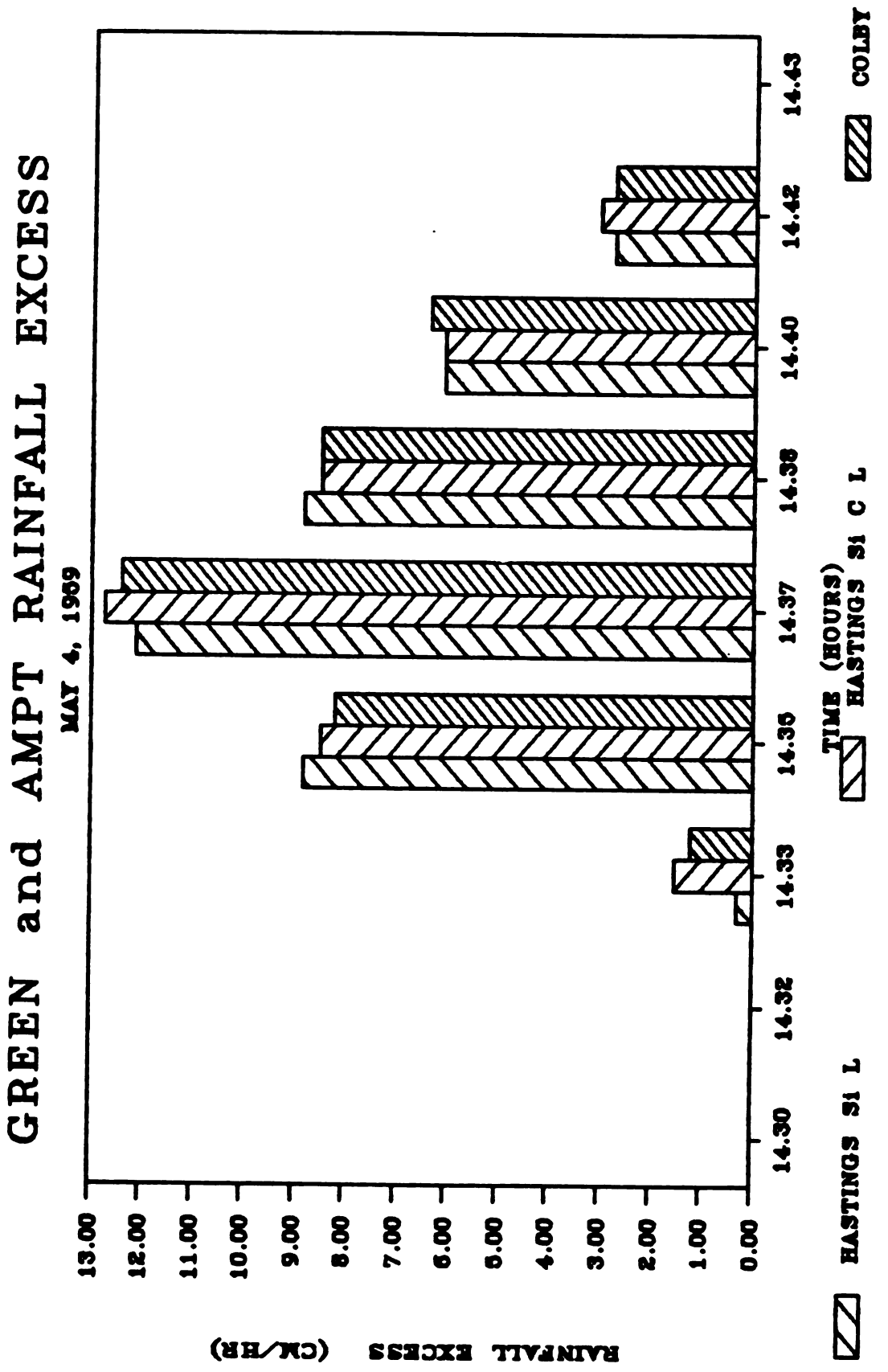

Figure 12 Rainfall Excess for Three Soils.

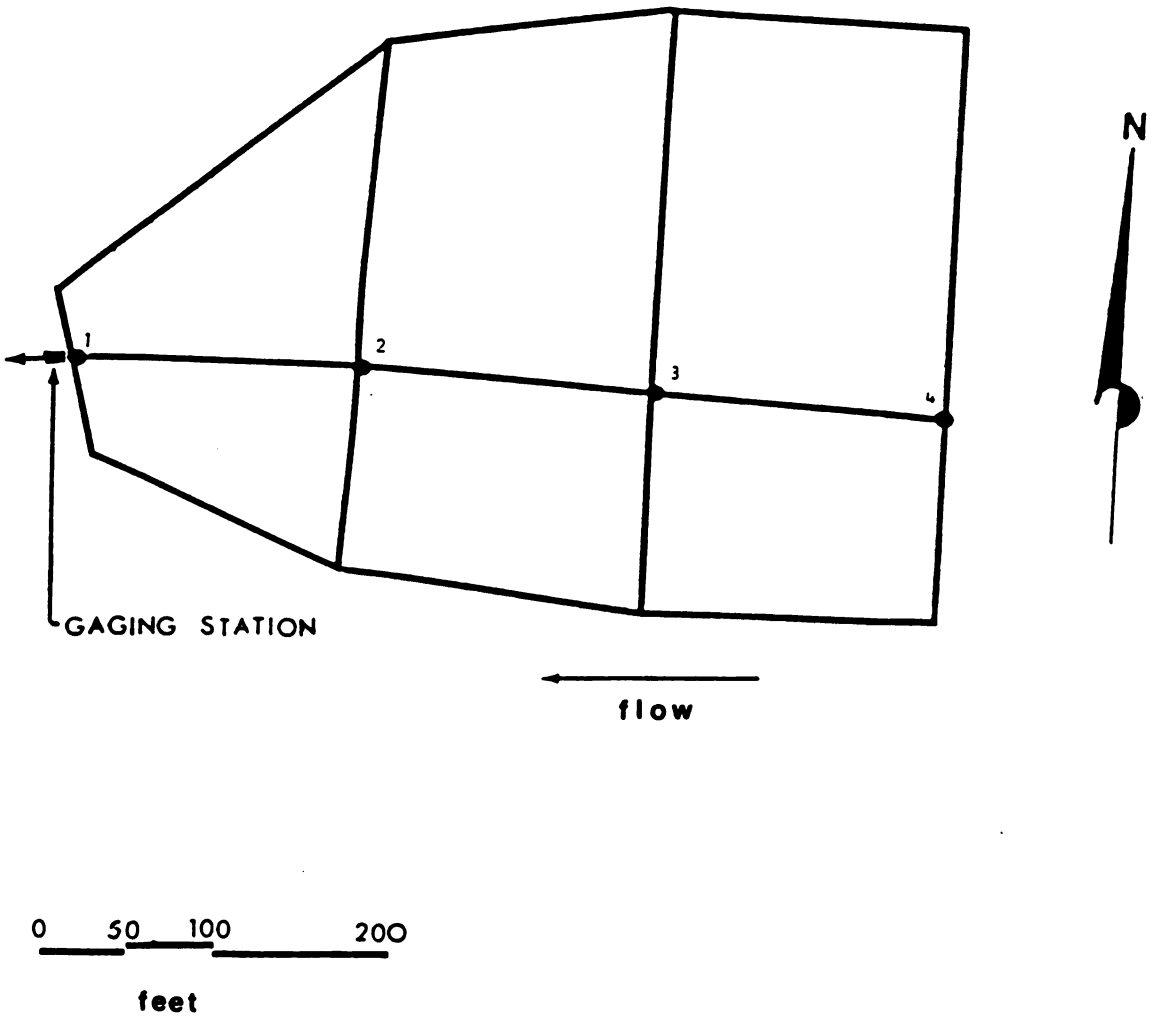

Figure 13 Finite Element Grid of Arbitrary Spatial Form.

The topography, in this particular watershed, is the one parameter of known spatial nonhomogeneity. Slopes defined by the 10-foot contour intervals, were used to form the finite element grid. Nodal points were located at the intersections of the 10-foot contour lines and the watershed boundary and the stream channel. The slope on a two-dimensional finite element grid possesses both x- and y-direction slopes. Even though two nodes lie on a contour, the element has an x- and/or y-direction slope due to the skewed spatial form with respect to the coordinate system. If the slope is spatially nonhomogeneous within the element then it should be averaged over the element to obtain the slope for the element. The scale of the variation defines the scale of the finite element grid. The 10-foot contour intervals were used in order to limit the number of elements representing the watershed. This was done in order that the comparison of the arbitrary-grid to the hydrologic-response-area grid would not be obscured by the increased accuracy gained from a large increase in the number of elements.

In order to model the hydrologic response areas, two-dimensional elements are required. The elements selected for this research were the three-node triangle and the four-node quadrilateral, isoparametric elements. A computer program was written that performs the coordinate transformation and computes the partial derivatives and

other components of the two-dimensional flow equation [109]. The nodal coordinates were obtained from the GIS overlay of the finite element grid over the watershed. The watershed is represented in the state plane coordinate system, defined by the plane table survey of 1942 of the watershed available from the USDA-ARS-Water Data Laboratory, Beltsville, Maryland. These coordinates are in Table 3 listed by node number. Each element is represented by the nodes associated with it. Thus, for Element (8) in Figure 14, the node numbers 1, 9, and 10 represent the three-node triangular element.

Table 3 Hydrologic Response Area Nodal Coordinates and Slopes

NODE NUMBERS	X-COORD.	Y-COORD.	ELEVATION	SLOPE	ASPECT	X-SLOPE	Y-SLOPE
1	1618	1302	1946.00	0.000	0.00	0.000	0.000
2	1610	1345	1950.00	0.081	-177.30	0.004	0.081
3	1707	1467	1960.00	0.049	-119.50	0.043	0.024
4	1897	1529	1970.00	0.063	-110.90	0.059	0.022
5	2079	1538	1978.00	0.032	-76.30	0.031	0.008
6	2111	1309	1976.30	0.022	-127.00	0.018	0.013
7	1977	1309	1970.00	0.064	-113.60	0.059	0.026
8	1841	1313	1960.00	0.159	-159.90	0.055	0.149
9	1710	1320	1950.00	0.086	-75.70	0.083	0.021
10	1625	1274	1950.00	0.118	-29.50	0.058	0.103
11	1739	1188	1960.00	0.089	-75.90	0.086	0.022
12	1931	1161	1970.00	0.033	-91.80	0.033	0.001
13	2077	1160	1975.00	0.016	-91.90	0.016	0.001

1. Coordinates are state plane (feet).
2. Elevation is mean sea level (feet).
3. Aspect is in degrees measured from north: negative is counter-clockwise from 0 to 180 and positive is clockwise from 0 to 180.
4. Slopes in the x- and y-direction are the absolute values of slopes in the polar coordinate system with zero degrees due east.

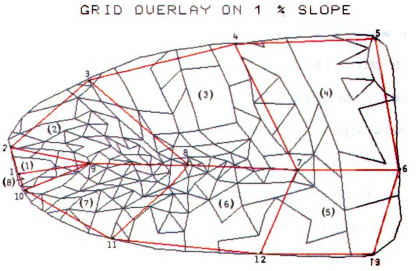

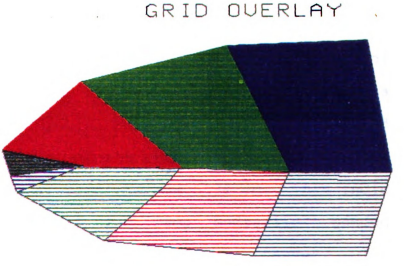

Figure 14 Finite Element Grid Representing Hydrologic Response Areas based on slope.

C. Hydrograph Response.

Several cases were investigated to test the accuracy of the proposed methodology. The first case was a representation of the watershed using a finite element grid of arbitrary spatial form. The spatial form of this grid is shown in Figure 13. The second case was a representation of the watershed using a hydrologic response area, finite element grid. Difficulties arose due to the anisotropic nature of the hydrologic response area grid which led to consideration of an isotropic finite element grid.

1. Arbitrary Finite Element Grid Model Calibration.

Several modeling runs were performed in order to produce an outflow hydrograph that matched the actual outflow hydrograph. The initial Green and Ampt parameters were estimated after Brakenseik (1983). After calculating the runoff intensities for the three soils it was determined that the soils could be treated as a single soil possessing spatial homogeneity at the watershed scale. The total volume of the resulting runoff was 1.31 cm. The actual runoff reported was 0.38 cm. This indicated that a combination of increased hydraulic conductivity and depressional storage would be needed. The range of hydraulic conductivities due to crusting was estimated as 0.15 cm to 0.06 cm. Values of hydraulic conductivity and depressional storage were selected such that the peak and volume were predicted as accurately as possible. The

depressional storage was estimated as 0.55 cm for a recently tilled silty clay loam (personal correspondence from Dr. R.J. Rawls, ARS, Beltsville). The other Green and Ampt parameters were

Wetting Front suction = 31 cm,

Bulk Density = 1.0 g/ccm.

The resulting hydrograph shown in Figure 15 has a peak of 0.114 m^3/s at 14:31 hours on May 4, 1959. This is compared to 0.13 m^3/s at 14:29 hours. The calculated hydrograph had a volume of 0.21 cm compared to an actual volume of 0.55 cm. The tabulated results, outflow at node-4 and rainfall/runoff intensities are in Table 4.

The hydrograph shown in Figure 15 has a larger volume than the actual hydrograph. The volume and peak could not be matched precisely. If sufficient depressional storage to match the outflow volume was removed, then the intense part of the storm was removed resulting in very low peak rates. The final calibration was found by inspection of the rainfall intensities that resulted from a varying hydraulic conductivities in the range reported above.

The difficulty in finding a set of depressional storages and hydraulic conductivities that would produce a hydrograph suggests that the Green and Ampt model does not define a unique set of parameters. The formulation of the arbitrary finite element grid as linear elements with variable width also affects the resulting calibrated parameters. The form of the finite element grid affects

the results since it makes the assumption of uniform flow across the width of the element. This assumption governs the form of the hydrograph as the rainfall excess is routed downstream.

Table 4 Arbitrary Finite Element Grid Outflow.

TIME (HR)	RAINFALL CM/HR	RUNOFF INTENSITY FT/S	CALCULATED OUTFLOW M3/S	ACTUAL OUTFLOW M3/S
14.30	0.00	0.00E+00	0.00E+00	0.00E+00
14.32		0.00E+00	0.00E+00	0.00E+00
14.33		0.00E+00	0.00E+00	0.00E+00
14.35	2.67	0.00E+00	0.00E+00	0.00E+00
14.37		0.00E+00	0.00E+00	0.00E+00
14.38		0.00E+00	0.00E+00	0.00E+00
14.40		0.00E+00	0.00E+00	0.00E+00
14.42	12.70	3.60E-05	7.18E-04	0.00E+00
14.43		1.30E-04	1.27E-02	3.20E-03
14.45		1.00E-04	4.68E-02	2.52E-02
14.47		3.60E-05	8.08E-02	8.92E-02
14.48		-1.80E-07	1.02E-01	1.28E-01
14.50	7.92	-1.80E-07	1.13E-01	1.15E-01
14.52		-1.80E-07	1.14E-01	1.04E-01
14.53		-1.80E-07	1.08E-01	8.82E-02
14.55		-1.80E-07	9.56E-02	7.28E-02
14.57		-1.80E-07	8.19E-02	6.04E-02
14.58	1.83	-1.80E-07	6.88E-02	4.79E-02
14.60		-1.80E-07	5.73E-02	3.92E-02
14.62		-1.80E-07	4.77E-02	3.05E-02
14.63		-1.80E-07	3.97E-02	2.54E-02
14.65		-1.80E-07	3.32E-02	2.03E-02
14.67		-1.80E-07	2.80E-02	1.74E-02
14.68	0.76	-1.80E-07	2.37E-02	1.44E-02
14.70		-1.80E-07	2.02E-02	1.14E-02
14.72		-1.80E-07	1.73E-02	9.82E-03
14.73		-1.80E-07	1.50E-02	8.21E-03

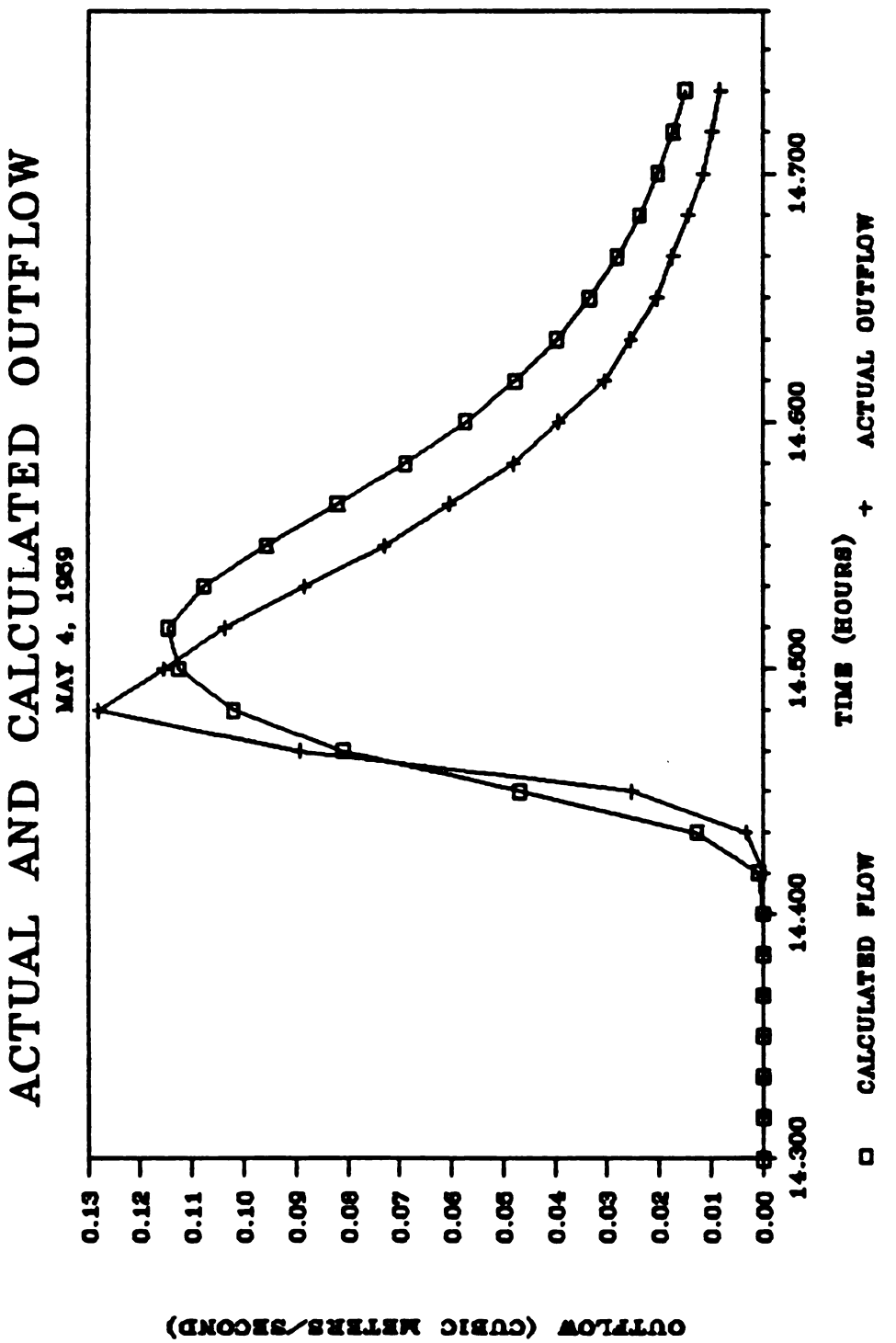

Figure 15 Hydrograph From Arbitrary Finite Element Grid.

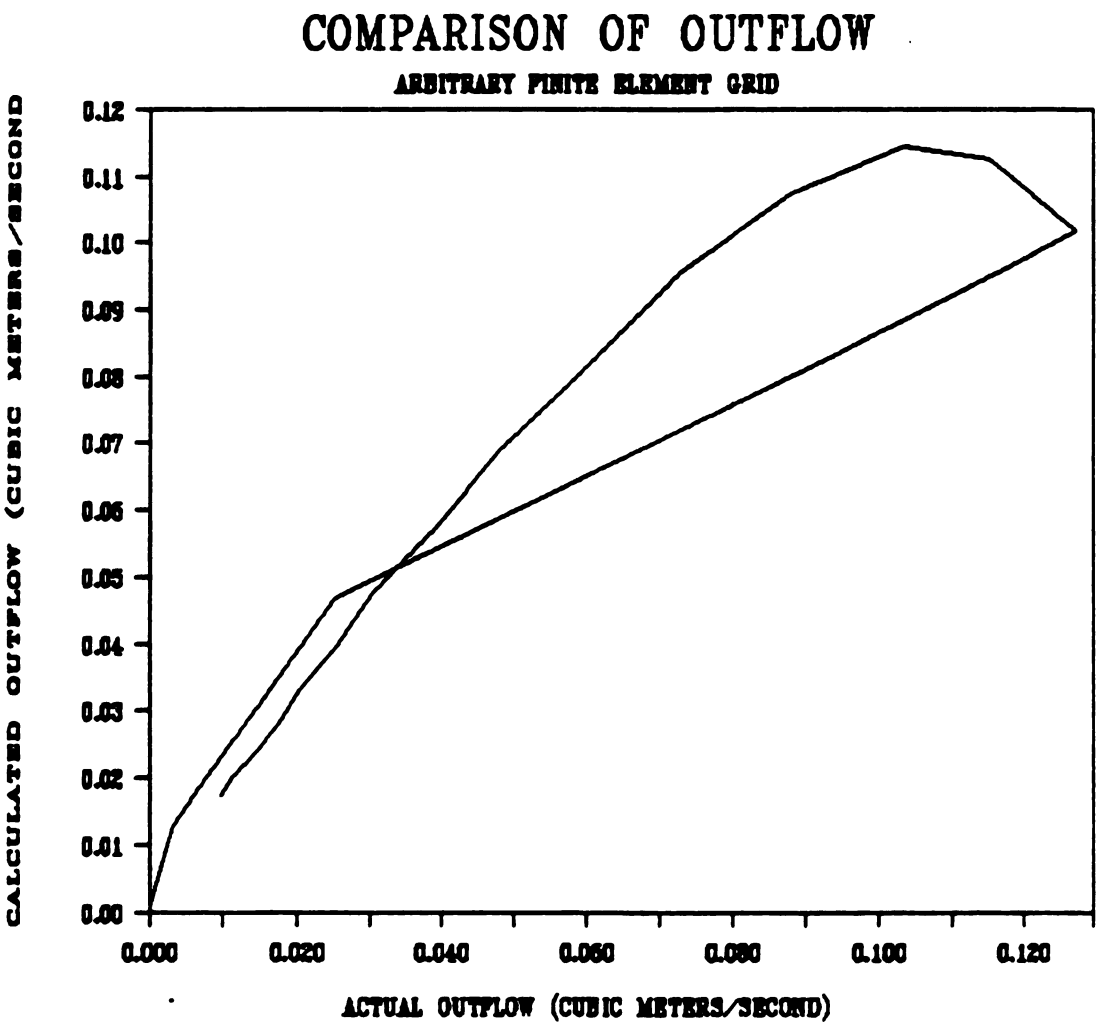

Figure 16 Comparison of Outflows for the Arbitrary Finite Element Grid.

2. Hydrologic Response Area Finite Element Grid.

The finite element grid shown in Figure 14 was formed using the spatial distribution of slope as defined by the ten foot elevation contours. The parameters used for this case were the same as those used in the calibrated, arbitrary grid model. This was chosen so that differences would not arise from two different calibrated sets of parameters. The effect of better defined finite elements formed from hydrologic response areas was expected to result in a more accurate prediction of the outflow hydrograph.

Difficulty in obtaining a solution for the hydrologic response area finite element grid was encountered. During the solution, a negative flow depth occurred at node number eight. This effectively precluded solution since no flow could pass this element because of the connectivity associated with the finite element grid.

The cause of this difficulty was investigated through extensive analysis of the matrices associated with the Galerkin finite element formulation for the surface water flow equations. These matrices are the [C], [bx] and [by] matrices as defined in [109]. The first difficulty examined was the first derivative term represented by [bx] and [by]. These matrices are asymmetric and therefore are difficult to integrate properly when anisotropy exists in the slope term. Anisotropy in the slope results from the two dimensional representation of overland flow. The

control volume in Figures 2 and 3 assume that the flow is orthogonal to the x-y coordinate system. The Manning equation relates the total flow Q to the flow depth h as a function of slope. This slope is the slope in the principal direction and therefore the flow rate Q is a vector quantity. The resolution of the flow into the respective x-y direction components is accomplished after the computation of the flow in the principal direction. The flow rates Q in [109] are the respective flow rates per unit width in the x-y directions.

Due to the derivation from the control volume and the form of the finite element formulation, each element must be rotated in a local coordinate system such that the finite element nodal coordinates are orthogonal to the principal direction of the slope. This rotation is performed for each coordinate pair using the rotation matrix

$$\begin{bmatrix} x' \\ y' \end{bmatrix} = \begin{bmatrix} \cos\theta & \sin\theta \\ -\sin\theta & \cos\theta \end{bmatrix} \begin{bmatrix} x \\ y \end{bmatrix} \qquad [110]$$

where

θ = angle of the principal slope in the global coordinate system.

This rotation must be done before the integration of the element matrices.

The integration of the element matrices is performed

numerically for the isoparametric element using the Gauss-Legendre Quadrature. The Jacobian matrix is calculated in this integration procedure using the global coordinates. If anisotropy exists, then the global coordinates must be rotated as in [111] and the local used in place of the global coordinates.

When rotation occurs for a randomly oriented four node quadrilateral finite element, it becomes unclear as to which nodal coordinate pair must be the first pair associated with node i or (-1,-1) in the ξ-η coordinate system. This importance can not be over emphasized since the existence of the solution depends on it. The difficulty arises when integrating the [bx] and [by] matrices in [110]. A four node quadrilateral finite element that is rectilinear and oriented with the ξ-axis parallel to the x-axis and the η-axis parallel to the y-axis would be integrated such that the lower left node closest to the origin would be associated with the (-1,-1) node in the ξ-η coordinate system. If this principle is not adhered to then the integrated result represented by the [b] matrices is not accurate and a solution is not achieved.

A four node quadrilateral finite element was investigated to demonstrate the difficulty imposed by rotation and node ordering when integrating the [b] matrices. Under a steady rainstorm intensity the equilibrium value of the outflow equals the product of

intensity and the surface area of the finite element. The solution yields unit width nodal flow rates which must be integrated over the sides of the element in order to compare the outflow with the inflow. The finite element modeled is shown in Figure 17. The outflow is 0.4 m^3/s for a 0.00001 m/s intensity over the 200x200 m finite element. Continuity is achieved since the inflow is the product of intensity and the surface area or 0.4 m^3/s. Note that the nodal slopes are orthogonal to the global coordinate system and that no rotation to a local coordinate system was performed.

The effect of rotation to a local coordinate system was investigated by observing the effect on the outflow that the direction of slope has. By assigning slopes of 45 degrees at the nodes and assigning boundary conditions at the nodes 1,2, and 4, outflow at node 3 results. The outflow was 0.424 m^3/s. The inflow was 0.40 m^3/s resulting in a 6% error. This is not a large error in this case.

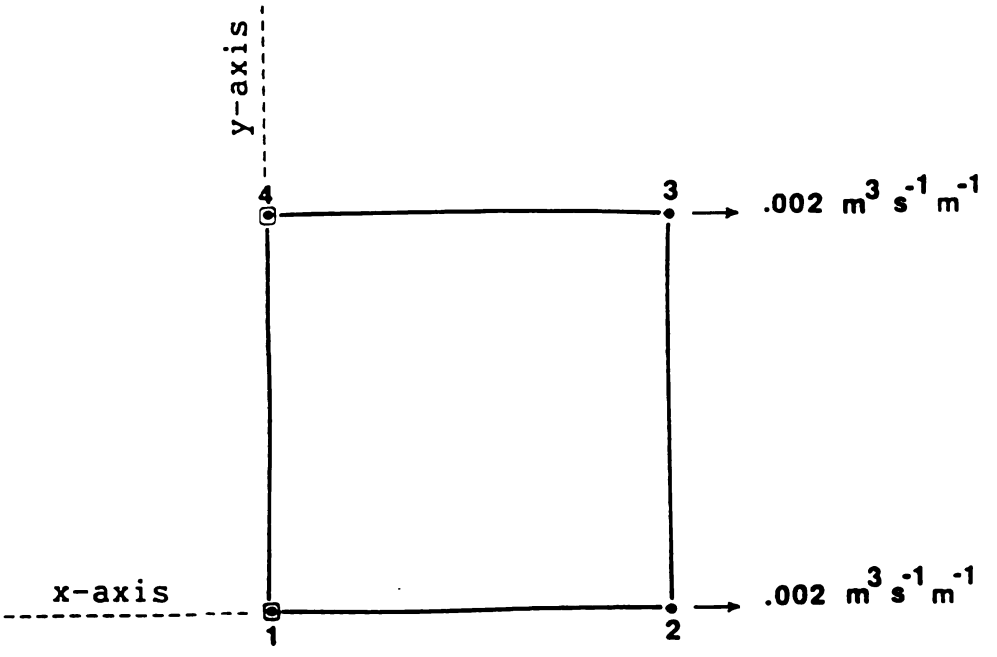

Figure 17 Four Node Quadrilateral Finite Element Outflow.

A more serious error occurs when several finite elements are combined in a system with slopes that are not orthogonal to the coordinate system. In Figure 18 two elements are shown with nodal slopes at 45 degrees. The outflow totaled 1.155 m^3/s whereas the inflow totaled 0.6 m^3/s.

These errors arise because of the difficulty in integrating the [b] matrices. These matrices are shown below for the four node quadrilateral when successive nodes are interpreted as node i in the integration. This amounts to extreme cases of rotation such that different nodes become the closest node to the global origin. The slope angle with respect to north and the first node are shown for each case.

Slope Aspect = 90

First Node = 1

$$[bx] = \frac{200}{12}\begin{bmatrix} -2 & 2 & 1 & -1 \\ -1 & 1 & 2 & -2 \\ -1 & 1 & 2 & -2 \\ -2 & 2 & 1 & -1 \end{bmatrix}$$

Slope Aspect = 90

First Node = 2

$$[bx] = \frac{200}{12}\begin{bmatrix} -1 & 1 & 2 & -2 \\ -2 & 2 & 1 & -1 \\ -2 & 2 & 1 & -1 \\ -1 & 1 & 2 & -2 \end{bmatrix}$$

Slope Aspect = 90

First Node = 3

$$[bx] = \frac{200}{12}\begin{bmatrix} -2 & 2 & 1 & -1 \\ -1 & 1 & 2 & -2 \\ -1 & 1 & 2 & -2 \\ -2 & 2 & 1 & -1 \end{bmatrix}$$

Slope Aspect = 90

First Node = 4

$$[bx] = \frac{200}{12}\begin{bmatrix} -1 & 1 & 2 & -2 \\ -2 & 2 & 1 & -1 \\ -2 & 2 & 1 & -1 \\ -1 & 1 & 2 & -2 \end{bmatrix}$$

Because of the incompatibility of the four node quadrilateral finite element with the computation of the [b] matrices when rotation occurs, it should not be used for the solution of the surface water equations when anisotropy exists in the slope.

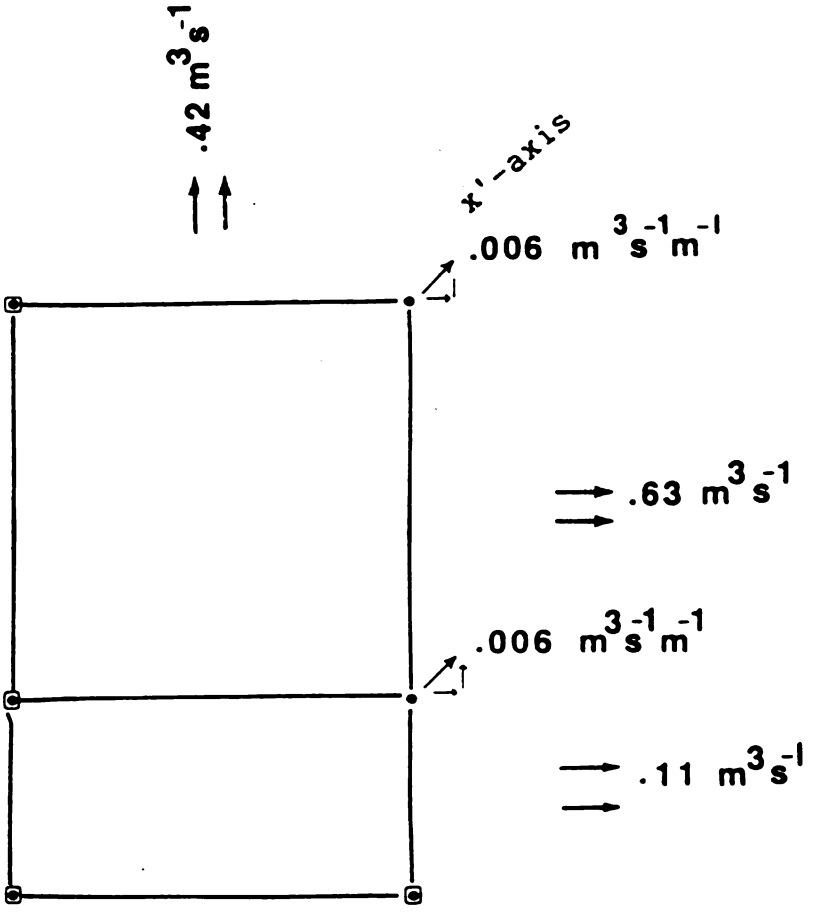

Figure 18 Two Element System Outflow.

The three node triangle was investigated in a similar manner. Figure 19 shows the three node triangle used to demonstrate the effect of rotation on the outflow and the integrated value of the [b] matrix. Successive nodes were used as the node associated with node i or the first shape function for the triangle finite element. The effect on the [b] matrices was observed for each of the following cases.

Slope Aspect = 90

First Node = 1

$$[bx] = \frac{200}{6}\begin{bmatrix} -1 & 0 & 1 \\ -1 & 0 & 1 \\ -1 & 0 & 1 \end{bmatrix}$$

Slope Aspect = 90

First Node = 2

$$[bx] = \frac{200}{6}\begin{bmatrix} -1 & 0 & 1 \\ -1 & 0 & 1 \\ -1 & 0 & 1 \end{bmatrix}$$

Slope Aspect = 90

First Node = 3

$$[bx] = \frac{200}{6}\begin{bmatrix} -1 & 0 & 1 \\ -1 & 0 & 1 \\ -1 & 0 & 1 \end{bmatrix}$$

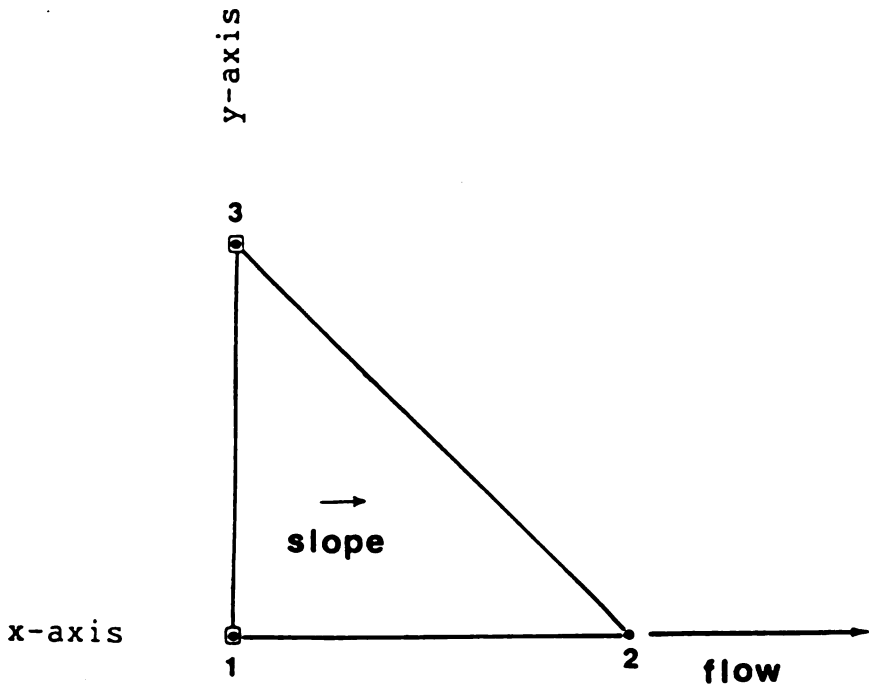

Figure 19 Three Node Triangle Isotropic Outflow.

The result is that the node ordering and hence the rotation has no effect on the magnitude or sign of the [bx] matrix. This indicates that the triangle is less sensitive to node ordering and rotation than the four node quadrilateral finite element in the effect on the [b] matrices. This fact recommends the use of the triangle for use in anisotropic surface water flow problems.

Rotation of the three node triangle finite element is done so that the x'-y' axes are orthogonal to the principal direction of slope. This is done in the same manner as in [111]. The boundary conditions are applied to the triangle as with the quadrilateral. Another difficulty arises, however, since all three nodes must be specified as boundary values of zero when the principal slope direction is in a direction away from two sides as shown in Figure 20. The solution for the triangle shown cannot be obtained. This is due to the difficulty in specifying the boundary condition. If only one or two nodes are specified, then the boundary conditions are under specified for anisotropic slopes. If three nodes are specified then the element is a null solution since all nodes are zero for all time.

The use of the three node triangle finite element for anisotropic flow requires that the element be oriented in the global coordinate system such that one side is parallel to the principal direction of slope. If this is done, then the triangle may be used with any node ordering and

orientation in the global coordinate system since rotation does not result in an invalid integration of the [b] matrix.

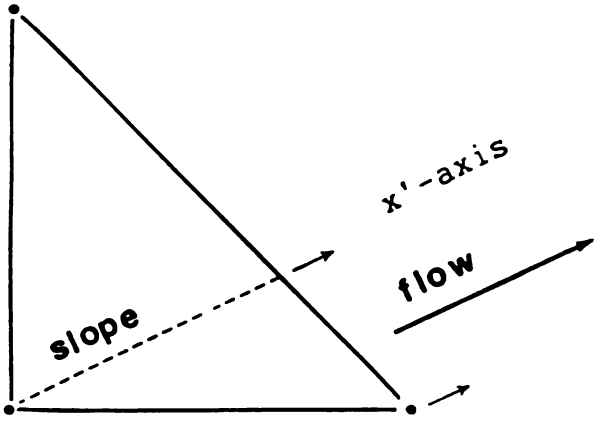

Figure 20 Three Node Anisotropic Triangle.

3. Isotropic Finite Element Grid

Inorder to investigate the hydrologic response of this watershed using a two-dimensional finite element configuration it was necessary to create a rectilinear grid that is oriented such that each element is orthogonal to the principal direction of slope. Due to difficulties arising from node ordering and rotation, the slopes derived from the ARC/INFO TIN slope map in Figure 11 were used with a realigned aspect of 90 degrees or due west. A new grid that possesses only isotropic slopes was used. The node ordering preserves the ordering necessary to achieve correct integraton of the [b] matrices. This ordering is preserved since no rotation is necessary due to the isotropic slopes. Figure 21 shows the isotropic finite element grid derived from the hydrologic response area grid and the TIN slope map.

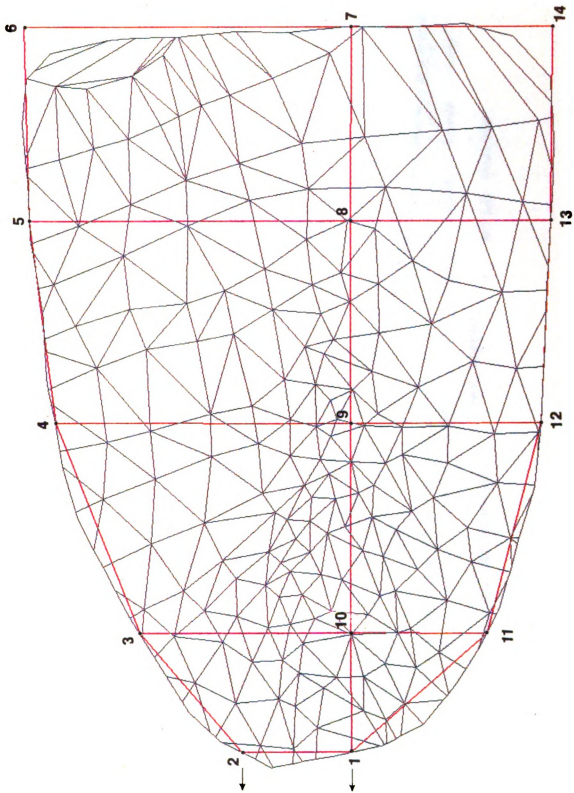

Figure 21 Isotropic Finite Element Grid.

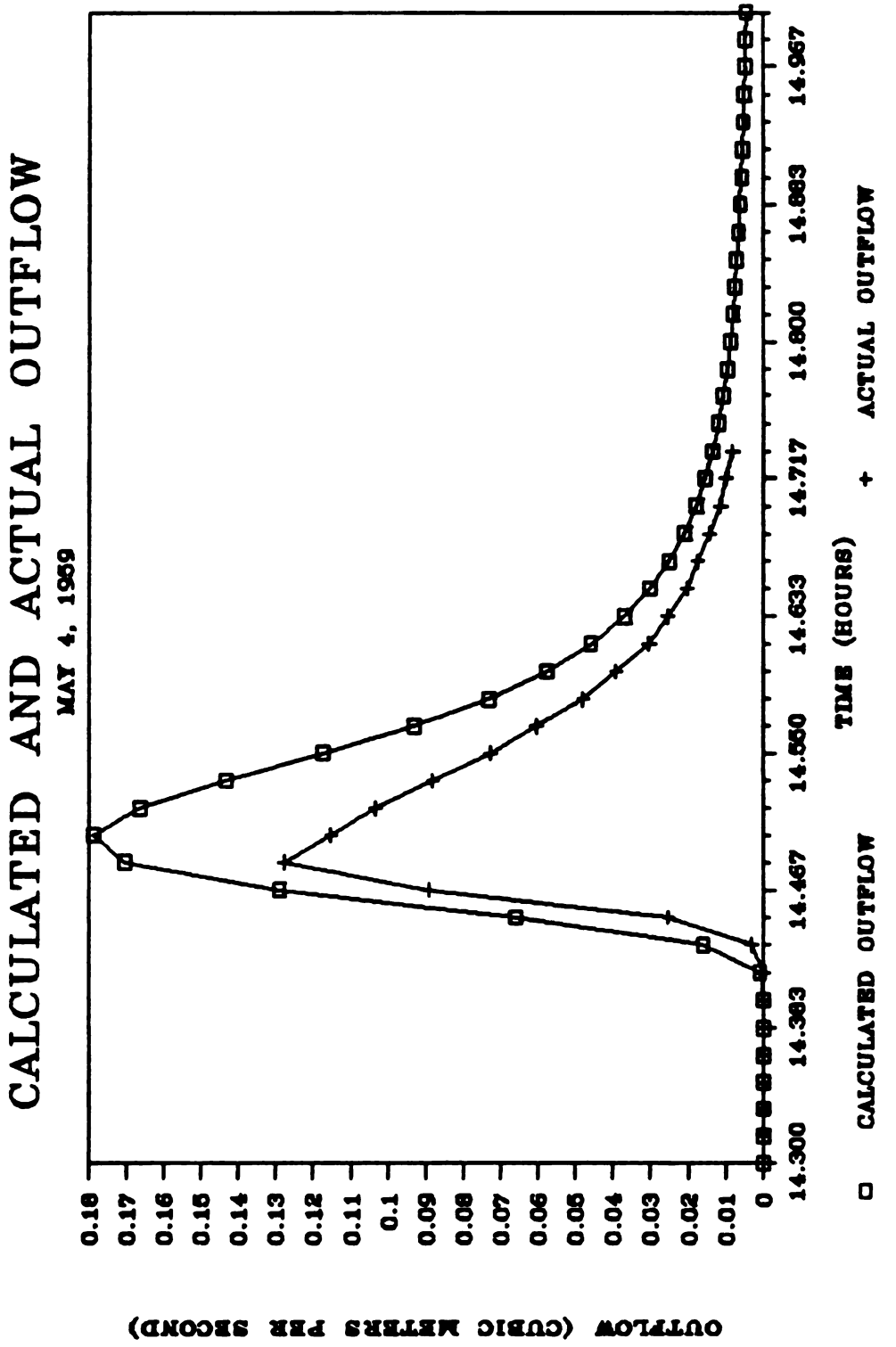

Figure 22 Hydrograph From Isotropic Finite Element Grid.

The hydrologic response from the isotropic finite element grid is shown in Figure 22. The isotropic finite element grid yields a hydrograph that exceeds the actual outflow hydrograph. The peak outflow of 0.18 m^3/s compares to the actual of 0.13 m^3/s. The time to peak is at 14:30 which compares to the actual time to peak of 14:29 hours. The rainfall excesses used were the same as those used for the arbitrary finite element grid. The tabulated results, outflow at node 1 and 2 integrated across the edges of elements (1) and (8) are presented in Table 5.

Table 5 Isotropic Finite Element Grid Outflow.

TIME HRS	INTEGRATED OUTFLOW NODES 1,2 CFS	CALCULATED OUTFLOW M3/S	ACTUAL OUTFLOW M3/S
14.400	0.00	0.00	0.00
14.417	0.03	0.00	0.00
14.433	0.60	0.02	0.00
14.450	2.44	0.07	0.03
14.467	4.78	0.13	0.09
14.483	6.31	0.17	0.13
14.500	6.62	0.18	0.12
14.517	6.16	0.17	0.10
14.533	5.31	0.14	0.09
14.550	4.35	0.12	0.07
14.567	3.45	0.09	0.06
14.583	2.71	0.07	0.05
14.600	2.14	0.06	0.04
14.617	1.70	0.05	0.03
14.633	1.37	0.04	0.03
14.650	1.12	0.03	0.02
14.667	0.93	0.03	0.02
14.683	0.78	0.02	0.01
14.700	0.66	0.02	0.01
14.717	0.57	0.02	0.01
14.733	0.50	0.01	0.01

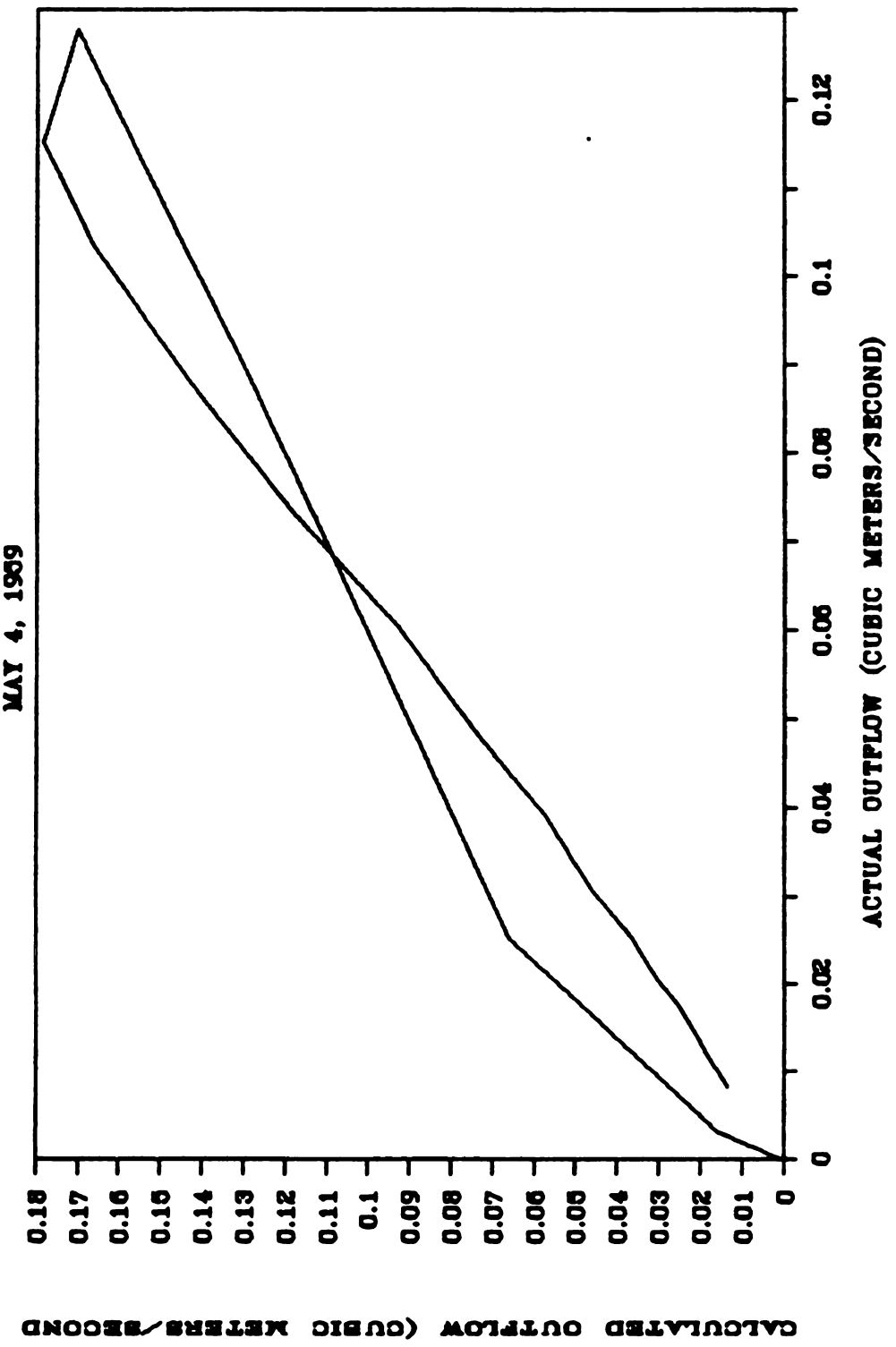

Figure 23 Comparison of Outflows for the Isotropic Finite Element Grid.

4. Statistical Comparison of Arbitrary Grid Outflows

The statistical comparison of the arbitrary finite element grid outflow hydrograph with the actual outflow is facilitated by plotting the calculated versus the actual outflows. The close agreement between the calculated and actual values would result in a line plotted along a 45^0 axis. Figure 16 shows close agreement in the rising limb.

Regression analysis presented in the Appendix represents values for both the ascending and recession limbs and a correlation coefficient of .92. The regression analysis was performed with Lotus 1-2-3 release 2.01. The regression analysis is a measure of goodness of fit. This technique does not address the sensitivity of the output (flow depth) to the input (slope, Manning n, and rainfall excess) parameters. Nor does it define the uniqueness of the calibrated parameters in the solution.

The hydrologic response area finite element grid did not result in an improvment over the arbitrary finite element grid. The more correct representation of the slope parameter by GIS analysis may improve the predictive capability of the finite element model but is not identyfiable by the approach taken. This approach assumed that the Green and Ampt parameters calibrated for the arbitrary finite element grid would result in accurate results when used with the hydrologic response area finite element grid. The difficulty with this approach is that the hydraulic conductivity and depressional storage are not

unique nor known apriori from measurable characteristics of the soil-landuse complex. Due to the difficulty in identifying a unique set of infiltration parameters as well as others such as Manning n, further calibration or statistical comparison was not pursued.

D. Discussion

Three cases were investigated, the arbitrary finite element grid, a hydrologic response area finite element grid and the isotropic finite element grid for use in modeling watershed outflow under an unsteady rainfall event. The arbitrary grid consisted of one-dimensional, linear elements of variable width. These linear elements were of the same spatial form as used by Peters, Blandford and Meadows (1983). This grid was termed arbitrary because they do not necessarily conform to spatially distributed parameters. The hydrologic response areas were defined using a Geographic Information System. The finite element grid used to represent the hydrologic response areas conforms to the spatially distributed parameters. The isotropic finite element grid was investigated because of significant difficulties in modeling randomly oriented finite elements that possess anisotropic slope.

1. Input Parameters

The essence of the difficulty lies in the representation of the watershed topography using finite

elements. Two dimensional analysis of the surface water equations was complicated by the use of a four node quadrilateral for computation of first order derivatives when anisotropy required rotation to an orthogonal set of local axes. The rotation caused errors in the integration of the [b] matrices. The other finite element investigated was the three node triangle. This finite element could be rotated to the orthogonal local axes without error in the [b] matrices integration. However, the proper assignment of boundary values requires that the triangle be oriented such that one node lies on a stream line, i.e. an isotropic finite element grid.

The arbitrary grid representation of slope, i.e., a uniformly sloped plane incorrectly represents the flow paths on a curvilinear surface. The flow paths are always perpendicular to the elevation contours if inertia is insignificant as in the kinematic wave equation. This amounts to a solution of the Laplacian equation for potential and streamlines. The equipotential lines are in this case the equi-elevation lines and the streamlines or orthogonal trajectories are the flow paths. Of course, depending on the scale of the modeled flow, micro-scale topography changes may obscure a smooth trend in flow path across the watershed. Significant difficulties arise when the element grid is not orthogonal to the principal direction of the slope as it varies over the watershed surface.

In the present watershed, the slope was defined by the contour intervals from the topographic survey. The variation of the elevation contours sets the scale of the spatial variation of the slope parameter. Between the contour lines, nothing is known of the micro-scale topography and therefore is assumed to be purely stochastic. The average slope within this interval was used to define the slope for the elements. The ARC-INFO, TIN program was used to determine the slope and aspect at each node. The TIN program simply determines the slope of the ground surface as defined by the digitized elevation contours. As more and more finite elements are used to represent the curvilinear, spatially nonhomogeneous watershed, the nodal slopes tend toward elemental representation of slope, and in the limit, they are the same.

In the case of the arbitrary grid, the slope is averaged over the plane by taking several measurements within the plane. This does not allow accurate representation of the slope by the finite element grid since the spatial nonhomogeneity is lost by averaging. The linear element is not well suited to representing the curvature of the watershed surface. However, as more and more linear, one-dimensional elements of decreasing size are used to represent the watershed, the representation of topography improves as with any other element. The difficulty arises from the use of one-dimensional elements

of variable width to represent two-dimensional, spatially variable, parameters. Difficulties were found when using a two-dimensional scheme in the modeling of two-dimensional, spatially variable parameters that are anisotropic. In such a case the finite element grid must be orthogonal to the principal direction of slope at each element.

A two-dimensional finite element grid is capable of more accurately representing the spatial nonhomogeneity of the spatially variable parameters. The nodal slopes were determined by the value of the slope and aspect represented by the TIN Slope map in Figure 11. These slopes vary over the element in the case of the four-node quadrilateral because this element is capable of representing a warped surface.

The average slope could have been determined by integrating the slope over the element and dividing this integrand by the area, and the consistent stress method used to obtain the nodal slope values to be used in the modeling. This procedure, however, ignores micro-scale slope variation interior to the finite element. It is though, responsive to meso-scale slope variation represented by the spatial form of the 10-foot contour lines. Two-foot contour intervals could have been used but this would have resulted in considerably more finite elements than the first case of the arbitrary grid. This increased fineness in the grid representation would have increased the accuracy due to the increased number of

elements not due, solely, to the better finite element representation of a spatially variable parameter.

Soil properties were found to produce very little difference in the Green and Ampt parameters and consequently in the rainfall excess intensities. The watershed was therefore treated as one soil. The effect of the lumping of the soils is obscured by the difficulty in defining a unique set of infiltration parameters. Based on evidence from other researchers (Brakenseik and Onstad, 1977) the relative error in peak runoff to hydraulic conductivity is 2.68 percent. If a one percent error exists in the hydraulic conductivity then a 2.68 percent error in peak runoff rate results. In this case the hydraulic conductivities predicted according to the method of Rawls, Lane and Nicks (1987) method were as follows

Hastings Silt Loam, K = 0.0198 cm/hr,

Hastings Silty Clay Loam, K = 0.0087 cm/hr,

Colby Silt Loam, K = 0.0167 cm/hr,

Average, K = 0.0151 cm/hr

This average was not actually used in the modeling run since the effect of crusting obscured the range of different soil hydraulic conductivities. The hydraulic conductivities are estimated to range from 0.15 to 0.06 cm/hr due to the crusting. This range is estimated by using the variation of the CEC/Clay ratio from 0.2 to 0.65. The hydraulic conductivity used in the modeling of the May 4, 1959 rainstorm event, was K = 0.056 cm/hr. This

corresponds to the CEC/CLAY ratio of 0.65, which was the high end of the range of data used in the WEPP Model development (cf. Rawls, Lane and Nicks). The actual CEC/CLAY ranged from 0.67-0.79.

The Green and Ampt parameters used in both the arbitrary finite element grid and the hydrologic response area finite element grid are not a unique set. The rainfall intensitites used in calibration were found by inspection from a range of intensities produced by a range of hydraulic conductivities. Extreme difficulty was encountered in matching both volume and peak rate of outflow. When these same rainfall intensities were used with the hydrologic response area finite element grid a more accurate solution did not result. In fact a poorer agreement was found. This suggests that not only are the Green and Ampt parameters nonunique but the calibration is dependent on the finite element grid representation of the watershed domain. Depending on the spatial form of the finite element grid, different sets of input parameters will result from the calibration procedure. This difficulty obscures the advantages of better representation of spatially nonhomogeneous parameters.

2. Numerical Errors

Numerical errors also result from the mathematical formulation of the solution. These errors result from several sources within the finite element method itself. Other errors in represetation of the physical phenomenon

have been previously discussed.

Numerical oscillations and stability errors arise from the size of the eigenvalues in the equation

$$[C]\{\dot{A}\} = \{F^*\} \quad . \qquad [112]$$

The eigenvalues are calculated by solving for the eigenvector [E],

$$\{A\} = [E]\{Z\} \qquad [113]$$

or,

$$\{\dot{A}\} = [E]\{\dot{Z}\} \qquad [114]$$

where,

{Z} = solution vector of flow depths.

Writing [114] as

$$[C][E]\{\dot{Z}\} = \{F^*\} \qquad [115]$$

and multiplying by $[E]^{-1}$,

$$[E]^{-1}[C][E]\{\dot{Z}\} = [E]^{-1}\{F^*\} \qquad [116]$$

The matrices $[E]^{-1}[C][E]$ form the eigenvector [λ],

$$\begin{bmatrix} \lambda_1 & 0 & \cdots & \cdots & 0 \\ 0 & \lambda_2 & 0 & \cdots & 0 \\ 0 & 0 & \lambda_3 & 0 & \cdots \\ \cdots & \cdots & \cdots & \cdots & 0 \\ 0 & \cdots & 0 & \lambda_n & 0 \end{bmatrix} \begin{Bmatrix} Z_1 \\ Z_2 \\ Z_3 \\ \vdots \\ Z_n \end{Bmatrix} = \begin{Bmatrix} R^*_1 \\ R^*_2 \\ R^*_3 \\ \vdots \\ R^*_n \end{Bmatrix} \qquad [117]$$

For any row i,

$$\lambda_i \dot{Z}_i = R^*_i \qquad [118]$$

and

$$\dot{Z}_i = R^*/\lambda_i \qquad [119]$$

or

$$Z_i = \int R^*/\lambda_i \, dt = \Delta t(R^*/\lambda_i) \; . \qquad [120]$$

Writing [119] as

$$\dot{Z}_i = \frac{Z_{new} - Z_{old}}{\Delta t} \qquad [121]$$

the recursive formulation results in

$$\begin{aligned} Z_1 &= a\Delta t + Z_0 \\ Z_2 &= a\Delta t + Z_1 = 2a\Delta t + Z_0 \\ &\cdot \\ \dot{Z}_n &= na\Delta t + Z_0 \; . \end{aligned} \qquad [122]$$

Equation [122] does not amplify errors that may occur in the right-hand side term $na\Delta t$ since it does not contain any Z terms. Because of this the solution of the kinematic wave equaitons in general may proceed without numerical oscillations or stability errors. This is a consequence of the partial differential equation form and the finite difference solution in the time domain.

Nonlinearity in the partial differential equation however can pose difficulties in the solution algorithm. It is necessary to start with sufficiently close values of flow depth at each time step such that the iterative solution converges. If large step increases in rainfall excess intensities occurs or large values of rainfall excesses occur, the iterative solution will not converge but rather flow depths becomes negative. If initial estimates of flow depth at each time step are used that are not the previous solution values, the solution again does not converge. Convergence was achieved by using the dry bed initial values at the first time step and the previous-time flow depths as the beginning values for iterative solution at succeeding time-steps.

As evidenced in the literature, the difficulties encountered in applying a deterministic, distributed parameter model to watershed hydrology fell into three categories. These categories largely center around the types of errors encountered in the literature for the type of modeling performed for this research. These categories

are numeric errors, model equation errors, and parameter estimation errors. The approaches taken to meet the project objectives were performed in order to reach the overall goal of this research to more accurately predict the actual outflow hydrograph from a watershed of nonuniform, spatially distributed parameters. Conclusions derived from this research follow together with recommendations and future applications of the method developed.

Numeric errors are those that arise from the method itself such as inaccuracies and instability in the time solution of the finite element method. These errors arise due to the form of the time dependent equation that is solved by standard finite difference techniques such as in equation [92]. Numeric errors can be subdivided into physical reality, numerical oscillations, accuracy, and stability.

Physical reality is observed whenever rainfall excess added to a node causes surrounding nodes to also increase. In the solution of heat flow and groundwater flow, it is possible to obtain solutions that for initial time steps the temperature or pressure head decreases when it should be increasing (Segerlind, 1984). A physical reality error results whenever this occurs.

Numerical oscillations occur when at each time step the solution is first higher then lower than the true solution thus causing oscillations about the solution.

Stability errors occur when an incremental error at each time step grows until the solution deteriorates.

As a result of the equation [116], the solution of the kinematic wave equation as represented by [106] does not suffer from stability and oscillation errors prevalent in other governing equations such as the field equation for heat flow. The only other possible source of numeric errors are those arising from the accuracy of the ordinary differential equations, e.g. the time dependent equation [105] in representing the partial differential equations, i.e., the conservation of mass equation [55]. This error is accounted for by observing the Courant condition. The Courant condition is a consequence of the partial differential equation theory, the Method of Characteristics. It was observed through the choice of the time step for the maximum rainfall excess and the longest plane. This choice of time step resulted in a solution that was accurate and free of oscillations or instability. The computation of the Courant condition from known physical parameters allows selection of the time step prior to modeling using the finite element method. As seen in Figures 14 and 15, a solution free of instability and oscillations resulted.

Model equation errors arise from the simplification of the full dynamic equation by the kinematic or diffusion analogy and kinematic shocks. The kinematic shocks that plagued previous researchers were avoided in the method

developed by this research. The method used here calculates the nodal flow rates using nodal slopes and Manning n values. This improvement over previous methods allowed an accurate solution of the kinematic wave equations using the finite element method. Both linear one-dimensional and two-dimensional elements were used successfully in this solution in the modeling of a two-dimensional domain of spatially nonhomogeneous slopes. This two-dimensional domain possessed complex topographical curvature as represented by the TIN slope map in Figure 11. This slope map provided the basis for the selection of nodal slope values that resulted in the solution of the kinematic wave equation free of kinematic shock.

Parameter estimation errors arise from uncertainty and from spatial variation of infiltration, rainfall, roughness and other parameters over the watershed domain. The spatial variation of the watershed parameters were represented by the finite element grid by assigning to each element and node the appropriate parameters. Rainfall excess was assigned as an element constant as well as assumed constant over the watershed.

Errors in rainfall excess arise from many sources including the assumption that infiltration, rainfall, roughness and other parameters are uniform over the entire watershed. Where the accuracy and the number of sampling points are sufficient, spatial statistics may be used to advantage to interpolate with known variance at a specified

location the value of a parameter. The location of the parameter is dictated by the finite element grid which in turn is dictated by the spatial variability of the parameters. Lack of knowledge apriori of the infiltration parameters and the inability to select an unique set by calibration limit the viability of calibrating.

Proper representation arises from the proper selection or the use of elements that maintain faithful representation of the hydrologically homogeneous character of subareas within the watershed. Improper representation may result from an incomplete knowledge of the parameters and the variation over the watershed or with time during the modeling process. The Geographic Information System allowed proper representation of the spatially nonhomogeneous parameter, slope. By utilizing the hydrologic response area, finite-element grid proper representation occurred.

Accurate modeling of the hydrologic response areas within the watershed during an unsteady rainstorm is possible if the infiltration parameters used to define rainfall excess is sufficiently well known. Better definition of the rainfall-runoff relation is needed. The finite element method holds promise as a mathematical model capable of accurately and efficiently solving the distributed, deterministic surface water equations in a watershed. The Geographic Information System holds promise as an efficient means of handling the large volume of input

data required by distributed, deterministic models.

The goal of this research has been achieved by accomplishing the following three objectives using the following approaches. The objectives and approaches were:

Objective 1. Define hydrologic response areas that exhibit similar soil infiltration parameters, surface roughness, and slope for a given watershed.

Approach: A Geographic Information System was used to search, smooth and aggregate areas of similar soil infiltration parameters, surface roughness, and slope thus producing the specific hydrologic response areas.

The approach to Objective 1 utilized the ARC-INFO GIS to digitize the maps of soils, landuse, and topography. Based on the infiltration parameters associated with the soils, the Manning n associated with the landuse, and the slope calculated from the 2-foot contour elevation map; hydrologic response areas were produced. Due to the homogeneity of the soils and landuse, slope was the only spatially nonhomogeneous parameter modeled. The ARC-INFO Triangular Irregular Network (TIN) program was used to define the slope and aspect from the 2-foot contour elevation map. From the TIN Slope map, nodal slope values were determined for each node of each element. The Slope map shown in Figure 11 was produced for a 1% interval. The hydrologic response area finite element grid was based on the 10-foot contour elevations. The GIS proved to be an

effective means of searching, smoothing and aggregating values of the slope parameter and thus defining hydrologic response areas for the anisotropic finite element grid. The GIS was also used to determine the slopes at the nodes for the isotropic finite element grid, however, the aspects were aligned such that the slope was parallel to the sides of the elements representing streamlines.

Objective 2. Apply the finite element method to the specific hydrologic response areas to compute and route the overland flow to the outlet.

Approach: The rate and volume of infiltration was modeled by the Green and Ampt infiltration equation. The equation parameters were calibrated for the watershed using an arbitrary finite element grid. The rainfall excess thus defined becomes the lateral inflow for use in solution of the overland flow equations.

The approach to Objective 2 utilized the Green and Ampt infiltration equation. The Green and Ampt parameters along with the rainfall excess were computed using the WEPP project programs with the aid of Dr. Walter Rawls, ARS Water Data Laboratory, Beltsville Maryland. For a description of the procedures used see Rawls, Lane and Nicks (1987). The initial estimates of the Green and Ampt parameters used measured soil properties. The rainfall excesses computed for the three soils were nearly identical during the rainstorm event. Due to the similarity, the watershed was modeled as having one soil.

Calibration of the Green and Ampt parameters was performed by varying the hydraulic conductivity and the initial abstraction until the calculated volume and peak outflow rate matched as closely as possible the actual outflow rate. The calibration was performed for the arbitrary finite element grid. The final values of initial abstraction and hydraulic conductivity were not determined directly but rather the rainfall excess intensities were determined by inspection of several sets of hydraulic conductivities and initial abstraction values. These Green and Ampt parameters appear to vary during the storm. The simply infiltration model was not capable of predicting the correct Green and Ampt parameters and resulting rainfall intensities.

After calibrating the Green and Ampt parameters for the arbitrary finite element grid, the hydrologic response area grid was modeled using the calibrated rainfall excess. The purpose for this was to investigate the effect of better description of the spatial parameters such as slope by the two dimensional, hydrologic response area grid. The Galerkin finite element formulation was applied to the kinematic wave equations producing the flow rate and flow depth solution. The solution was performed in the time domain during the unsteady rainstorm event. The time solution was performed using the central difference, finite difference form. This formulation resulted in a solution free from the physical reality, numerical oscillations,

instability, kinematic shock and accuracy errors reported previous literature.

It was necessary to form an isotropic finite element grid such that the solution may be obtained. The resulting finite element grid was a better representation of the spatially varying slope and the solution to a spatially varying flow depth in two-dimensions. The relative accuracy of the hydrologic response area finite element grid to the arbitrary finite element grid is unknown due to uncertainty in the infiltration parameters and resulting rainfall excesses.

Objective 3. Compare the accuracy of the outflow hydrographs to the actual outflow hydrograph for a given rainstorm event for the following two cases:

a. A finite element grid that is of an arbitrary spatial form.

b. A finite element grid formed from hydrologic response areas defined by the Geographic Information System.

Approach: The rate and volume of runoff was modeled by the finite difference/finite element method of solving the kinematic wave equation for overland flow. The excess rainfall was defined by the infiltration equation. The outflow hydrograph was calculated for the outlet of the watershed for the two cases described above. A finite

element model, utilizing linear, one-dimensional and two-dimensional finite elements was used to compute the overland flow equations. Lotus 1-2-3 release 2.01 was used for the solution of the linear, one-dimensional finite element grid. A FORTRAN computer program identical in algorithm to the Lotus 1-2-3 spread sheet was used for the linear, two-dimensional finite element grid. The spread sheet formulas and the computer program are contained in the Appendix. The validity of the method was checked by comparing the computed and analytical solution outflow hydrographs. The validity was checked for a single plane with the results contained in the Appendix.

The finite element solution of the kinematic wave equations when solved with nodal rather than elemental flow rates produces a close approximation to the analytic solution and resulted in a close approximation of the actual outflow hydrograph for this rainstorm event. The flexibility of this method allows modeling of watershed runoff using spatially nonhomogeneous parameters. The spatial variability must be lumped interior to the finite element. Finite elements corresponding to the spatially nonhomogeneous parameter allow a much more accurate representation of the parameters. It was not determined whether the hydrologic response area, finite element grid produced a better agreement between the calculated and actual hydrograph due to the uncertainty in the infiltration parameters.

The method developed through this research calculates the two-dimensional solution to the kinematic wave equation hydrograph for a watershed of nonuniform, spatially nonhomogeneous parameters such as slope. Further, this method is free from kinematic shocks which had prevented earlier researchers from solving the problem as a continuum.

V. CONCLUSIONS AND RECOMMENDATIONS

The approaches taken to meet the project objectives were performed in order to reach the overall goal of this research--to more accurately predict the actual outflow hydrograph from a watershed of nonuniform, spatially distributed parameters. Conclusions derived from this research follow together with recommendations and future applications of the method developed.

A. Conclusions

The method developed through this research calculates the two-dimensional solution to the kinematic wave equation hydrograph for a watershed of nonuniform, spatially nonhomogeneous parameters such as slope. From this research it may be concluded that:

1. The GIS was effective in searching, smoothing and aggregating values of the spatially variable slope parameter for use in the finite element model.

2. The Green and Ampt infiltration model used did not adequately predict the rainfall excess intensities in order to accurately simulate runoff from an actual storm using the finite

element model.

3. The finite element model developed through this research results in a solution free from kinematic shock for the two-dimensional kinematic wave equation in a watershed continuum.

B. Recommendations

The ability of the Geographic Information System and the finite element method to model and display modeled results of the watershed surface runoff recommends its use for further research. It is recommended that:

1. Further research is needed to better measure and describe the spatially variable parameters affecting surface flow, particularly infiltration.

2. The use of geostatistics may provide valuable information as to the detail required to accurately model spatially variability in the input parameters.

3. This research should be extended to consider both overland and channel flow for larger watershed systems. This extension should include diffusion and full dynamic equation modeling.

4. Better calibration techniques should be investigated that are capable of handling the

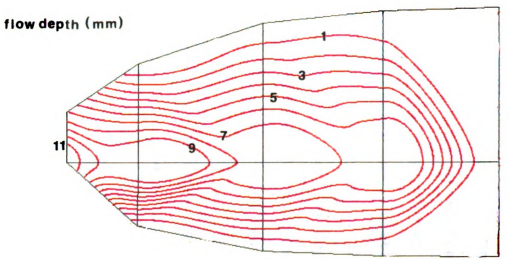

Figure 24 Spatial Distribution of Peak Runoff Flow Depth.

the nodes were used in producing the contours. The peak values occur at different times during the storm runoff period.

The value of predicting the spatial distribution of surface flow is realized if the distribution of concentration of nutrients or pesticides is capable of being predicted for a watershed. This ability provides insight into the location and source of contaminants in overland flow. The flow depth shown in Figure 24 may be interpreted as the highest concentrations of contaminants. Since the flow rate over any particular location during a storm event is related to the flow depth by the Manning or Chezy equation', the concentration expressed as a mass fraction of the flow rate will correspond to the flow depth.

Further research is needed to better describe the spatially variable parameters affecting surface flow, particularly infiltration. The method developed through this research provides a better description of the hydrologic processes in a two-dimensional domain. It also provides insight into the transport phenomena of agricultural pollution by pesticides and nutrients in surface and subsurface water as affected by overland flow and infiltration for an agricultural watershed.

VI. REFERENCES

Abdel-Razaq, A.Y., W. Viessman, and J.W. Hernandez. "A Solution to the Surface Runoff Problem," Journal of the Hydraulics Division, ASCE, Vol. 93, No. HY6 (November 1967), 335-352.

Andrews, R.G. "The Use of Relative Infiltration Indices in Computing Runoff." Paper presented at the American Society of Agricultural Engineers, 1954. In R.E. Rallison, q.v.

Band, L.E. "Topographic Partition of Watersheds with Digital Elevation Models," Water Resources Research, Vol. 22, No. 1 (January 1986). Published by the American Geophysical Union.

Bartholic, J. and K. Kittleson. "Temperature and Reflectance Monitoring from Satelites as an Indication of Shift and Impact of Vegetation Change." Paper presented at the Nineteenth International Symposium on Remote Sensing of Environment, Ann Arbor, Michigan, October 1985.

Biswas, A.K. "Beginning of Quantitative Hydrology," Journal of the Hydraulics Division, ASCE, Vol. 94, No. HY5 (September 1968), 1299-1316.

Brakenseik, D.L. and C.A. Onstad. "Parameter Estimation of the Green and Ampt Infiltration Equation," Water Resources Research, Vol. 13, No. 6 (December 1977). Published by the American Geophysical Union.

_____ and W.J. Rawls. "Agricultural Effects on Soil Water Processes, Part II: Green and Ampt Parameters for Crusting Soils," Transactions of the ASAE, 26:(1983), 1753-1757.

Brutsaert, W. "The Initial Phase of the Rising Hydrograph of Turbulent Free Surface Flow with Unsteady Lateral Inflow," Water Resources Research, Vol. 4, No. 6 (December 1968), 1189-1192.

_____. "De Saint Venant Equations Experimentally Verified," Journal of the Hydraulics Division, ASCE, Vol. 97, No. HY9 (September 1971), 1387-1401.

"Central Great Plains Experimental Watershed, A Summary Report of 30 Years of Hydrologic Research," Agricultural

Research Service, USDA, n.d.

Chen, C.L. and Ven Te Chow. "Formulation of the Mathematical Watershed-Flow Model," Journal of the Mechanics Division, ASCE, Vol. EM3 (June 1971), 809-828.

Chu, S.T. "Infiltration During an Unsteady Rain," Water Resources Research, Vol. 14, No. 3 (June 1978). Published by the American Geophysical Union.

Crandall, S.H. Engineering Analysis, A Survey of Numerical Procedures. McGraw-Hill Book Company, Inc., New York, 1956, pp. 322-324.

Grace, R.A. and P.S. Eagleson. "The Modeling of Overland Flow," Water Resources Research, Vol. 2, No. 3 (1966), 393-403.

Grayman, W.M. "Land-Based Modeling System for Water Quality Management Studies," Journal of the Hydraulics Division, ASCE, Vol. 101, No. HY5 (May 1975), 567-580.

Gupta, S.K. and S.I. Solomon. "Distributed Numerical Model for Estimating Runoff and Sediment Discharge of Ungaged Rivers, 1. The Information System," Water Resources Research, Vol. 13, No. 3 (June 1977). Published by the American Geophysical Union.

Guymon, G.L. "Application of the Finite Element Method for Simulation of Surface Water Transport Problems," Institute of Water Resources Report No. IWR-21, University of Alaska, Anchorage, 1972.

Handbook of Chemistry and Physics, 40th ed., Chemical Rubber Publishing Co., Cleveland, Ohio, 1972-1973.

Henderson, F.M. Open Channel Flow, Macmillan Publishing Co., Inc., New York, 1966, pp. 288-324.

Huggins, L.F. and J.R. Burney. "Surface Runoff, Storage and Routing, Chapter 5." In Hydrologic Modeling of Small Watersheds, edited by C.T. Haan, ASAE Monograph No. 5 (1982), 169-225.

Huggins, L.F. and E.J. Monke. "The Mathematical Simulation of the Hydrology of Small Watersheds," Water Resource Research Center Technical Report No. 1, Purdue University, 1966.

Jayawardena, A.W. On The Application of the Finite Element Method to Catchment Modeling. Ph.D. Thesis, University of London, King's College, 1976.

_____ and J.K. White. "A Finite Element Distributed Catchment Model, II. Application to Real Catchments," Journal of Hydrology, Vol. 42, No. 3/4 (July 1979). Published by the Elsevier Scientific Publishing Company, Amsterdam, Oxford, New York.

Judah, O.M. Simulation of Runoff Hydrographs from Natural Watersheds by Finite Element Method, Ph.D. Thesis, Virginia Polytechnic Institute and State University, Blacksburg, Virginia, 1973.

_____, V.O. Shanholtz, and D.N. Contractor. "Finite Element Simulation of Flood Hydrographs," Transactions of the ASAE, 1975, pp. 518-522.

Kibler, D.F. and D.A. Woolhiser. The Kinematic Cascade, Colorado State University, Fort Collins, Publication No. 39, March 1970.

Liggett, J.A. Unsteady Flow in Open Channels, Volume I, edited by Mahmood and Yevjevich, Water Resources Publications, Fort Collins, Colorado, 1975.

Mein, R.G. and C.L. Larson, Modeling Infiltration Component of the Rainfall-Runoff Process. Water Resources Research Center, University of Minnesota, Graduate School, 1971.

Mockus, Victor. "Estimation of Total (and Peak Rates of) Surface Runoff for Individual Storms," Exhibit A of Appendix B, Interim Survey Report Grand Neosho River Watershed, USDA, December 1, 1949. In Rallison, q.v.

Morris, E.M., K. Blyth, and R.T. Clarke. "Watershed and River Characteristics, and Their Use in a Mathematical Model to Predict Flood Hydrographs," in Remote Sensing Application in Agriculture and Hydrology, ed. by Georges Fraysse, A.A. Balkema, Rotterdam, 1980.

Morris, E.M. and D.A. Woolhiser. "Unsteady One-Dimensional Flow over a Plane: Partial Equilibrium and Recession Hydrographs," Water Resources Research, Vol. 16, No. 2 (April 1980), 355-360.

Peters N., G. Blandford, and M.E. Meadows. "Finite Element Simulation of Overland Flow," Proceedings of the Specialty Conference on Advances in Irrigation and Drainage: Surviving External Pressures, ASCE, July 1983, pp. 466-475.

"Phase I Oconee Basin Pilot Study Trail Creek Test." Hydrologic Engineering Center, U.S. Army Corps of Engineers, Davis California, September 1975.

Potter, M.C. and J.F. Foss, Fluid Mechanics. Great Lakes Press, Inc., Okemos, Michigan, 1982.

Rallison, R.E. "Origin and Evolution of the SCS Runoff Equation," Proceedings of the Symposium on Watershed Management '80, ASCE, 1980.

Rawls, W. J., D.L. Brakensiek, and B. Soni. "Agricultural Management Effects on Soil Water Processes, Part I: Soil Water Retention and Green and Ampt Infiltration Parameters." Transactions of the ASAE 26 (1983).

_____, L.J. Lane, and A.D. Nicks. "Hydrologic Components." In Compilation of Water Erosion Prediction Project (WEPP) Papers, presented at the 1987 International Winter Meeting of ASAE, Chicago, Illinois, 1987.

Segerlind, L.J. Applied Finite Element Analysis, 1st ed., John Wiley and Sons, New York, 1976.

_____. Applied Finite Element Analysis, 2nd ed., John Wiley and Sons, New York, 1984.

Smith, R.E. and D.A. Woolhiser. "Mathematical Simulation of Infiltrating Watersheds," Hydrology Papers, No. 47, Colorado State University, Fort Collins, January 1971.

Smith, V.E. Philosophical Physics, Harper & Brothers, New York, 1950, p. 8.

Taylor, C. "A Computer Simulation of Direct Run-Off," in Finite Elements in Water Resources, edited by W.G. Gray, G.F.Pinder, and C.A. Brebbia, Pentech Press, London, 1976.

_____, G. Al-Mashidani, and J.M. Davis. "A Finite Element Approach to Watershed Runoff," Journal of Hydrology, Vol. 21, No. 3 (March 1974), 231-246.

_____ and P.S. Huyakorn. "A Comparison of Finite Element Based Solution Schemes for Depicting Overland Flow," Applied Mathematical Modelling, edited by C.A. Brebbia, Vol. 2, No. 3 (September 1978), 185-190.

Vitruvius, Ten Books on Architecture. Translated by Morris H. Morgan, Dover Publications, Inc., New York, 1960, pp. 225-232.

Woolhiser, D.A. Unsteady Flow in Open Channels, Volume II, edited by Mahmood and Yevjevich, Water Resources Publications, Fort Collins, Colorado, 1975, pp. 485-508.

_____ and J.A. Liggett. "Unsteady, One-dimensional Flow over a Plane--the Rising Hydrograph," Water Resources

Research, Vol. 3, No. 3 (Third Quarter, 1967), 753-771.

Yen, B.C. "Open Channel Flow Equations Revisited," Journal of the Engineering Mechanics Division, ASCE, Vol. 99, No. EM5 (October 1973), 979-1009.

Zobrist, A.L. "Elements of an Image Based Information System," Manual of Remote Sensing, 2nd ed., Volume 1, American Society of Photogrammetry, p. 946.

APPENDIX

Modeling Data

The following is a listing of the Lotus 1-2-3 work sheet for the arbitrary finite element grid solution. The cell formulas are printed unformatted for each section of the worksheet separated by headings describing the function of the section.

ELEMENT DATA HEADING

```
A1: [W12] 'ELEMENT
B1: 'DATA
H1: [W12] 66
A3: [W12] ^element
B3: ^node1
C3: [W12] ^node2
D3: [W12] ^node3
E3: [W12] ^node4
F3: [W12] ^slope1
G3: [W12] ^slope2
H3: [W12] ^slope3
I3: [W12] ^slope4
J3: [W14] ^n1
K3: ^n2
L3: [W12] ^n3
M3: ^n4
N3: ^width
O3: ^ROLD
P3: [W12] ^RNEW
A4: [W12] ^1
B4: 0
C4: [W12] 171
F4: [W12] 0.0406
G4: [W12] 0.0406
J4: [W14] 0.035
K4: 0.035
N4: 353
O4: 0
P4: [W12] 0
A5: [W12] ^2
B5: 171
C5: [W12] 342
F5: [W12] 0.0406
G5: [W12] 0.0669
J5: [W14] 0.035
K5: 0.035
N5: 333
A6: [W12] ^3
B6: 342
C6: [W12] 507
F6: [W12] 0.0669
G6: [W12] 0.0562
J6: [W14] 0.035
K6: 0.035
N6: 206
```

ELEMENTAL EQUATIONS OF THE FORM $[C]\{\dot{A}\} = \{F\}$

```
A9: [W12] 'ELEMENT NO 1
A10: [W12] ^[C]
C10: [W12] ^{h}new
D10: [W12] '{F}=
E10: [W12] ^[C]
F10: [W12] ^*{AOLD)
G10: [W12] ^DT/2[K]*
H10: [W12] 'QOLD+QNEW
A11: [W12] 2*($C$4-$B$4)*$N$4/6
B11: ($C$4-$B$4)*$N$4/6
D11: [W12] +$E$11+$F$11+$G$11+$H$11+$I$11
E11: [W12] 2*($C$4-$B$4)*$N$4*$B$27/6
F11: [W12] ($C$4-$B$4)*$N$4*$B$28/6
G11: [W12] -($B$37/2)*(-1)*((1-$B$38)*$D$27+$B$38*$D$33)
H11: [W12] -($B$37/2)*(1)*((1-$B$38)*$D$28+$B$38*$D$34)
I11: [W12] +$B$37*($C$4-$B$4)/2*((1-$B$38)*$N$4*$O$4+
     $B$38*$N$4*$P$4)
A12: [W12] ($C$4-$B$4)*$N$4/6
B12: 2*($C$4-$B$4)*$N$4/6
D12: [W12] +$E$12+$F$12+$G$12+$H$12+$I$12
E12: [W12] ($C$4-$B$4)*$N$4*$B$27/6
F12: [W12] 2*($C$4-$B$4)*$N$4*$B$28/6
G12: [W12] -($B$37/2)*(-1)*((1-$B$38)*$D$27+$B$38*$D$33)
H12: [W12] -($B$37/2)*(1)*((1-$B$38)*$D$28+$B$38*$D$34)
I12: [W12] +$B$37*($C$4-$B$4)/2*((1-$B$38)*$N$4*$O$4+
     $B$38*$N$4*$P$4)
A13: [W12] 'ELEMENT NO2
A14: [W12] ^[C]
C14: [W12] ^{h}new
D14: [W12] '{F}=
E14: [W12] ^[C]
F14: [W12] ^*{AOLD)
G14: [W12] ^DT/2[K]*
H14: [W12] 'QOLD+QNEW
A15: [W12] 2*($C$5-$B$5)*$N$5/6
B15: ($C$5-$B$5)*$N$5/6
D15: [W12] +$E$15+$F$15+$G$15+$H$15+$I$15
E15: [W12] 2*($C$5-$B$5)*$N$5*$B$28/6
F15: [W12] ($C$5-$B$5)*$N$5*$B$29/6
G15: [W12] -($B$37/2)*(-1)*((1-$B$38)*$D$28+$B$38*$D$34)
H15: [W12] -($B$37/2)*(1)*((1-$B$38)*$D$29+$B$38*$D$35)
I15: [W12] +$B$37*($C$5-$B$5)/2*((1-$B$38)*$N$5*$O$4+
     $B$38*$N$5*$P$4)
A16: [W12] ($C$5-$B$5)*$N$5/6
B16: 2*($C$5-$B$5)*$N$5/6
D16: [W12] +$E$16+$F$16+$G$16+$H$16+$I$16
E16: [W12] ($C$5-$B$5)*$N$5*$B$28/6
F16: [W12] 2*($C$5-$B$5)*$N$5*$B$29/6
G16: [W12] -($B$37/2)*(-1)*((1-$B$38)*$D$28+$B$38*$D$34)
H16: [W12] -($B$37/2)*(1)*((1-$B$38)*$D$29+$B$38*$D$35)
```

```
I16: [W12] +$B$37*($C$5-$B$5)/2*((1-$B$38)*$N$5*$O$4+
     $B$38*$N$5*$P$4)
A17: [W12] 'ELEMENT NO3
A18: [W12] ^[C]
C18: [W12] ^{h}new
D18: [W12] '{F}=
E18: [W12] ^[C]
F18: [W12] ^*{AOLD)
G18: [W12] ^DT/2[K]*
H18: [W12] 'QOLD+QNEW
A19: [W12] 2*($C$6-$B$6)*$N$6/6
B19: ($C$6-$B$6)*$N$6/6
D19: [W12] +$E$19+$F$19+$G$19+$H$19+$I$19
E19: [W12] 2*($C$6-$B$6)*$N$6*$B$29/6
F19: [W12] ($C$6-$B$6)*$N$6*$B$30/6
G19: [W12] -($B$37/2)*(-1)*((1-$B$38)*$D$29+$B$38*$D$35)
H19: [W12] -($B$37/2)*(1)*((1-$B$38)*$D$30+$B$38*$D$36)
I19: [W12] +$B$37*($C$6-$B$6)/2*((1-$B$38)*$N$6*$O$4+
     $B$38*$N$6*$P$4)
A20: [W12] ($C$6-$B$6)*$N$6/6
B20: 2*($C$6-$B$6)*$N$6/6
D20: [W12] +$E$20+$F$20+$G$20+$H$20+$I$20
E20: [W12] ($C$6-$B$6)*$N$6*$B$29/6
F20: [W12] 2*($C$6-$B$6)*$N$6*$B$30/6
G20: [W12] -($B$37/2)*(-1)*((1-$B$38)*$D$29+$B$38*$D$35)
H20: [W12] -($B$37/2)*(1)*((1-$B$38)*$D$30+$B$38*$D$36)
I20: [W12] +$B$37*($C$6-$B$6)/2*((1-$B$38)*$N$6*$O$4+
     $B$38*$N$6*$P$4)
```

FLOW DEPTHS AND FLOW RATES AT EACH NODE, BOTH NEW AND OLD VALUES DEFINED BY THE MANNING EQUATION. INVERSE AND SOLUTION MACROS ARE PRECEEDED BY '/.

```
A27: [W12] ^h1old
B27: U 0
C27: [W12] ^Q1old
D27: [W12] 1.486/$J$4*$F$4^0.5*$B$27^(5/3)*$N$4
F27: [W12] 'INVERSE
G27: U [W12] 'SOLUTION\D
A28: [W12] ^h2old
B28: U 0.0017120387
C28: [W12] ^Q2old
D28: [W12] (1.486/$K$4)*$F$4^0.5*$B$28^(5/3)*($N$4+$N$5)/2
F28: [W12] '/DMI~~~
G28: [W12] '/DMM~~~
A29: [W12] ^h3old
B29: U 0.0037515851
C29: [W12] ^Q3old
D29: [W12] 1.486/$K$5*$G$5^0.5*$B$29^(5/3)*($N$5+$N$6)/2
A30: [W12] ^h4old
B30: U 0.0072532181
C30: [W12] ^Q4old
D30: [W12] (1.486/$K$6)*$G$6^0.5*$B$30^(5/3)*$N$6
```

```
F32: U [W12] 'COPY\C
G32: U [W12] 'NEXT TIME STEP
A33: [W12] ^h1NEW
B33: U 0
C33: [W12] ^Q1NEW
D33: [W12] 1.486/$J$4*$F$4^0.5*$B$33^(5/3)*$N$4
E33: U [W12] 6
F33: U [W12] '/C$B$34..$B$36~$B$28..$B$30~/C$P$4~$O$4~
A34: [W12] ^h2NEW
B34: U 0.0015953261
C34: [W12] ^Q2NEW
D34: [W12] (1.486/$K$4)*$F$4^0.5*$B$34^(5/3)*($N$4+$N$5)/2
A35: [W12] ^h3NEW
B35: U 0.0034417683
C35: [W12] ^Q3NEW
D35: [W12] 1.486/$K$5*$G$5^0.5*$B$35^(5/3)*($N$5+$N$6)/2
A36: [W12] ^h4NEW
B36: U 0.00667484
C36: [W12] ^Q4NEW
D36: [W12] (1.486/$K$6)*$G$6^0.5*$B$36^(5/3)*$N$6
```

TIME STEP IN SECONDS AND TIME WEIGHTING COEFFICIENT

```
A37: [W12] 'DELTA
B37: 60
A38: [W12] 'THETA
B38: 0.5
```

DIRECT STIFFNESS METHOD SUMMING THE ELEMENTAL MATRIX ENTRIES TOGETHER WITH BOUNDARY CONDITIONS INTO THE GLOBAL MATRIX

```
G38: U [W12] ^'{F}
G38: U [W12] ^'{F}
C39: U [W12] \-
D39: U [W12] \-
E39: U [W12] \-
F39: U [W12] \-
G39: U [W12] \-
C40: U [W12] +B12+A15
D40: U [W12] +B15
E40: U [W12] 0
G40: U [W12] +D12+D15
C41: U [W12] +A16
D41: U [W12] +B16+A19
E41: U [W12] +B19
G41: U [W12] +D16+D19
C42: U [W12] 0
D42: U [W12] +A20
E42: U [W12] +B20
G42: U [W12] +D20
```

INVERSE OF THE GLOBAL [C] MATRIX MULTIPLIED TIMES THE $\{F^*\}$ VECTOR FOR THE SOLUTION OF THE NODAL FLOW DEPTHS h2,h3,h4

```
C45: U [W12] 0.0000279141
D45: U [W12] -0.0000096409
E45: U [W12] 0.0000048205
C46: U [W12] -0.0000096409
D46: U [W12] 0.0000397219
E46: U [W12] -0.0000198609
C47: U [W12] 0.0000048205
D47: U [W12] -0.0000198609
E47: U [W12] 0.0000981917
```

The worksheet solution and methodology was tested for a single plane consisting of the same input data for element No. 1. The solution was compared to the analytic solution using the Method of Characteristics. The analytic solution states that prior to equilibrium the flow depth is

$$h = i*t$$

where,

i = rainfall intensity,
t = time since start of the rainfall excess.
h = flow depth.

The flow rate is

$$q = mh^{\alpha}$$

where,

$m = (1.486/n)*S^{1/2}$,
$\alpha = 5/3$ for overland flow.

The following Figure A1 shows the comparison of the finite element analysis and the analytic solution for a single plane. The parameters used for this plane is the upper plane in the arbitrary grid finite element solution.

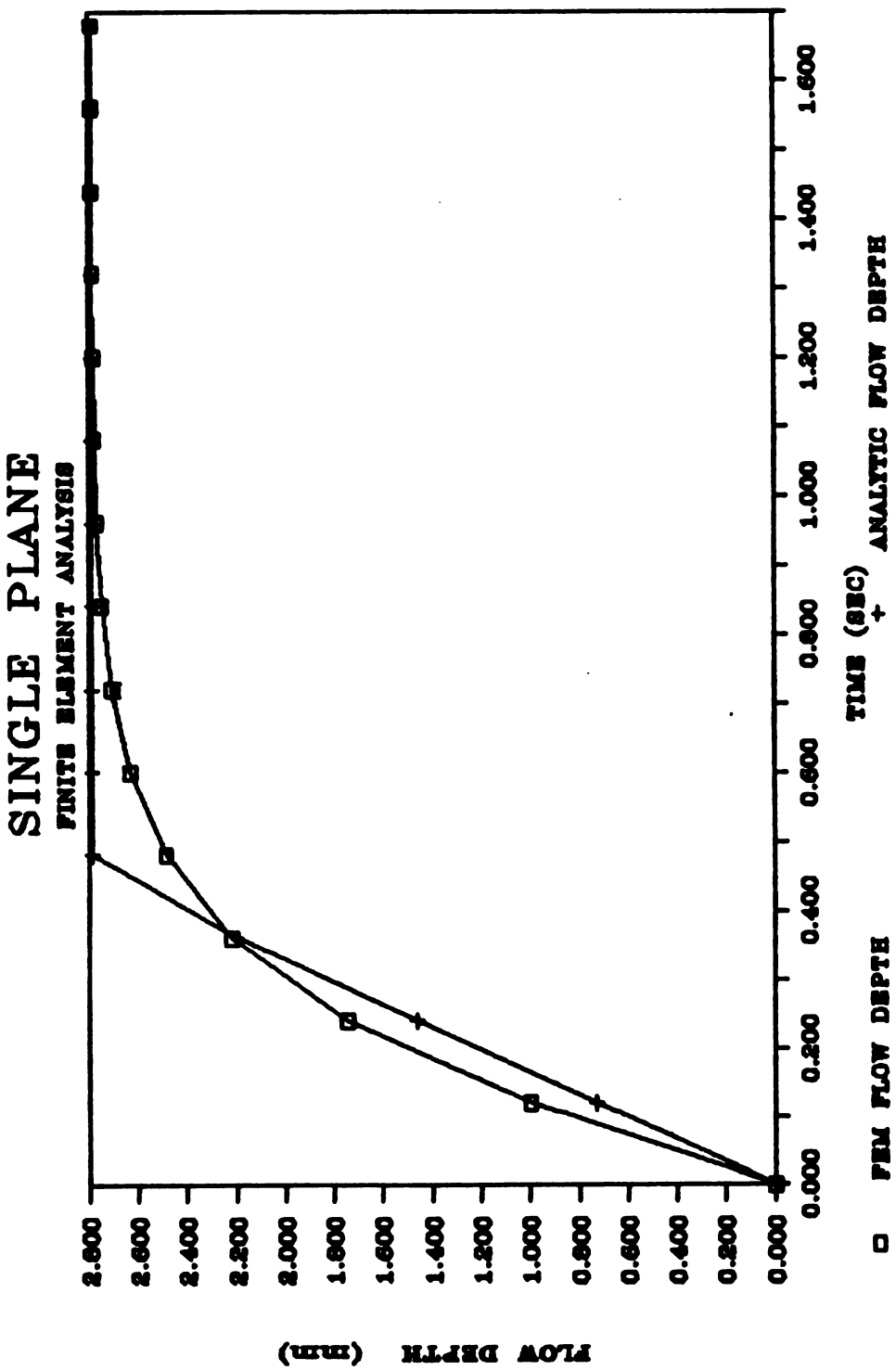

Figure A1 Comparison of the Finite Element and Analytic Solution for Flow Depth on a Single Plane.

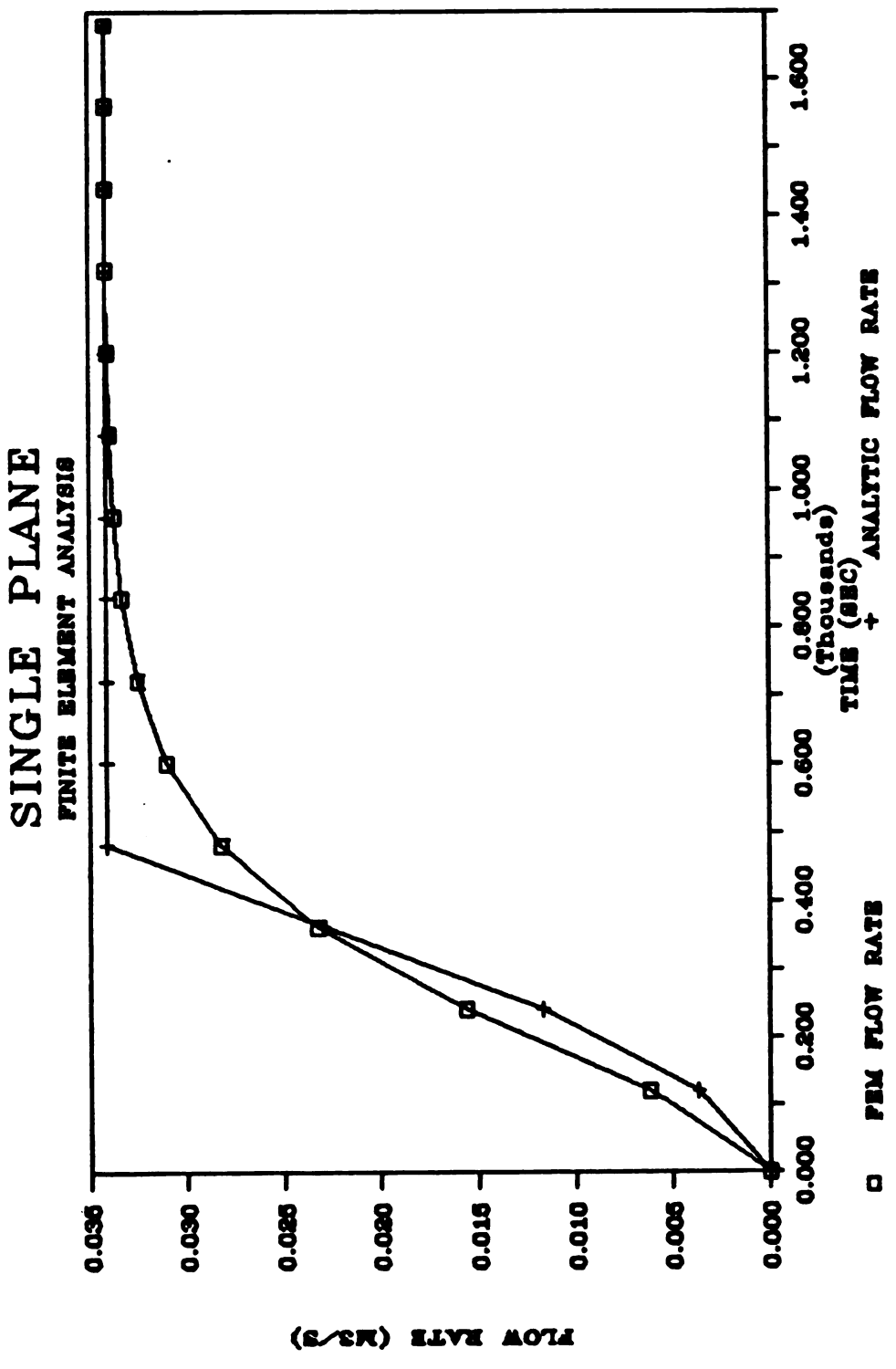

Figure A2 Comparison of the Finite Element and Analytic Solution for Flow Rate from a Single Plane.

Conputer solution of the hydrologic response area finite element grid was performed utilizing the following listing of FORTRAN code.

```
**************************************************************************

      PROGRAM MAINSTRM

C     This program finds a linear solution to a finite element overland
C     flow problem for a global system of two-dimensional elements.

C     Units of measurement are taken from the English System.

C     To avoid internal storage of large amounts of data, this program
C     reads element and node information from external files as needed.

C     In the variable listing below, the X-direction is identical to the
C     direction of flow at a given node.

C     DELTAT     = Length (seconds) of time step.
C     GCHOLD( ) = GCM( , ) * GHOLD(2)
C     GCM( , )  = Global Capacitance Matrix f    T
C                                              j½N½ ½N½
C     GF( )      = Global Force vector
C     GHNEW(I)  = Flow depth H (feet) at node I at end of current
C                 time step.
C     GHOLD(I)  = Flow depth H (feet) at node I at end of previous
C                 time step.
C     GHTRY(I)  = Flow depth H (feet) at node I tried for solution
C                 iteration. When solution GHNEW is close to GHTRY,
C                 solution is accepted.
C     GQR(I)     = Resultant of flow rate per unit width (ft**2/sec) in X
C                 and Y directions at node I.
C     GQX(I)     = Weighted flow rate per unit width (ft**2/sec) in
C                 X-direction at node I for given time step.
C     GQXNEW(I) = Flow rate per unit width (ft**2/sec) in X-direction
C                 at node I at end of current time step.
C     GQXOLD(I) = Flow rate per unit width (ft**2/sec) in X-direction
C                 at node I at tend of previous time step.
C     GRF( )     = GF * ½weighted rainfall½
C     GSMX( )    = Global Stiffness Matrix for X-direction f    T
C                                                          j½N½ ½dN/dx½
C     GSMQX( )  = GSMX * GQX
C     HLOLIM     = Negative tolerance for flow depth H (feet).
C     HUPLIM     = Largest expected flow depth H (feet).
C     INDEXN( ) = Index for array of node numbers.
C     NODE( )    = Array of node numbers.
C     NP         = Total number of nodal points being evaluated.
C     NSOLV      = Solution iteration number.
C     MANNGN     = Mannings N.
C     MAXNOD     = Maximum number of nodes associated with an element in
C                 the system.
C     MAXSOL     = Maximum number of solution iterations expected.
C     PI         = 3.14159...
C     QNEW       = Flow rate per unit width at a node calculated
C                 from GHTRY(I).
```

```
C       RAINN      = Rate of rainfall at end of present  time step (ft/sec).
C       RAINO      = Rate of rainfall at end of previous time step (ft/sec).
C       SLOPE      = Slope (ft/ft) at a node.
C       SLOPEX     = Slope (ft/ft) in X direction at a node.
C       THETA      = Weighting coefficient.
C       TIMEN      = Clock time (seconds) at end of present time step.
C       TIMEO      = Clock time (seconds) at end of previous time step.

C       Tracing definitions:
C       ILEVEL     = Tracing level for downstream write statements.
C       ITRACK     = Unit (TRACE.OUT) to which results of intermediate
C                    calculations are written.
C       LEVELT     = Tracing level relative to the calling program.
C       LTRACE     = Tracing level for entire program.

        COMMON/TRACE/LTRACE,ITRACK
        COMMON/MATRIX/GSMX(20,20),GSMY(20,20),GCM(20,20),GF(20)
        COMMON/NODES/NP,NBW,NODE(20),INDEXN(20)
        DIMENSION GHNEW(20),GHOLD(20),GRF(20),GCHOLD(20),GSUM(20),
       +    GQXNEW(20),GQXOLD(20),GQX(20),GSMQX(20),GHTRY(20),
       +    GQYNEW(20),GQYOLD(20),GQY(20),GSMQY(20),GQRES(20)
        INTEGER HOUR
        REAL MANNGN
        CHARACTER*40 TITLE
        DOUBLE PRECISION ASPECT,ASPRAD,PI
        DATA THETA/.5/, MANNGN/.035/, PI/3.141592653589794/
        DATA MAXNOD/4/ LEVELT/0/ HUPLIM/10./ HLOLIM/-0.1E-06/
        DATA GHNEW,GQXNEW,GQYNEW/60*0./

        ITRACK = 8
        OPEN(1,FILE='SYSTEM.IN')
        OPEN(3,FILE='STORM.IN')
        OPEN(7,FILE='STREAM.OUT')
        OPEN(ITRACK,FILE='TRACE.OUT')

        READ(1,10) TITLE
10      FORMAT(40X,40A)
        WRITE(7,20) TITLE
        WRITE(ITRACK,20) TITLE
20      FORMAT(/,5X,40A,/)

        ILEVEL = LEVELT+1
        WRITE(6,70)
70      FORMAT(1X,'Enter the program tracing (debug) level: ')
        READ(*,*) LTRACE
        WRITE(ITRACK,60) LTRACE
60      FORMAT(/,10X,'The program tracing level is ',I2)

        WRITE(6,72)
72      FORMAT(5X,'Executing MAINSTRM:  Running main program.')

C       Determine the total number of elements and nodes in the global system:
        CALL COUNT(ILEVEL,NELTOT,NODTOT)
```

```
C     Determine which elements and nodes and their coordinates
C     are associated with the subsystem selected for analysis:
      CALL SUBSYS(ILEVEL,NELTOT,NODTOT)

C     Construct the global stiffness and capacitance matrices and the
C     force vector:
      CALL BUILDG(ILEVEL,NELTOT)

C     Modify the global matrices:
      Call MODGM(ILEVEL)

      READ(3,10) TITLE
      WRITE(ITRACK,20) TITLE
      WRITE(7,20) TITLE
      WRITE(7,722) (NODE(I),I=1,NP)
722   FORMAT(6X,10I10)

      ILEV1=ILEVEL+1
      IF(ILEV1.LE.LTRACE) WRITE(ITRACK,102)
102   FORMAT(5X,'Executing time loop...')

      MAXSOL = NP*10

************** BEGIN TIME DEPENDENT CALCULATIONS ***************


C     Read the rainfall at the beginning of the time period:
      READ(3,237) HOUR,MINUTE,RAINN
237   FORMAT(I2,1X,I2,F10.5)
      TSTART = (HOUR*60.+MINUTE)*60
      TIMEN = TSTART
      DELTAT=0
      WRITE(6,235) HOUR,MINUTE,RAINN,DELTAT
      IF(ILEV1+2.LE.LTRACE) THEN
      WRITE(ITRACK,'(1X)')
      WRITE(ITRACK,235) HOUR,MINUTE,RAINN,DELTAT
235   FORMAT(5X,'At ',I2,':',I2,' rain intensity is ',
     1   E10.3,' ft/sec       DELTAT = ', F5.1,' sec.')
      ENDIF
      WRITE(7,720) HOUR,MINUTE,(GQRES(I),I=1,NP)

****************** START TIME LOOP *************************

1000  DO 2000 ITIME=1,1000

      TIMEO = TIMEN
      RAINO = RAINN
      READ(3,237,ERR=3000) HOUR,MINUTE,RAINN
      TIMEN = (HOUR*60+MINUTE)*60
      DELTAT = TIMEN - TIMEO
      IF(DELTAT.LT.0) THEN
         WRITE(6,236)
236      FORMAT(1X,'TIME STEPS NOT CONSECUTIVE. PROGRAM STOPPED.')
         STOP
```

```
      ENDIF

      WRITE(6,235) HOUR,MINUTE,RAINN,DELTAT
      IF(ILEV1+2.LE.LTRACE) THEN
         WRITE(ITRACK,'(1X)')
         WRITE(ITRACK,235) HOUR,MINUTE,RAINN,DELTAT
      ENDIF
C     Assign the last computed values to the 'old' locations:
      DO 1030 I = 1,NP
        GHOLD(I) = GHNEW(I)
        GQXOLD(I) = GQXNEW(I)
        GQYOLD(I) = GQYNEW(I)
1030  CONTINUE

C     Multiply the global capacitance matrix times the old depth values:
        DO 497 I=1, NP
             GCHOLD(I) = 0.0
             DO 497 K=1,NP
                GCHOLD(I) = GCHOLD(I) + GCM(I,K)*GHOLD(K)
497     CONTINUE

      NSOLV= 0


** ** ** ** ** **  START SOLUTION LOOP  ** ** ** ** ** **
      WRITE(6,'(1X)')
      ILEV4=ILEV1+3
300   NSOLV=NSOLV+1
      IF(ILEV4.LE.LTRACE) THEN
          WRITE(ITRACK,'(1X)')
          WRITE(ITRACK,301) NSOLV
      ENDIF
      WRITE(6,301) NSOLV
301   FORMAT('+',4X,'Executing solution iteration number',I4)

C     Compute the flow in each direction:
      IFILE=1
600   DO 700 I=1,NP
        GHTRY(I)  = GHNEW(I)
        NSKIP=NELTOT+NODE(I)+1
        CALL SKIP(IFILE,NSKIP)
        READ(IFILE,610) SLOPE, WIDTH
610      FORMAT(25X,2F10.3)
        GQXNEW(I) = 1.486/MANNGN * SLOPE**0.5 * GHTRY(I)**(5./3.)
        IF(WIDTH.GT.0) GQXNEW(I) = GQXNEW(I) * WIDTH
        GQX(I)    = (1.-THETA)*GQXOLD(I) + THETA * GQXNEW(I)
        GQY(I)    = (1.-THETA)*GQYOLD(I) + THETA * GQYNEW(I)
        GRF(I)    = (1.-THETA)*GF(I)*RAINO + THETA * GF(I) * RAINN
700   CONTINUE

C     Write intermediate results:
      IF(ILEV4+1.LE.LTRACE) THEN
      WRITE(ITRACK,704)
704   FORMAT(/5X,' NODE     GHTRY        GQXNEW        GQYNEW          GQX',
```

```
     1   '          GQY          GRF')
         WRITE(ITRACK,706) (NODE(I),GHNEW(I),GQXNEW(I),GQYNEW(I),
     1    GQX(I),GQY(I),GRF(I),I=1,NP)
706    FORMAT(5X,I5,6E12.4)
       ENDIF

C      Multiply the global X-stiffness matrix times the X-flow vector:
         DO 498 I=1, NP
              GSMQX(I) = 0.0
              DO 498 K=1,NP
                 GSMQX(I) = GSMQX(I) + GSMX(I,K) * GQX(K)
498       CONTINUE

C      Multiply the global Y-stiffness matrix times the Y-flow vector:
         DO 499 I=1, NP
              GSMQY(I) = 0.0
              DO 499 K=1,NP
                 GSMQY(I) = GSMQY(I) + GSMY(I,K) * GQY(K)
499       CONTINUE

C      Compute the global SUM vector:
800    DO 900 I=1,NP
          GSUM(I) = GCHOLD(I) + DELTAT * ( GRF(I)-
     1       (GSMQX(I) + GSMQY(I)) )
900    CONTINUE

C      Write intermediate results:
       IF(ILEV4.LE.LTRACE) THEN
       WRITE(ITRACK,904)
904    FORMAT(/5X,' NODE     CHOLD          GSMQX          GSMQY          GSUM')
       WRITE(ITRACK,906) (NODE(I),GCHOLD(I),GSMQX(I),GSMQY(I),
     1    GSUM(I),I=1,NP)
906    FORMAT(5X,I5,4E12.4)
       ENDIF

C      Solve the system of equations ½GCM½*½GHNEW½=½GSUM½
       N=20
       CALL SLVSYS(GCM,GHNEW,GSUM,NP,N)

C      Check estimated depth against result:
       FLAG = 0.
       DO 1400 I=1,NP
          IF(ABS(GHNEW(I)-GHTRY(I)).LT.1.E-08) GO TO 1400
          FLAG = 1.
1400   CONTINUE

C      If all differences are within tolerance, go to next time step.
       IF(FLAG.EQ.0) GO TO 1997

       IF(NSOLV.GE.MAXSOL) THEN
          WRITE(6,1440) MAXSOL
1440       FORMAT('+',5X,'Solution considered convergent after ',I4,
     +        ' iterations.')
          GO TO 1930
```

```
      ENDIF

C     Compare solution at each node with upper and lower limits:
      DO 1500 I=1,NP
         IF(GHNEW(I).LT.0) THEN
            IF(GHNEW(I).LT.HLOLIM) THEN
               WRITE(ITRACK,712)
712             FORMAT(5X,'NODE     DEPTH')
               WRITE(ITRACK,715)(NODE(J),GHNEW(J),J=1,NP)
715             FORMAT(5X,I4,E12.4)
               WRITE(ITRACK,1520)
               WRITE(6,1520)
1520            FORMAT(5X,'SOLUTION FOR FLOW DEPTH IS NEGATIVE. ',
     +         'PROGRAM EXECUTION STOPPED.')
               STOP
            ELSE
               GHNEW(I)=0.
               WRITE(6,1521) NODE(I)
1521            FORMAT(5X,'SMALL NEGATIVE FLOW DEPTH AT NODE ',I4,
     1         '.  0 DEPTH ASSUMED.'/)
            ENDIF
         ELSEIF(GHNEW(I).GT.HUPLIM) THEN
            WRITE(ITRACK,712)
            WRITE(ITRACK,715)(NODE(J),GHNEW(J),J=1,NP)
            WRITE(6,1530) HUPLIM,NODE(I)
            WRITE(ITRACK,1530) HUPLIM,NODE(I)
1530         FORMAT(10X,'SOLUTION FOR FLOW DEPTH ½ ',F5.1,
     1        'AT NODE ',I4,'.  PROGRAM EXECUTION STOPPED.')
            STOP
         ENDIF
1500  CONTINUE

C     Iterate solution again:
      GO TO 300

** ** ** ** ** **  END SOLUTION LOOP  ** ** ** ** ** ** **
1997  CONTINUE
1999  IF(ILEV4.LE.LTRACE) WRITE(6,1920) NSOLV
1920  FORMAT('+',5X,'Solution converges after ',I3,' iterations.')

C     Compute resultant flow for each direction:
1930  DO 1940 I=1,NP
1940  GQRES(I) = SQRT(ABS(GQXNEW(I))**2.+ABS(GQYNEW(I))**2.)

      IF(ILEVEL+1.LE.LTRACE) THEN
      WRITE(ITRACK,702)
702    FORMAT(/5X,'NODE     DEPTH          FLOWX          FLOWY     TOTAL FLOW')
      WRITE(ITRACK,705) (NODE(I),GHNEW(I),
     1 GQXNEW(I),GQYNEW(I),GQRES(I),I=1,NP)
705    FORMAT(5X,I4,4E12.4)
      ENDIF

      WRITE(7,720) HOUR, MINUTE, (GQRES(I),I=1,NP)
720    FORMAT(3X,I2,':',I2,2X,100E10.3)
```

```
2000  CONTINUE

************** END TIME LOOP **************

3000  CONTINUE

      WRITE(6,3001)
      IF(ILEVEL.LE.LTRACE) WRITE(ITRACK,3001)
3001  FORMAT(//,1X,'END OF PROGRAM REACHED')

      STOP
      END

*******************************************************************************

      SUBROUTINE BUILDG(LEVELT,NELTOT)

C     This subroutine reads the nodal coordinates associated with each
C     element, rotates the element so that the local X axis lies in the
C     direction of the element aspect angle,
C     and sends the transformed coordinates to MATRIC for computation of
C     element matrices.  ASSMBL is called to place the coefficients of
C     the element matrices into their respective positions in the global
C     matrices.

C     Subroutine arguments LEVELT and NELTOT are sent TO this subroutine.

C     ASPECT     = The aspect angle (degrees) for an element.
C     ASPRAD     = The aspect angle (radians) for an element.
C     GLOBAL( , ) = Global coordinates associated with an element.
C     GTRAN( , )  = Transformed global coordinates.
C     LABELE( ) = Array of element numberals associated with subsystem.
C     MAXNOD     = Maximum number of nodes which is associated with any
C                  element in the subsystem.
C     NELEMS     = Number of elements associated with the subsystem.
C     NELTOT     = Total number of elements in the global system.
C     NNODEL( ) = Array of nodes associated with an element.
C     SLOPE( )   = Slope at a node.
C     TRANSF( , ) = Transformation matrix.
C     WIDTH(I)   = Width of linear element at node I.

      COMMON/ELEMS/NELEMS,LABELE(20)
      COMMON/TRACE/LTRACE,ITRACK
      DIMENSION GLOBAL(4,2),NNODEL(4),WIDTH(4),SLOPE(4)
      DIMENSION TRANSF(2,2),GTRAN(4,2)
      DOUBLE PRECISION PI,ASPECT,ASPRAD
      DATA PI/3.141592653589794D0/
      DATA MAXNOD/4/

      ILEVEL=LEVELT+1

      WRITE(6,10)
      IF(ILEVEL.LE.LTRACE) WRITE(ITRACK,10)
```

```
10    FORMAT(5X,'Executing BUILDG: Building global matrices.')
      WRITE(6,11)
11    FORMAT(1X)

100   DO 600 INDEXE=1,NELEMS
        IFILE=1
        NSKIP=LABELE(INDEXE)
        CALL SKIP(IFILE,NSKIP)
        READ(IFILE,120) NELEM,(NNODEL(J),J=1,MAXNOD),ASPECT
120      FORMAT(5I5,F10.2)
        WRITE(6,130) NELEM
        IF(ILEVEL+2.LE.LTRACE) WRITE(ITRACK,130) NELEM
130      FORMAT('+',4X,'Computing matrices for element number ',I3)
C       Determine how many nodes are associated with the element:
        NODSEL=MAXNOD
140      DO 160 J=1,MAXNOD
160      IF(NNODEL(J).EQ.0) NODSEL=NODSEL-1

C       Determine the element matrices:

520      DO 560 I=1,NODSEL
           NSKIP = NELTOT+NNODEL(I)+1
           CALL SKIP(IFILE,NSKIP)
           READ(1,540) NODNUM,(GLOBAL(I,J),J=1,2),SLOPE(I),WIDTH(I)
540         FORMAT(I5,4F10.2)
560      CONTINUE

        IF(NODSEL.EQ.2) THEN
          CALL LINMAT(ILEVEL,NODSEL,NNODEL,GLOBAL,WIDTH)
          GO TO 599
        ENDIF

        ASPRAD=PI/180.D0*ASPECT

C       Compute the coefficents of the transformation matrix:
        TRANSF(1,1)= DSIN(ASPRAD)
        TRANSF(1,2)= DCOS(ASPRAD)
        IF(ABS(ASPECT).EQ.90.) TRANSF(1,2)=0.
        TRANSF(2,1)=-TRANSF(1,2)
        TRANSF(2,2)= TRANSF(1,1)

        IF(ILEVEL+2.LE.LTRACE) WRITE(ITRACK,714) ASPECT,ASPRAD
714        FORMAT(5X,'Element aspect angle is ',F6.2,
     1       ' degrees or ',F7.4,' radians.')
        IF(ILEVEL+4.LE.LTRACE) THEN
          WRITE(ITRACK,716)
716        FORMAT(/5X,'Coordinate transformation matrix:')
          WRITE(ITRACK,718)((TRANSF(I,J),J=1,2),I=1,2)
718        FORMAT(5X,2E10.3)
        ENDIF

C       Transform the global coordinates:
720      DO 730 I=1,NODSEL
           DO 726 J=1,2
```

```
                GTRAN(I,J)=0.
                DO 726 K=1,2
                  GTRAN(I,J)=GTRAN(I,J)+TRANSF(J,K)*GLOBAL(I,K)
726           CONTINUE
730         CONTINUE

            IF(ILEVEL+3.LE.LTRACE) THEN
              WRITE(ITRACK,510)
510           FORMAT(5X,'The following coordinates are associated with ',
     1          'this element:',/,5X,' NODE    XGLOBAL    YGLOBAL',
     2          '      Slope      Xlocal     Ylocal')
              DO 542 I=1,NODSEL
542           WRITE(ITRACK,550) NNODEL(I),(GLOBAL(I,J),J=1,2),SLOPE(I),
     1          (GTRAN(I,J),J=1,2)
550           FORMAT(5X,I5,5F10.2)
              WRITE(ITRACK,'(1X)')
            ENDIF

C           Determine the element matrices:
            CALL MATRIC(ILEVEL,NODSEL,NNODEL,GTRAN)

C           Add the element matrices to the global matrices:
599         CALL ASSMBL(ILEVEL,NODSEL,INDEXE,NELEMS,NELEM,NNODEL)

600       CONTINUE

C         End element loop.

          WRITE(6,660)
          IF(ILEVEL+1.LE.LTRACE) WRITE(ITRACK,660)
660       FORMAT('+',4X,'Returning from BUILDG:  ',
     1        'Global matrices complete.',/)
          RETURN
          END

*******************************************************************************

          SUBROUTINE COUNT(LEVELT,NELEMS,NODSYS)

C         This subroutine determines the total number of nodes and elements
C         in the major global system data file.  This permits subsequent
C         reading from the correct lines of input data.

C         The subroutine arguments NELEMS and NODSYS are passed FROM the
C         subroutine.

C         NELEMS = The total number of elements in the major global system.
C         NODSYS = The total number of nodes    in the major global system.

          COMMON/TRACE/LTRACE,ITRACK
          DATA IFILE/1/

          ILEVEL=LEVELT+1
          IF(ILEVEL.LE.LTRACE) THEN
```

```
          WRITE(ITRACK,10)
          WRITE(6,10)
10        FORMAT(5X,'Executing COUNT: Counting nodes and elements in ',
     1    'global system...')
        ENDIF

C       Skip the record containing input column headings:
        NSKIP=1
        CALL SKIP(IFILE,1)

100     DO 200 IELEM=1,100
          READ(1,120,ERR=220) NELEM
120       FORMAT(I5)
          NELEMS = IELEM
200     CONTINUE

220     NSKIP=NELEMS+2
        CALL SKIP(IFILE,NSKIP)
        DO 400 INODE=1,100
          READ(1,120,ERR=420) NODNUM
          NODSYS = INODE
400     CONTINUE

420     IF(ILEVEL+2.LE.LTRACE) THEN
          WRITE(ITRACK,80) NELEMS,NODSYS
80        FORMAT(/5X,'Total number of elements in global system= ',I3,
     1      /5X,'Total number of nodes      in global system= ',I3,/)
        ENDIF

        IF(ILEVEL+1.LE.LTRACE) THEN
          WRITE(6,510)
          WRITE(ITRACK,510)
510       FORMAT(5X,'Returning from COUNT: Counting complete.',/)
        ENDIF
        RETURN
        END
```

****

****

```
C       PROGRAM MAINSTRM

C       This program finds a linear solution to a finite element overland
C       flow problem for a global system of two-dimensional elements.

C       Units of measurement are taken from the English System.

C       To avoid internal storage of large amounts of data, this program
C       reads element and node information from external files as needed.

C       In the variable listing below, the X-direction is identical to the
C       direction of flow at a given node.
```

```
C     DELTAT     = Length (seconds) of time step.
C     GCHOLD( ) = GCM( , ) * GHOLD(2)
C     GCM( , )   = Global Capacitance Matrix f    T
C                                              j½N½ ½N½
C     GF( )      = Global Force vector
C     GHNEW(I)   = Flow depth H (feet) at node I at end of current
C                  time step.
C     GHOLD(I)   = Flow depth H (feet) at node I at end of previous
C                  time step.
C     GHTRY(I)   = Flow depth H (feet) at node I tried for solution
C                  iteration. When solution GHNEW is close to GHTRY,
C                  solution is accepted.
C     GQR(I)     = Resultant of flow rate per unit width (ft**2/sec) in X
C                  and Y directions at node I.
C     GQX(I)     = Weighted flow rate per unit width (ft**2/sec) in
C                  X-direction at node I for given time step.
C     GQXNEW(I) = Flow rate per unit width (ft**2/sec) in X-direction
C                  at node I at end of current time step.
C     GQXOLD(I) = Flow rate per unit width (ft**2/sec) in X-direction
C                  at node I at tend of previous time step.
C     GRF( )     = GF * ½weighted rainfall½
C     GSMX( )    = Global Stiffness Matrix for X-direction f    T
C                                                          j½N½ ½dN/dx½
C     GSMQX( )   = GSMX * GQX
C     HLOLIM     = Negative tolerance for flow depth H (feet).
C     HUPLIM     = Largest expected flow depth H (feet).
C     INDEXN( ) = Index for array of node numbers.
C     NODE( )    = Array of node numbers.
C     NP         = Total number of nodal points being evaluated.
C     NSOLV      = Solution iteration number.
C     MANNGN     = Mannings N.
C     MAXNOD     = Maximum number of nodes associated with an element in
C                  the system.
C     MAXSOL     = Maximum number of solution iterations expected.
C     PI         = 3.14159...
C     QNEW       = Flow rate per unit width at a node calculated
C                  from GHTRY(I).
C     RAINN      = Rate of rainfall at end of present  time step (ft/sec).
C     RAINO      = Rate of rainfall at end of previous time step (ft/sec).
C     SLOPE      = Slope (ft/ft) at a node.
C     SLOPEX     = Slope (ft/ft) in X direction at a node.
C     THETA      = Weighting coefficient.
C     TIMEN      = Clock time (seconds) at end of present time step.
C     TIMEO      = Clock time (seconds) at end of previous time step.

C     Tracing definitions:
C     ILEVEL     = Tracing level for downstream write statements.
C     ITRACK     = File to which results of intermediate calculations are
C                  written.
C     LEVELT     = Tracing level relative to the calling program.
C     LTRACE     = Tracing level for entire program.

*************************************************************************
```

```
      SUBROUTINE MATRIC(LEVELT,NODSEL,NSEND,GLOBAL)

C     This subroutine calculates the stiffness and capacitance matrices
C     and the force vector for a triangular or quadrilateral element
C     having a node at each corner.

C     Subroutine arguments LEVELT,NODSEL,NSEND,XGLOBL,YGLOBL are sent TO
C     this subroutine. Coefficients of KX,KY,C,F are sent FROM this
C     subroutine via COMMON/ELMATS.

C-----------------------------------------------------------------------

C     B( , )       = Matrix containing the derivatives of shape function N
C                    with respect to the global coordinate system
C     B(1, )       = ½dN/dx½
C     B(2, )       = ½dN/dy½
C     C( , )       = Capacitance matrix for the element = f    T
C                                                        j½N½ ½N½
C     DNDNAT(I,J) = Array of derivatives of N with respect to KSI (I=1) and
C                    ETA (I=2) in ¢natural' coordinate system.
C     F( )         = Force vector for the element.
C     GLOBAL( ,J) = Array of X (J=1) and Y (J=2) coordinates for an element.
C     ILEVEL       = Tracing level used for debugging this subroutine.
C     IJACOB(I,J) = Inverse of JACOBian matrix.
C     JACOB(I,J)  = JACOBian matrix of partial derivatives of global
C                    coordinates with respect to natural coordinates
C                    ETA and KSI.
C     KX( , )     = Stiffness matrix with respect to rotated local direction X.
C                 = f    T
C                   j½N½ ½dN/dx½
C     KY( , )     =     "      "     "     "     "     "     "     "     Y.
C     LEVELT       = Tracing level sent from upstream program.
C     NODSEL       = Number of nodes associated with the element.
C     NSEND( )     = Node numerals associated with the element.
C     VN(I)        = Shape function  N at node I in ¢natural' coordinate system
C                    for given integration point.

C     Dhatt, G. and G. Touzot. The finite element method displayed.
C     John Wiley and Sons, NY, 1984.  509pp.  (See pp. 45, 102.)

C     Segerlind, L. Applied finite element analysis (2nd ed.). John Wiley
C     and Sons, NY, 1984.  427pp.  (See pp. 73, 365, 372-374.)

C-----------------------------------------------------------------------

      COMMON/ELMATS/KX(4,4),KY(4,4),C(4,4),F(4)
      COMMON/TRACE/LTRACE,ITRACK
      DIMENSION VN(4),DNDNAT(2,4),NSEND(4),GLOBAL(4,2),B(2,4)
      REAL KX,KY, JACOB(2,2),IJACOB(2,2)

      ILEVEL=LEVELT+1
      IF(ILEVEL.LE.LTRACE) WRITE(ITRACK,12)
 12   FORMAT(5X,'Executing MATRIC: Calculating elemental matrices.')
```

```
      IF(ILEVEL+2.LE.LTRACE) WRITE(ITRACK,16) NODSEL
16    FORMAT(5X,'There are ',I2,' nodes associated with this element.')

      IF(ILEVEL+3.LE.LTRACE) THEN
         WRITE(ITRACK,17)
17        FORMAT(/12X,'NODE',8X,'X',14X,'Y')
         WRITE(ITRACK,18) (NSEND(I),(GLOBAL(I,J),J=1,2),I=1,NODSEL)
18        FORMAT(4(10X,I5,2E15.6,/))
      ENDIF

C     Initialize the element matrices:
100   DO 200 I=1,NODSEL
110      DO 190 J=1,NODSEL
            C(I,J) = 0.
            KX(I,J) = 0.
            KY(I,J) = 0.
190      CONTINUE
         F(I) = 0.
200   CONTINUE

      IF(NODSEL.EQ.4) INTPTS = 4
      IF(NODSEL.EQ.3) INTPTS = 1

      ILEV5=ILEVEL+5

      DO 2000 INTPT = 1,INTPTS

         IF(NODSEL.EQ.4) CALL QSHAPE(ILEV5,INTPT,VN,DNDNAT)
         IF(NODSEL.EQ.3) CALL TSHAPE(VN,DNDNAT)

C        Calculate the Jacobian matrix: JACOB=DNDNAT*GLOBAL
         DO 499 I=1,2
            DO 499 J=1,2
               JACOB(I,J) = 0.0
               DO 499 K=1,NODSEL
                  JACOB(I,J) = JACOB(I,J) + DNDNAT(I,K) * GLOBAL(K,J)
499      CONTINUE

C        Determine the inverse of the Jacobian matrix:
         CALL INV2X2(JACOB,IJACOB,DETJAC)

C        Multiply : IJACOB * DNDNAT = B
         DO 498 I=1, 2
            DO 498 J=1, NODSEL
               B(I,J) = 0.0
               DO 498 K=1,2
                  B(I,J) = B(I,J) + IJACOB(I,K)*DNDNAT(K,J)
498      CONTINUE

         IF(ILEVEL+5.LE.LTRACE) THEN
            WRITE(ITRACK,315)
315         FORMAT(/5X,'½-----JACOBIAN-----½      ½----JACOBIANinv---½')
            DO 316 I=1,2
316         WRITE(ITRACK,318)(JACOB(I,J),J=1,2),(IJACOB(I,J),J=1,2)
```

```
318         FORMAT(5X,2E10.3,5X,2E10.3)

           WRITE(ITRACK,310) INTPT
310         FORMAT(/5X,'B matrix at integration point',I2,' :')
           WRITE(ITRACK,311) (NSEND(J),J=1,NODSEL)
311         FORMAT(5X,I5,5X,I5,5X,I5,5X,I5)
           DO 312 I=1,2
312         WRITE(ITRACK,314) (B(I,J),J=1,NODSEL)
314         FORMAT(5X,8E10.3)
         ENDIF

         IF(NODSEL.EQ.3 .AND. ILEVEL+4.LE.LTRACE) THEN
           AREA=ABS(DETJAC/2.)
           WRITE(ITRACK,510) AREA
510         FORMAT(5X,'Area of triangle = ',E10.4)
         ENDIF

C        Compute the element matrices:

         IF(NODSEL.EQ.4) WC = 1.0
         IF(NODSEL.EQ.3) WC = 0.5
         SCALAR = WC * ABS(DETJAC)

700      DO 800 I=1,NODSEL

710         DO 790 J=1,NODSEL

C              The capacitance matrix C is the sum over the integration
C              points of N½transpose * N multipled by a scalar value.

               C(I,J)  = C(I,J)  + VN(I) * VN(J) * SCALAR

C              The stiffness matrix K is determined for each direction as
C              the sum over the integration points of N½transpose * B
C              multiplied by a scalar value

               KX(I,J) = KX(I,J) + VN(I) * B(1,J) * SCALAR
               KY(I,J) = KY(I,J) + VN(I) * B(2,J) * SCALAR

790         CONTINUE

C           The force vector F is the sum over the integration points
C           of N multiplied by a scalar value.

            F(I) = F(I) + VN(I) * SCALAR

800      CONTINUE

2000  CONTINUE

C     Write the element matrices:
2010  IF(ILEVEL+4.LE.LTRACE) CALL WRITEM(4,NODSEL,NSEND,KX,KY,C,F)

      IF(ILEVEL+1.LE.LTRACE) WRITE(ITRACK,2140)
```

```
2140  FORMAT(5X,'Returning from MATRIC: Elemental matrix complete.',/)

      RETURN
      END


*************************************************************************

      SUBROUTINE QSHAPE(LEVELT,INTPT,VN,DNDNAT)

C     For a quadrilateral having a node at each corner, this subroutine
C     determines the shape functions and the derivatives of the shape
C     function with respect to the natural (KSI-ETA) coordinate system.

C     Subroutine argument INTPT is passed TO this subroutine, while
C     subroutine arguments VN and DNDNAT are passed FROM this subroutine.

C     INTPT = Number associated with the integration point in the KSI-ETA
C             coordinate system.
C
C     VKSIN(I)  = Value of KSI at node I in 'natural' coordinate system.
C                 ( = Abscissa of node I "       "          "        "     )
C     VETAN(I)  = Value of ETA at node I "       "          "        "
C                 ( = Ordinate of node I "       "          "        "     )

C     XINTEG(I) = Abscissa of integration point in 'natural' coord. system.
C     YINTEG(I) = Ordinate of integration point in 'natural' coord. system.

      COMMON/TRACE/LTRACE,ITRACK
      DIMENSION VKSIN(4),VETAN(4),XINTEG(4),YINTEG(4),VN(4),DNDNAT(2,4)
      DATA VKSIN/-1.0, 1.0, 1.0, -1.0/, VETAN/-1.0, -1.0, 1.0, 1.0/

C
C     Calculate the location of the integration points in the 'natural'
C     KSI-ETA coordinate system for the linear quadrilateral.

      ILEVEL=LEVELT+1

      IF(ILEVEL.LE.LTRACE) WRITE(ITRACK,10)
10    FORMAT(5X,'Executing QSHAPE: Determining shape functions for ',
     1  'an integration point.')
      WHERE = .577350
      DO 100 I=1,4
         XINTEG(I) = WHERE * VKSIN(I)
         YINTEG(I) = WHERE * VETAN(I)
100   CONTINUE

C        At each integration point :
         DO 450 I=1,4
C           Compute the shape function N at each node I:
            VN(I) = 0.25 * (1.+VKSIN(I) * XINTEG(INTPT))
     +                   * (1.+VETAN(I) * YINTEG(INTPT))
C           Compute the derivatives of N wrt natural coordinates:
```

```
            DNDNAT(1,I) = 0.25 * VKSIN(I) * (1+VETAN(I) * XINTEG(INTPT))
            DNDNAT(2,I) = 0.25 * VETAN(I) * (1+VKSIN(I) * YINTEG(INTPT))
450       CONTINUE

        IF(ILEVEL+2.LE.LTRACE) THEN

          WRITE(ITRACK,460)
460       FORMAT(/,5X,'INTPT     XINTEG      YINTEG      VN1         VN2    ',
     +       '    VN3         VN4')
          WRITE(ITRACK,470)INTPT,XINTEG(INTPT),YINTEG(INTPT),
     +       (VN(I),I=1,4)
470       FORMAT(5X,I3,2X,6F10.5)

          WRITE(ITRACK,521)
521       FORMAT(/5X,'DNDNAT :')
          WRITE(ITRACK,522) ((DNDNAT(I,J),J=1,4),I=1,2)
522       FORMAT(5X,4E10.3)

        ENDIF

        IF(ILEVEL+1.LE.LTRACE) WRITE(ITRACK,610)
610     FORMAT(5X,'Returning from QSHAPE.',/)

        RETURN
        END

*************************************************************************

        SUBROUTINE TSHAPE(VN,DNDNAT)

        DIMENSION VN(4),DNDNAT(2,4)

        DO 100 I=1,3
100     VN(I) = 1./3.

        DNDNAT(1,1) = 1.
        DNDNAT(1,2) = 0.
        DNDNAT(1,3) =-1.
        DNDNAT(2,1) = 0.
        DNDNAT(2,2) = 1.
        DNDNAT(2,3) =-1.

        RETURN
        END

*************************************************************************

        SUBROUTINE INV2X2(RM, RINV, D)
        DIMENSION RM(2,2), RINV(2,2)
C
C       FIND THE INVERSE OF A 2 X 2 MATRIX (I.E.)
C
C                -1
C       ½ a   b ½       ½ d/D     -b/D ½
```

```
C      ½        ½    =  ½              ½
C      ½ c    d ½       ½ -c/D     a/D ½
C
C
C      WHERE
C
C                      ½a    b½
C            D = det ½       ½
C                      ½c    d½
C
C     AND
C            D .NE. 0
C

      D = RM(1,1) * RM(2,2) - RM(2,1) * RM(1,2)
      IF(ABS(D).LT. 0.0001) THEN
        WRITE(*,*)'2 X 2 MATRIX IS SINGULAR'
        STOP
      ENDIF
        RINV(1,1) = RM(2,2) / D
        RINV(1,2) = -RM(1,2) / D
        RINV(2,1) = -RM(2,1) / D
        RINV(2,2) = RM(1,1) / D
      RETURN
      END

*******************************************************************************


*******************************************************************************

      SUBROUTINE SKIP(IFILE,NSKIP)
C     This subroutine skips to the selected line in an input file:
      REWIND IFILE
      DO 100 I=1,NSKIP
100    READ(IFILE,'(1X)')
      RETURN
      END

*******************************************************************************

$INCLUDE:'COUNT.FOR'
$INCLUDE:'SUBSYS.FOR'
$INCLUDE:'BUILDG.FOR'
$INCLUDE:'LINQUIK.FOR'
$INCLUDE:'MATRIC.FOR'
$INCLUDE:'ASSEMBLE.FOR'
$INCLUDE:'MODGM.FOR'
$INCLUDE:'SLVSYS.FOR'
$INCLUDE:'WRITEM.FOR'

*******************************************************************************

      SUBROUTINE MODGM(LEVELT)
```

```
C       This subroutine modifies the stiffness and capacitances matrices
C       and the force vector for the global subsystem.

C       Subroutine argument LEVELT is sent TO this subroutine, which refers
C       to the global matrices via COMMON/MATRIX.

        COMMON/MATRIX/GSMX(20,20),GSMY(20,20),GCM(20,20),GF(20)
        COMMON/NODES/NODSUB,NBW,NODE(20),INDEXN(20)
        COMMON/BOUND/NKNOWN,NBOUND(20),BVALUE(20)
        COMMON/TRACE/LTRACE,ITRACK

        ILEVEL=LEVELT+1
        IF(ILEVEL.LE.LTRACE) THEN
           WRITE(6,10)
           WRITE(ITRACK,10)
10          FORMAT(5X,'Executing MODGM: Modifying global matrices.')
        ENDIF

100     DO 200 IBOUND=1,NKNOWN
           INDEX=INDEXN(NBOUND(IBOUND))
110         DO 190 IJ=1,NODSUB
              GSMX(IJ,INDEX)=0.
              GSMX(INDEX,IJ)=0.
              GSMY(IJ,INDEX)=0.
              GSMY(INDEX,IJ)=0.
              GCM(IJ,INDEX)=0.
              GCM(INDEX,IJ)=0.
190         CONTINUE
           GF(INDEX)=0.
           GCM(INDEX,INDEX)=1.
200     CONTINUE

        IF(ILEVEL+2.LE.LTRACE) THEN
C          Write the modified global matrices:
           WRITE(ITRACK,260)
260         FORMAT(5X,'The MODIFIED global matrices:')
           NDIM=20
           CALL WRITEM(NDIM,NODSUB,NODE,GSMX,GSMY,GCM,GF)
        ENDIF
        IF(ILEVEL+1.LE.LTRACE) THEN
           WRITE(6,310)
           WRITE(ITRACK,310)
310         FORMAT(5X,'Returning from MODGM: Modification complete.',/)
        ENDIF

        RETURN
        END



        subroutine slvsys(a,x,b,n,np)
C                                    physical dim     logical dim
C                                    ------------     -----------
```

```
C       a : coeff matrix                (np x np)        (n x n used)
C       x : soln matrix                 (np)             (n used)
C       b : right hand side of eqn      (np)             (n used)
C       np : physical dimensions of a,x and b   (how big it really it is)
C       n : logical dimensions of a,x and b     (how much you use)
C
        dimension a(np,np),x(np),b(np)
        dimension awork(20,20), bwork(20,1)

        do 100 i=1,n
          do 200 j=1,n
            awork(i,j) = a(i,j)
200       continue
          bwork(i,1) = b(i)
100     continue
        call gaussj(awork,n,20,bwork,1,1)
        do 300 i = 1,n
          x(i) = bwork(i,1)
300     continue
        return
        end


        SUBROUTINE GAUSSJ(A,N,NP,B,M,MP)
C
C       solves the set of matrix eqns:
C       A½x1 x2 ... xn½ = ½b1 b2 ... bn½
C       to solve for: Ax=b call with:
C
C       CALL GAUSSJ(A,N,NP,B,1,1)
C
C       From:
C       Press, W.H., B.P. Flannery, S.A. Teukolsky, W.T. Vetterling.
C       Numerical recipes, the art of scientific computing.  Cambridge
C       University Press, Cambridge.  1986.  pp. 19-29.
C

        PARAMETER (NMAX=50)
        DIMENSION A(NP,NP),B(NP,MP),IPIV(NMAX),INDXR(NMAX),INDXC(NMAX)
        DO 11 J=1,N
          IPIV(J)=0
11      CONTINUE
        DO 22 I=1,N
          BIG=0.
          DO 13 J=1,N
            IF(IPIV(J).NE.1)THEN
              DO 12 K=1,N
                IF (IPIV(K).EQ.0) THEN
                  IF (ABS(A(J,K)).GE.BIG)THEN
                    BIG=ABS(A(J,K))
                    IROW=J
                    ICOL=K
                  ENDIF
                ELSE IF (IPIV(K).GT.1) THEN
```

```
                PAUSE 'Singular matrix'
              ENDIF
12            CONTINUE
            ENDIF
13        CONTINUE
          IPIV(ICOL)=IPIV(ICOL)+1
          IF (IROW.NE.ICOL) THEN
            DO 14 L=1,N
              DUM=A(IROW,L)
              A(IROW,L)=A(ICOL,L)
              A(ICOL,L)=DUM
14          CONTINUE
            DO 15 L=1,M
              DUM=B(IROW,L)
              B(IROW,L)=B(ICOL,L)
              B(ICOL,L)=DUM
15          CONTINUE
          ENDIF
          INDXR(I)=IROW
          INDXC(I)=ICOL
          IF (A(ICOL,ICOL).EQ.0.) PAUSE 'Singular matrix.'
          PIVINV=1./A(ICOL,ICOL)
          A(ICOL,ICOL)=1.
          DO 16 L=1,N
            A(ICOL,L)=A(ICOL,L)*PIVINV
16        CONTINUE
          DO 17 L=1,M
            B(ICOL,L)=B(ICOL,L)*PIVINV
17        CONTINUE
          DO 21 LL=1,N
            IF(LL.NE.ICOL)THEN
              DUM=A(LL,ICOL)
              A(LL,ICOL)=0.
              DO 18 L=1,N
                A(LL,L)=A(LL,L)-A(ICOL,L)*DUM
18            CONTINUE
              DO 19 L=1,M
                B(LL,L)=B(LL,L)-B(ICOL,L)*DUM
19            CONTINUE
            ENDIF
21        CONTINUE
22      CONTINUE
        DO 24 L=N,1,-1
          IF(INDXR(L).NE.INDXC(L))THEN
            DO 23 K=1,N
              DUM=A(K,INDXR(L))
              A(K,INDXR(L))=A(K,INDXC(L))
              A(K,INDXC(L))=DUM
23          CONTINUE
          ENDIF
24      CONTINUE
        RETURN
        END
*******************************************************************************
```

```
      SUBROUTINE LINMAT(LEVELT,NODSEL,NNODEL,GLOBAL,WIDTH)

C     Without integrating, this subroutine supplies the capacitance and
C     stiffness matrices and the force vector for the given linear
C     element.

C     See Segerlind 1984, pp. 70-71, 371-372, 375-376.

C     GLOBAL( )   = Set of node coordinates associated with the element.
C     C( , )      = Capacitance matrix.
C     EWIDTH      = Width of element.
C     F( )        = Force vector.
C     GLOBAL( , ) = Array of global coordinates.
C     KX( , )     = Stiffness matrix.
C     LENGTH      = Length of element.
C     NNODEL( )   = Node numbers associated with the element.
C     WIDTH( )    = Width at a node.

      COMMON/ELMATS/KX(4,4),KY(4,4),C(4,4),F(4)
      COMMON/TRACE/LTRACE,ITRACK
      DIMENSION GLOBAL(4,2),NNODEL(4),WIDTH(4)
      REAL KX,KY,NTN(2,2),NTB(2,2),LENGTH
      DATA NTN/2,1,1,2/ NTB/-.5,-.5,.5,.5/

      ILEVEL=LEVELT+1
      IF(ILEVEL.LE.LTRACE) WRITE(ITRACK,12)
12    FORMAT(5X,'Executing LINMAT: Calculating elemental matrices.')

      IF(ILEVEL+2.LE.LTRACE) WRITE(ITRACK,16) NODSEL
16    FORMAT(5X,'There are ',I2,' nodes associated with this element.')

      IF(ILEVEL+3.LE.LTRACE) THEN
         WRITE(ITRACK,17)
17       FORMAT(/12X,'NODE',8X,'X',14X,'Y')
         WRITE(ITRACK,18) (NNODEL(I),(GLOBAL(I,J),J=1,2),I=1,NODSEL)
18       FORMAT(4(10X,I5,2E15.6,/))
      ENDIF

      LENGTH = SQRT( (GLOBAL(1,1)-GLOBAL(2,1))**2.
     1              + (GLOBAL(1,2)-GLOBAL(2,2))**2.)

      EWIDTH = (WIDTH(1)+WIDTH(2))/2.

      DO 900 I=1,2
         DO 890 J=1,2
            C(I,J) = NTN(I,J) * LENGTH/6. * EWIDTH
            KX(I,J) = NTB(I,J)
890      CONTINUE
         F(I) = LENGTH/2. * EWIDTH
900   CONTINUE

      RETURN
      END
```

```
**************************************************************************
      SUBROUTINE ASSMBL(LEVELT,NRC,IELEM,NELEMS,NUMEL,NSEND)
C
C     This subroutine places the coefficients of an element's stiffness
C     matrices, capacitance matrix, and force vector into the proper
C     positions in the respective global arrays.
C
C     All of the subroutine arguments are passed TO this subroutine.
C     The element matrices are passed from MATRIC via COMMON/ELMATS.  The
C     global matrices are referenced by COMMON/MATRIX.
C
C     ECM( , )    = Element Capacitance Matrix.
C     EF( )       = Element Force vector.
C     ESMX( , )   = Element Stiffness Matrix for X-direction.
C     ESMY( , )   = Element Stiffness Matrix for Y-direction.
C
C     GCM( , )    = Global Capacitance Matrix.
C     GF( )       = Global Force vector.
C     GSMX( , )   = Global Stiffness Matrix for X-direction.
C     GSMY( , )   = Global Stiffness Matrix for Y-direction.
C
C     INDEXN( )   = Array nodal indices.
C     NODE( )     = Array of nodal numerals.
C     NODSUB      = Number of nodes in watershed subsystem.
C     NRC         = Number of rows and columns in element matrices.
C     NSEND       = Array of node numerals corresponding to the element.

C     Tracing constants:
C          ILEVEL = Local (subroutine) tracing level.
C          ITRACK = Unit to which intermediate values are written.
C          LTRACE = Global tracing level.


      DIMENSION NSEND(4)
      COMMON/ELMATS/ESMX(4,4),ESMY(4,4),ECM(4,4),EF(4)
      COMMON/TRACE/LTRACE,ITRACK
      COMMON/MATRIX/GSMX(20,20),GSMY(20,20),GCM(20,20),GF(20)
      COMMON/NODES/NODSUB,NBW,NODE(20),INDEXN(20)

      ILEVEL=LEVELT+1
      IF(ILEVEL.LE.LTRACE) WRITE(ITRACK,5) NUMEL
5        FORMAT(5X,'Executing ASSMBL: Adding element ',I3, ' matrices ',
     1      'to global matrices:')

       IF(ILEVEL+3.LE.LTRACE) THEN
          WRITE(ITRACK,10)
10         FORMAT(/1X,'Element matrices passed from MATRIC:')
          NDIM=4
          CALL WRITEM(NDIM,NRC,NSEND,ESMX,ESMY,ECM,EF)
       ENDIF

       DO 30 I=1,NRC
          IROW=INDEXN(NSEND(I))
```

```
            DO 20 J=1,NRC
               JCOL=INDEXN(NSEND(J))
               GSMX(IROW,JCOL)=GSMX(IROW,JCOL)+ESMX(I,J)
               GSMY(IROW,JCOL)=GSMY(IROW,JCOL)+ESMY(I,J)
               GCM(IROW,JCOL) =GCM(IROW,JCOL)+ECM(I,J)
20          CONTINUE
            GF(IROW)=GF(IROW)+EF(I)
30       CONTINUE

C  RETURN OPTIONS
         IF(ILEVEL+2.LE.LTRACE .AND. IELEM.EQ.NELEMS) THEN
            WRITE(ITRACK,43)
43          FORMAT(/1X,'The fully assembled global matrices:')
            NDIM=20
            CALL WRITEM(NDIM,NODSUB,NODE,GSMX,GSMY,GCM,GF)
         ENDIF
44       IF(ILEVEL+1.LE.LTRACE) WRITE(ITRACK,45)
45       FORMAT(5X,'Returning from ASSMBL',/)
100      RETURN
         END


         SUBROUTINE WRITEM(NDIM,NRC,NSEND,KX,KY,C,F)

C        This subroutine prints the stiffness, and capacitance matrices and
C        the force vector.

C        All the subroutine arguments are passed TO this subroutine.
C
C        C( , )    = Capacitance matrix.
C        F( )      = Force vector.
C        KX( )     = Stiffness matrix in X direction.
C        KY( )     = Stiffness matrix in Y direction.
C        NDIM      = Physical storage DIMensions assigned by calling program.
C        NRC       = Number of Rows and Columns in the matrices.

         DIMENSION NSEND(NDIM),C(NDIM,NDIM),F(NDIM)
         REAL KX(NDIM,NDIM),KY(NDIM,NDIM)
         COMMON/TRACE/LTRACE,ITRACK

C           Write matrices to trace file:

2102      FORMAT(3X,8I10)

          WRITE(ITRACK,2103)
2103      FORMAT(/,1X,'Stiffness matrix KX:')
          WRITE(ITRACK,2102) (NSEND(J),J=1,NRC)
          DO 2104 I=1,NRC
          WRITE(ITRACK,2105) NSEND(I),(KX(I,J),J=1,NRC)
2104      CONTINUE

2105      FORMAT(1X,I3,8E10.3,20(/,4X,8E10.3))

          WRITE(ITRACK,2106)
```

```
2106    FORMAT(/,1X,'Stiffness matrix KY:')
        WRITE(ITRACK,2102) (NSEND(J),J=1,NRC)
        DO 2107 I=1,NRC
2107    WRITE(ITRACK,2105) NSEND(I),(KY(I,J),J=1,NRC)

        WRITE(ITRACK,2109)
2109    FORMAT(/,1X,'Capacitance matrix C:')
        WRITE(ITRACK,2102) (NSEND(J),J=1,NRC)
        DO 2110 I = 1, NRC
2110    WRITE(ITRACK,2105)  NSEND(I),(C(I,J),J=1,NRC)

        WRITE(ITRACK,2112)
2112    FORMAT(/,1X,'Force vector F:')
        WRITE(ITRACK,2102) (NSEND(J),J=1,NRC)
        WRITE(ITRACK,2113) (F(I),I=1,NRC)
2113    FORMAT(4X,8E10.3)

        WRITE(ITRACK,2120)
2120    FORMAT(1X)

        RETURN
        END

*******************************************************************************

      SUBROUTINE SUBSYS(LEVELT,NELEMS,NODSYS)

C     This subroutine reads the element numbers in the chosen subsystem,
C     develops an index for the nodes associated with those elements,
C     and reads the nodal boundary values.

C     The variables LEVELT,NELEMS,and NODSYS are passed TO the subroutine.
C     The nodal indexing system and boundary value array are stored in
C     COMMON arrays.

C     BVALUE(I) = The boundary value at node I.
C     INDEXN(I) = The INDEX of Node I.  This index is developed so that
C                 the global matrices are no larger than needed and no
C                 zeroes are placed in the diagonal.
C     ITRACK    = Output device to which results of intermediate
C                 calculations are written.
C     LABELE(I) = Number of the ELement I in SUBsystem
C     LEVELT    = Debug level to control output.
C     LTRACE    = Debug level for entire program.
C     NBOUND(I) = Node at which BOUNDary value is known.
C     NELEMS    = Number of elements in the major global system.
C     NELSUB    = Number of elements in the subsystem.
C     NKNOWN    = Number of nodes for which the boundary value is KNOWN.
C     NODE( )   = Vector containing node numerals associated with subsystem.
C     NODSUB    = Number of nodes associated with the subsystem.

      DIMENSION NNODEL(4)
      COMMON/ELEMS/NELSUB,LABELE(20)
      COMMON/TRACE/LTRACE,ITRACK
```

```
      COMMON/BOUND/NKNOWN,NBOUND(20),BVALUE(20)
      COMMON/NODES/NODSUB,NBW,NODE(20),INDEXN(20)
      DATA MAXNOD/4/

      ILEVEL = LEVELT+1
      IF(ILEVEL.LE.LTRACE) THEN
      WRITE(ITRACK,80)
      WRITE(6,80)
80    FORMAT(5X,'Executing SUBSYS: Determining range of subsystem.')
      ENDIF

C     Skip to the first line containing a boundary value:
      IFILE=1
      NSKIP = NELEMS + NODSYS + 3
      CALL SKIP(IFILE,NSKIP)

      DO 90 I=1,NELEMS
         READ(IFILE,85,ERR=91) LABELE(I)
85       FORMAT(I5)
         NELSUB=I
90    CONTINUE

91    IF(ILEVEL+2.LE.LTRACE) THEN
         WRITE(ITRACK,92)
92       FORMAT(/5X,'Elements chosen in subsystem:')
93       WRITE(ITRACK,95) (LABELE(I),I=1,NELSUB)
95       FORMAT(1X,16I5)
      ENDIF

C     Construct the indexing system for the subsystem nodes:

      NSKIP=LABELE(1)
      CALL SKIP(IFILE,NSKIP)
      READ(IFILE,299) NELEM,NNODEL(1)
299   FORMAT(16I5)

      NODSUB=1
      NODE(1) = NNODEL(1)
400   DO 500 IELEM=1,NELSUB
         NSKIP=LABELE(IELEM)
         CALL SKIP(IFILE,NSKIP)
         READ(IFILE,299) NELEM,(NNODEL(J),J=1,MAXNOD)
410      DO 490 J=1,MAXNOD
            IF(NNODEL(J).EQ.0) GO TO 490
420         DO 480 I=1,NODSUB
               IF(NNODEL(J).EQ.NODE(I)) GO TO 490
480         CONTINUE
            NODSUB = NODSUB + 1
            NODE(NODSUB)=NNODEL(J)
490      CONTINUE
500   CONTINUE

C     Sort nodes
590   IFLAG=0
```

```
600    DO 700 I=1,NODSUB-1
         IF(NODE(I).LE.NODE(I+1)) GO TO 700
         NTEMP=NODE(I)
         NODE(I)=NODE(I+1)
         NODE(I+1)=NTEMP
         IFLAG=1
700    CONTINUE
       IF(IFLAG.EQ.1) GO TO 590

       DO 800 I=1,NODSUB
800    INDEXN(NODE(I))=I

       IF(ILEVEL+3.LE.LTRACE) THEN
          WRITE(ITRACK,804)
804         FORMAT(/,16X,'NODE',5X,'INDEXN')
          WRITE(ITRACK,810) (NODE(I),INDEXN(NODE(I)),I=1,NODSUB)
810         FORMAT(10X,2I10)
       ENDIF

C      Read the boundary values:

       IFILE=1
       NSKIP=NELEMS+NODSYS+NELSUB+4
       CALL SKIP(IFILE,NSKIP)

100    DO 200 IBOUND=1,NODSYS
          READ(IFILE,110,ERR=210) NBOUND(IBOUND),BVALUE(IBOUND)
110         FORMAT(I5,F5.1)
          NKNOWN = IBOUND
200    CONTINUE

210    IF(ILEVEL+2.LE.LTRACE) THEN
          WRITE(ITRACK,240) NKNOWN
240         FORMAT(/,5X,'Boundary Values are known at ',I3,' nodes:')
          WRITE(ITRACK,260) (NBOUND(I),BVALUE(I),I=1,NKNOWN)
260         FORMAT(8(4X,I5,F5.1))
       ENDIF

       IF(ILEVEL+1.LE.LTRACE) THEN
       WRITE(ITRACK,280)
       WRITE(6,280)
280    FORMAT(5X,'Returning from SUBSYS:  Subsystem determined.'/)
       ENDIF
       RETURN
       END
```

Soils data was gathered from microfiche at the National Soil Survey Laboratory, Soil Conservation Service-USDA, Lincoln, Nebraska for the Hastings soil and from the SCS SOILS-5 for the Coly soil series which is the same as the Colby, 1939 soil series name. The Hastings Silty Clay Loam was assumed to be an eroded phase of the Hastings Silt Loam. The Hastings Silty Clay Loam data was taken from the A12 horizon on the following data sheets.

Soil Classification: Udic Argiustoll, fine, montmorillonitic, mesic
Soil: Hastings
Soil Nos.: 365NK-91-1
Location: Webster County, Nebraska. 0.15 mile west and 100 feet south of northeast corner of Sec. 1, T3N, R10W.
Elevation: 1,985 feet.
Climate: Subhumid.
Precipitation and Temperature: 24 inches; 52 degrees F.
Vegetation and Use: Native grasses, principally big bluestem, sideoats grama, Western wheatgrass, blue grama, Scribner panicum, Kentucky bluegrass, and June grass. Native hay.
Root Distribution: Good: no restrictive zones.
Drainage and Permeability: Moderately well drained; moderately slow permeability.
Slope and Land Form: 1 to 2 percent with east aspect; stable upper interfluve; dissected uplands.
Parent Material: Thorian loess.
Collected and Described by: R. H. Jordan and J. V. Drew, April 21, 1965.

A11 20449 0 to 13 cm (0 to 5 inches). Dark gray (10YR 4/1, dry) to black (10YR 2/1, moist) silt loam; moderate fine granular structure; soft, friable; roots abundant; noncalcareous; clear smooth boundary.

A12 20450 13 to 25 cm (5 to 10 inches). Dark grayish-brown (10YR 4/2, dry) to very dark brown (10YR 2/2, moist) silt loam; moderate fine to medium granular structure; soft, friable; roots abundant; few insect worm casts about 5 mm in diameter; noncalcareous; clear smooth boundary.

B1 20451 25 to 41 cm (10 to 16 inches). Dark grayish-brown (10YR 4/2, dry) to very dark grayish-brown (10YR 3/2, moist) silty clay loam; weak fine subangular blocky breaking to moderate medium granular structure; soft, friable; roots plentiful; few insect worm casts about 5 mm in diameter; noncalcareous; clear smooth boundary.

B2t 20452 41 to 58 cm (16 to 23 inches). Brown (10YR 5/3, dry) to dark brown (10YR 3/3, moist) with 40 percent dark gray (10YR 4/1, dry) to very dark gray (10YR 3/1, moist) coatings; silty clay; weak to moderate medium prismatic breaking to moderate medium and fine subangular blocky structure; hard, firm; roots numerous; noncalcareous; gradual smooth boundary.

B3 20453 58 to 79 cm (23 to 31 inches). Pale brown (10YR 6/3, dry) to grayish-brown (10YR 5/2, moist) with 30 percent dark gray (10YR 4/1, dry) to very dark gray (10YR 3/1, moist) coatings; silty clay loam; weak coarse prismatic breaking to moderate medium and fine angular blocky structure; hard, firm; few roots; noncalcareous; many medium to fine distinct mottles of brownish-yellow (10YR 6/8, moist) occur at 29 to 31 inches; abrupt smooth boundary.

C1ca 20454 79 to 102 cm (31 to 40 inches). Very pale brown (10YR 7/3, dry) to brown (10YR 5/3, moist) silt loam; common fine distinct mottles of brownish-yellow (10YR 6/8, moist); very weak coarse prismatic structure; slightly hard; friable; common fine tubular pores; some are lined with thin clay films; few roots; calcareous, carbonate occurs as soft to slightly hard segregations; gradual smooth boundary.

C2 20455 102 to 127 cm (40 to 50 inches). Very pale brown (10YR 7/3, dry) to pale brown (10YR 6/3, moist) silt loam; common fine distinct mottles of brownish-yellow (10YR 6/8, moist); massive structure; soft, friable; common fine tubular pores, a few are lined with clay films--fewer than horizon above; a local krotovina-like pocket contained numerous clay-lined tubular pores; calcareous, carbonate occurs as soft segregations, fewer than horizon above; gradual smooth boundary.

C3 20456 127 to 152 cm (50 to 60 inches). Very pale brown (10YR 7/3, dry) to pale brown (10YR 6/3, moist) silt loam; few fine distinct mottles of brownish-yellow (10YR 6/8, moist); massive structure; soft, friable; common fine tubular pores; calcareous, occasional soft carbonate segregations.

Remarks: A detailed discussion of the micromorphology and mineralogy is available in the Master's Thesis: Jordan, R. H. 1965. Formation and Transfer of Clay in Hastings Silt Loam, A Udic Argiustoll. University of Nebraska.

Soil Classification: Udic Argiustoll, fine, montmorillonitic, mesic
Soil: Hastings
Soil Nos.: S64[illegible]-91-2
Location: Webster County, Nebraska. 1,[illegible] feet north and 420 feet west of southeast corner of Sec. 31, T4[illegible], R[illegible]W. Small-Watershed 1-H, Central Great Plains Experimental Watershed1/, USDA-ARS, Hastings, Nebraska.
Vegetation and Use: Native grasses such as blue grama, sideoats grama, big bluestem, etc. Area has been cut for hay.
Slope and Land Form: Gently sloping (3 percent slightly convex slope) toward northeast.
Parent Material: Tuorian loess.
Collected by: L. T. Alexander, R. B. Grossman, G. S. Holmgren, L. E. Mitchell, W. C. Lynn, and H. E. Palen.
Described by: Harry E. Palen, September 29, 1964.

All 19956 0 to 15 cm (0 to 6 inches). Very dark brown (10YR 2/2, moist) silt loam; weak very fine granular structure; slightly hard when dry, friable when moist; clear smooth boundary.

A12 19957 15 to 28 cm (6 to 11 inches). Very dark brown (10YR 2/1.5, moist) silty clay loam; moderate, very fine granular structure; slightly hard when dry, friable when moist; clear smooth boundary.

B1 19958 28 to 38 cm (11 to 15 inches). Very dark gray (10YR 3/1, moist) silty clay loam; moderate, very fine sub angular blocky structure; hard when dry, friable when moist; clear smooth boundary.

B21t 19959 38 to 61 cm (15 to 24 inches). Dark grayish-brown (2.5Y 4/2, moist) silty clay loam; moderate, fine and very fine subangular blocky structure; hard when dry, friable when moist; clear smooth boundary.

B3 19960 61 to 81 cm (24 to 32 inches). Dark grayish-brown (2.5Y 4/2, moist) sil: loam; weak, fine prismatic structure separating to weak, medium blocky structure; distinct, common, medium yellowish-brown (10YR 5/8) mottles cover 2 to 20 percent of surface, mottles 5 to 15 mm in diameter; scattered nodules of iron; slightly hard when dry, friable when moist; clear smooth boundary.

C1 19961 81 to 102 cm (32 to 40 inches). Grayish-brown (2.5Y 4.5/2, moist) silt loam; weak medium prismatic structure; faint, few medium yellowish-brown (10YR 5/6) mottles cover less than 2 percent of surface, mottles 5 to 15 mm in diameter; slightly hard when dry, very friable when moist; gradual smooth boundary.

C2ca 19962 102 to 130 cm (40 to 51 inches). Grayish-brown (10YR 5/2, moist) silt loam; weak, coarse prismatic structure; slightly hard when dry, very friable when moist; calcareous; gradual wavy boundary.

C3ca 19963 130 to 157 cm (51 to 62 inches). Grayish-brown (10YR 5/2, moist) silt loam; weak, coarse prismatic structure; slightly hard when dry, very friable when moist; calcareous; gradual wavy boundary.

C4ca 19964 157 to 185 cm (62 to 73 inches). Grayish-brown (10YR 5/2, moist) silt loam; weak, coarse prismatic structure; slightly hard when dry, very friable when moist; calcareous; gradual wavy boundary.

C5 19965 185 to 213 cm (73 to 84 inches). Grayish-brown (10YR 5/2, moist) silt loam; weak, coarse prismatic structure; slightly hard when dry, very friable when moist; noncalcareous.

Remarks: Same moisture distribution as for S64[illegible]-91-1. Beginning at the top, twenty-three (23) 3/4-inch core samples of the upper 6 inches were taken along the transect at intervals of 20 feet for carbon and nitrogen determinations. This pedon description was written at station number 3 on this transect. Four clods for bulk density measurements (0-1, 1-3, 4-6, and 7-9 inch depths) were taken at each even-numbered station.

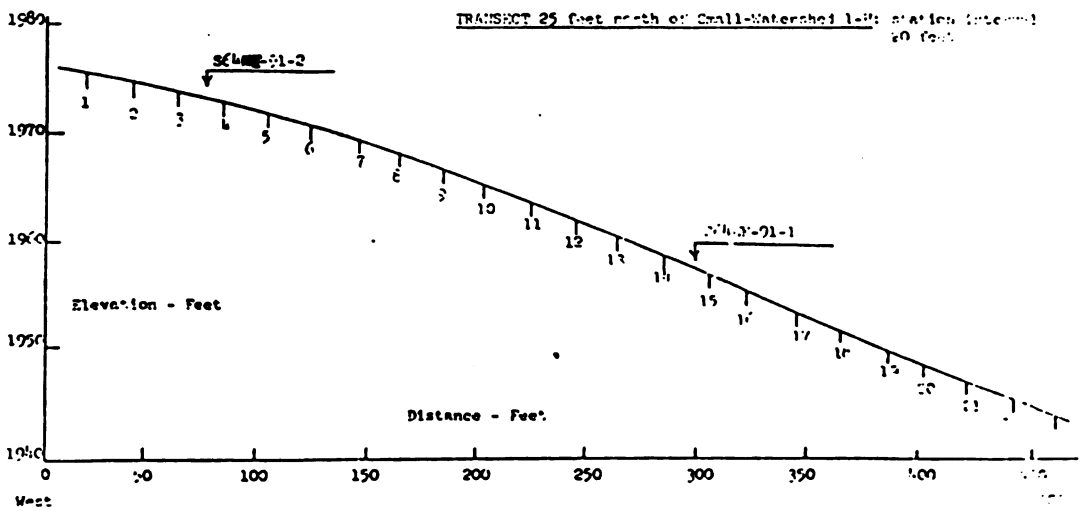

1/ Terminated 1967.

SOIL CLASSIFICATION-UDIC ARGIUSTOLL
FINE, MONTMORILLONITIC, MESIC
SERIES - - - - - - -HASTINGS

SOIL NO - - - - - - S65NE-91-1 COUNTY - - - WEBSTER

GENERAL METHODS- - -1A,1B2B,2A2,2B SAMPLE NOS. 20449-20456

U. S. DEPARTMENT OF AGRICULTURE
SOIL CONSERVATION SERVICE MATSC
SOIL SURVEY INVESTIGATIONS UNIT
LINCOLN, NEBRASKA

11-22-74

DEPTH	HORIZON	PARTICLE SIZE ANALYSIS, LT 2MM, 3A1, 3A1A, 3A1B															RATIO
					FINE	SAND					SILT			FAML	INTR	FINE	NON-	8O1
		SAND	SILT	CLAY	CLAY	VCOS	CORS	MEDS	FNES	VFNS	COSI	FNSI	VFSI	TEXT	II	CLAY	CO3-	15-
		2-	.05-	LT	LT	2-	1-	.5-	.25-	.10-	.05	.02	.005-	SAND	.2-	TO	CLAY	BAR
		.05	.002	.002	.0002	1	.5	.25	.10	.05	.02	.002	.002	2-.1	.02	CLAY		TO
CM		PCT LT 2MM														PCT	PCT	CLAY
000-013	A11	9.5	67.4	23.1	16.7	.0	.1	.1	.3	9.0	50.6	16.8	3.2	.5	59.9	72		.48
013-025	A12	7.5	59.3	33.2	25.9	.0	.0	.1	.1	7.3	41.5	17.8	3.5	.2	48.9	78		.42
025-041	B1	5.6	51.8	42.6	33.7	.0	.0	.0	.0	5.6	34.1	17.7	4.2	.0	39.7	79		.36
041-058	B2T	5.1	50.2	44.7	34.5	.0	.0	.0	.0	5.1	31.0	19.2	5.3	.0	36.1	77		.41
058-079	B3	6.4	56.8	36.8	23.4	.0	.0	.0	.1	6.3	35.6	21.2	4.5	.1	42.0	64		.43
079-102	C1CA	7.3	69.5	23.2	7.2	.1	.1	.1	.2	6.8	41.1	28.4	7.6	.5	48.1	31		.49
102-127	C2	7.8	67.2	25.0	9.4	.0	.0	.0	.1	7.7	41.6	25.6	5.8	.1	49.4	38		.47
127-152	C3	7.0	68.0	25.0	9.6	.0	.0	.1	.2	6.7	40.0	28.0	6.7	.3	46.9	38		.45
058-079	(A)	6.8	55.4	37.8	22.5	.0	.0	.1	.3	6.4	33.8	21.6	4.1	.4	40.4	60		.42
079-102	(A)	7.3	60.2	32.5	17.3	.0	.0	.1	.3	6.9	37.1	23.1	4.3	.4	44.2	53		.35
102-127	(A)	7.6	61.4	31.0	16.2	.0	.0	.1	.4	7.1	37.8	23.6	4.7	.5	45.2	52		.38
127-152	(A)	7.1	64.1	28.8	15.4	.0	.0	.1	.4	6.6	37.8	26.3	4.9	.5	44.7	53		.39

DEPTH	PARTICLE SIZE ANALYSIS, MM, 3B, 3B1, 3B2I					BULK DENSITY			WATER CONTENT				CARBONATE		PH	
	VCL.	WEIGHT				4A1D	4A1M	4D1	4B1C	4B1C	4B2	4C1	6E1B	3A1A	8C1A	8C1E
	GT	GT														
	2	75			.074	PCT	BAR	DRY		BAR	BAR	CM/			1/1	1/2
CM	PCT	PCT	75-20	20-5	5-2	LT 75	LT20	G/CC	G/CC		PCT	PCT	PCT	CM	LT 2 PCT	.002 PCT	H2O	CACL
000-013	0	0	0	0	0	0	1.22	1.31	.024		25.4	11.0	.18				5.9	5.2
013-025	0	0	0	0	0	0	1.27	1.43	.040		30.5	14.0	.21				5.9	5.3
025-041	0	0	0	0	0	0	1.34	1.72	.087		27.8	15.4	.17				6.0	5.6
041-058	0	0	0	0	0	0	1.46	1.78	.082		28.1	18.2	.14				6.6	6.1
058-079	0	0	0	0	0	0	1.40	1.62	.052		26.7	16.0	.15		0		7.1	6.4
079-102	0	0	0	0	0	0	1.29	1.39	.024		28.1	11.3	.22		3	0	8.1	7.2
102-127	0	0	0	0	0	0	1.28	1.38	.024		29.8	11.8	.23		1	0	8.1	7.3
127-152	0	0	0	0	0	0	1.28	1.	.028		29.0	11.3	.23		1	0	8.2	7.3
058-079																		
079-102																		
102-127																		
127-152																		

DEPTH	ORGANIC MATTER		C/N	IRON	PHOS	EXTRACTABLE BASES 5B4A					ACTY	AL	CAT EXCH	RATIO	RATIO	CA	BASE SAT	
	6A1A	6B1A		6C2A	6S1A	6M2E	6O2D	6P2A	6Q2A		6H1A	6G1D	5A3A	5A6A	8D1	8D3	5F	5C3	5C1
	CRGN	NITG		EXT	TOTL	CA	MG	NA	K	SUM	BACL	KCL	EXTB	NHAC	NHAC	CA	SAT	EXTB	NHAC
	CARB			FE						EXTB	TEA	EXT	ACTY		TO	TO	NHAC	ACTY	
CM	PCT	PCT		PCT	PCT	MEQ / 100 G									CLAY	MG	PCT	PCT	PCT
000-013	2.548	.202	13	.5		12.3C	3.7C	TR	1.1	17.1	7.7		24.8	18.2	.79	3.3	.9	94	
013-025	1.80	.199	11	.6		13.4C	5.7C	.1	1.3	22.5	7.7		30.2	22.4	.67	2.7	75	100	
025-041	1.24	.122	10	.7		18.7C	7.6C	.5	1.8	28.6	7.4		36.0	27.2	.64	2.5	79	103	
041-058	.75	.081	9	.6		17.5C	8.3C	.5	2.0	28.3	4.3		32.6	28.3	.63	2.1	87	100	
058-079	.39			.5		16.2C	8.1C	.6	1.9	26.8	2.8		29.6	29.7	.70	2.0	91	104	

MLRA(S): 63B, 71, 72, 73, 75
REV. LR, 12-87
TYPIC USTORTHENTS, FINE-SILTY, MIXED (CALCAREOUS), MESIC

COLY SERIES

THE COLY SERIES CONSISTS OF WELL DRAINED TO EXCESSIVELY DRAINED SILTY SOILS FORMED IN CALCAREOUS LOESS ON UPLANDS. THE SURFACE LAYER IS GRAYISH BROWN SILT LOAM SURFACE LAYER 4 INCHES THICK. THE NEXT 6 INCHES IS LIGHT BROWNISH GRAY SILT LOAM. THE SUBSTRATUM IS LIGHT GRAY SILT LOAM. SLOPES RANGE FROM 1 TO 60 PERCENT. MOST AREAS ARE USED FOR RANGELAND.

ESTIMATED SOIL PROPERTIES

DEPTH (IN.)	USDA TEXTURE	UNIFIED	AASHTO	FRACT >3 IN (PCT)	PERCENT OF MATERIAL LESS THAN 3" PASSING SIEVE NO. 4	10	40	200	LIQUID LIMIT	PLASTICITY INDEX
0-4	SIL, L	ML, CL, CL-ML	A-4, A-6, A-7	0	100	100	85-100	85-100	20-45	2-20
0-4	VFSL	ML, CL-ML, CL	A-4	0	100	100	85-95	50-65	22-35	3-10
4-60	SIL, VFSL, L	ML, CL, CL-ML	A-4, A-6	0	100	100	85-100	85-100	20-40	2-15

DEPTH (IN.)	CLAY (PCT)	MOIST BULK DENSITY (G/CM3)	PERMEABILITY (IN/HR)	AVAILABLE WATER CAPACITY (IN/IN)	SOIL REACTION (PH)	SALINITY (MMHOS/CM)	SHRINK-SWELL POTENTIAL	EROSION FACTORS K	T	WIND EROD. GROUP	ORGANIC MATTER (PCT)	CORROSIVITY STEEL	CONCRETE
0-4	18-24	1.30-1.50	0.6-2.0	0.20-0.24	7.4-8.4	-	LOW	.43	5	4L	1-2	HIGH	LOW
0-4	8-15	1.30-1.50	0.6-2.0	0.17-0.18	7.4-8.4	-	LOW	.43	5	3	1-2		
4-60	18-24	1.30-1.50	0.6-2.0	0.17-0.22	7.4-8.4	-	LOW	.43					

FLOODING FREQUENCY	FLOODING DURATION	FLOODING MONTHS	HIGH WATER TABLE DEPTH (FT)	HIGH WATER TABLE KIND	HIGH WATER TABLE MONTHS	CEMENTED PAN DEPTH (IN)	CEMENTED PAN HARDNESS	BEDROCK DEPTH (IN)	BEDROCK HARDNESS	SUBSIDENCE INIT. (IN)	SUBSIDENCE TOTAL (IN)	HYD GRP	POTENTIAL FROST ACTION
NONE			>6.0			-		>60		-		B	MODERATE

SANITARY FACILITIES

SEPTIC TANK ABSORPTION FIELDS	1-8%: SLIGHT 8-15%: MODERATE-SLOPE 15+%: SEVERE-SLOPE
SEWAGE LAGOON AREAS	1-2%: MODERATE-SEEPAGE 2-7%: MODERATE-SEEPAGE,SLOPE 7+%: SEVERE-SLOPE
SANITARY LANDFILL (TRENCH)	1-8%: SLIGHT 8-15%: MODERATE-SLOPE 15+%: SEVERE-SLOPE
SANITARY LANDFILL (AREA)	1-8%: SLIGHT 8-15%: MODERATE-SLOPE 15+%: SEVERE-SLOPE
DAILY COVER FOR LANDFILL	1-8%: GOOD 8-15%: FAIR-SLOPE 15+%: POOR-SLOPE

BUILDING SITE DEVELOPMENT

SHALLOW EXCAVATIONS	1-8%: SLIGHT 8-15%: MODERATE-SLOPE 15+%: SEVERE-SLOPE
DWELLINGS WITHOUT BASEMENTS	1-8%: SLIGHT 8-15%: MODERATE-SLOPE 15+%: SEVERE-SLOPE
DWELLINGS WITH BASEMENTS	1-8%: SLIGHT 8-15%: MODERATE-SLOPE 15+%: SEVERE-SLOPE
SMALL COMMERCIAL BUILDINGS	1-4%: SLIGHT 4-8%: MODERATE-SLOPE 8+%: SEVERE-SLOPE

CONSTRUCTION MATERIAL

ROADFILL	1-15%: FAIR-LOW STRENGTH 15-25%: FAIR-SLOPE,LOW STRENGTH 25+%: POOR-SLOPE
SAND	IMPROBABLE-EXCESS FINES
GRAVEL	IMPROBABLE-EXCESS FINES
TOPSOIL	1-8%: GOOD 8-15%: FAIR-SLOPE 15+%: POOR-SLOPE

WATER MANAGEMENT

POND RESERVOIR AREA	1-3%: MODERATE-SEEPAGE 3-8%: MODERATE-SEEPAGE,SLOPE 8+%: SEVERE-SLOPE
EMBANKMENTS DIKES AND LEVEES	SEVERE-PIPING
EXCAVATED PONDS AQUIFER FED	SEVERE-NO WATER
DRAINAGE	DEEP TO WATER
IRRIGATION	1-3% SIL,L: ERODES EASILY 3+% SIL,L: SLOPE,ERODES EASILY 1-3% VFSL: ERODES EASILY,SOIL BLOWING 3+% VFSL: SLOPE,ERODES EASILY,SOIL BLOWING

Topography, soils, and landuse were taken from "THE CENTRAL GREAT PLAINS EXPERIMENTAL WATERSHED, A Summary Report of 30 Years of Hydrologic Research". The following map and data are excerpts from this report and from Plane Table Topographic Surveys performed in 1942 by the Soil Conservation Service-USDA under Hugh Hammond Bennet. The report is available from the Water Data Laboratory, Agriculutral Research Service-USDA, Beltsville Maryland. The folio of maps is available for loan from the same Laboratory.

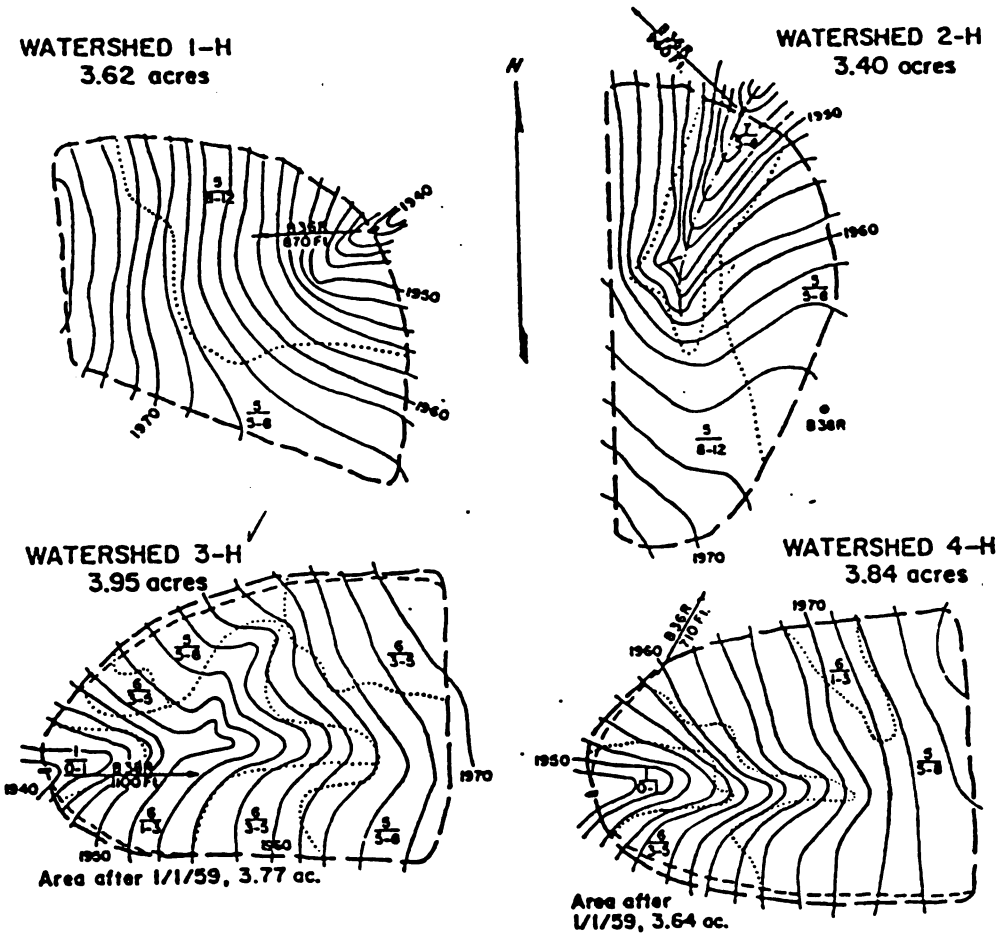

Watersheds 1-H, 2-H, 3-H, & 4-H.

Table 3 .—Crop and treatment plan for 4-acre watersheds for the period of 1958 through 1967

Watershed	Crop and treatment by years 1/									
	1958	1959	1960	1961	1962	1963	1964	1965	1966	1967
1-H	Mn	Mn	Mn	Mn	Mn	Mn	Sf	Sm	Fm	Wm
2-H	Mn	Mn	Mn	Mn	Mn	Mn	P	P	P	P
22-H					Mr	Mr	Mr	Mr	Mr	Mr
23-H					Mr	Mr	Mr	Mr	Mr	Mr
25-H						Mn	Mn	Mn	Mn	Mn
18-H	P	P	P	P	P	P	P	P	P	P
3-H'	Wm	Sm	Fm	Wm	Sm	Fm	Wm	Sm	Fm	Wm
8-H	Wm	Sm	Fm	Wm	Sm	Fm	Wm	Sm	Fm	Wm
4-H'	Sm	Fm	Wm	Sm	Fm	Wm	Sm	Fm	Wm	Sm
7-H'	Sm	Fm	Wm	Sm	Fm	Wm	Sm	Fm	Wm	Sm
5-H'	Fm	Wm	Sm	Fm	Wm	Sm	Fm	Wm	Sm	Fm
6-H	Fm	Wm	Sm	Fm	Wm	Sm	Fm	Wm	Sm	Fm

1/ Symbols used in columns are: Mn = native meadow; Mr = meadow of reseeded native grasses; Sf = forage sorghum; S = sorghum in rows for grain; W = wheat; F = fallow; P = native pasture; m = stubble mulch farmed.

A75

SELECTED RUNOFF EVENTS — WATERSHED 4-H (44.08)

ANTECEDENT CONDITION			RAINFALL				RUNOFF			
Date	P (in.)	Q (in.)	Date	Time	Rate (in/hr)	Acc. (in.)	Date	Time	Rate (in/hr)	Acc. (in.)
			Event of May 6, 1959							
				RG	B-J6-R					
4-10	.02	.00	5-4	1418	.00	.00	5-4	1425	.3700	.0000
4-17	.34	.09		1420	.90	.03		1427	.243	T
4-19	.51	.03		1422	2.10	.10		1429	1.23	.03
5-2	.25	.00		1424	3.60	.22		1431	.987	.07
5-3	.14	.00		1426	5.40	.40		1435	.461	.11
				1428	3.60	.52		1439	.196	.13
Watershed conditions:				1430	2.40	.60		1442	.110	.14
Fallow good residue cover.				1432	1.20	.64		1445	.0637	.15
				1507	.19	.75		1452	.0236	.15
				1527	.03	.76		1509	.0095	.16
				1630	.00	.76		1549	.0051	.16
				1750	.06	.84		1749	.0000	.16

Regression analysis of Table 4 outflows. This analysis was performed with Lotus 1-2-3 for the actual and calculated outflows. The pairs of values are at constant time for which the analysis was performed.

Regression Output:	
Constant	2.90E-01
Std Err of Y Est	3.96E-01
R Squared	9.26E-01
No. of Observations	2.70E+01
Degrees of Freedom	2.50E+01
X Coefficient(s)	3.43E+01
Std Err of Coef.	1.94E+00